Hydrologic Dynamics in Response to Natural and Anthropogenic Stresses on a Barrier Island: Saltwater Intrusion and Inundation.

By:

Kyle Prock

July 2020

Director of thesis: Alex Manda

Major Department: Geological Sciences

The impacts of climate change and sea-level rise on groundwater systems on barrier islands are not well documented in the literature. Globally, there is high competition for useable land in coastal regions because large populations of people live along the coast. If useable land and freshwater resources are lost to saltwater intrusion through sea-level rise or groundwater pumping, coastal communities may experience challenges with meeting high costs of mitigating resulting effects. The goals of this study were to (i) evaluate the impact of sea-level rise and groundwater pumping on saltwater intrusion in the surficial aquifer using an analytical model, and (ii) to evaluate how changes in tidal amplitudes due to sea-level rise may influence groundwater levels in surficial aquifers on barrier islands. To establish if groundwater pumping or sea-level rise has the greatest impact on saltwater intrusion models were used to delineate the location of the toe of the freshwater-saltwater interface as a proxy for the area of the aquifer that was lost to saltwater intrusion. The second objective was to assess the extent of marine and groundwater inundation under different tidal amplitude and sea-level rise scenarios using geospatial procedures. The results show that the percentage of the aquifer occupied by saltwater intrusion due to sea-level rise is greater (51%) than the percentage of the aquifer occupied by saltwater due to consumptive groundwater pumping (34%) for comparable magnitudes of movement of the toe of the saltwater wedge. The results also indicate that when tidal amplitudes are increased by 20%, marine inundation is greater (5%) than groundwater inundation (2%) in the most extreme sea level rise scenario (i.e., 1.5 m of sea-level rise by the year 2100). The results of this study provide estimates of potential changes in groundwater levels that could impact coastal communities and the amount of land that may become impaired. The results can also help water managers understand potential changes to the groundwater system and determine viable solutions to consequences. The relevance of this research is that it will help provide insight on how sea-level rise and groundwater pumping may affect saltwater intrusion and groundwater levels in surficial aquifers on barrier islands.

Hydrologic Dynamics in Response to Natural and Anthropogenic Stresses on a Barrier Island: Saltwater Intrusion and Inundation.

A Thesis

Presented to the Faculty of the Department of Geological Sciences

East Carolina University

To be submitted in partial fulfillment of the requirements for the degree of

Master of Science in Geology

By: Kyle Prock

July 2020

Hydrologic Dynamics in Response to Natural and Anthropogenic Stresses on a Barrier Island: Saltwater Intrusion and Inundation.

By:

Kyle Prock

July 2020

DIRECTOR OF THESIS:____

Alex K. Manda, PhD

COMMITTEE MEMBER:____

Michael O'Driscoll, PhD

COMMITTEE MEMBER:____

Terri Woods, PhD

COMMITTEE MEMBER:____

Randall Etheridge, PhD

CHAIR OF THE DEPARTMENT
OF GEOLOGICAL SCIENCES:____

Stephen J. Culver, PhD

DEAN OF THE GRADUATE SCHOOL:______________________________________

Paul J. Gemperline, PhD

DEDICATION

This thesis is dedicated to my family and friends.

ACKNOWLEDGMENTS

First, I would like to thank my family for all their support throughout this journey. To my mother Katherine, my father Donald, my sister Jessica, my dog Rocky. I can never thank you enough for all the love and support and for everything you’ve done to help me get this far.

I would like to thank my advisor, Alex Manda. Thank you for this opportunity to learn from your knowledge and experience, I am grateful for the opportunity you provided me.

I would also like to thank the other members of my committee. Dr. Michael O’Driscoll, Dr. Terri Woods, and Dr. Randall Etheridge. Thank you all for imparting your assistance during the journey.

Thank you to all of my friends and fellow graduate students for the support along this journey.

TABLE OF CONTENTS

LIST OF TABLES

LIST OF FIGURES

INTRODUCTION

Groundwater resources in coastal communities will be impacted by sea-level rise in response to climate change (Masterson et al., 2013a). This change will also have a significant impact on hydrologic processes of surficial aquifers on barrier islands. By the year 2100, sea-level is forecast to rise 0.2 to 1.5 m (Jevrejeva et al.; 2012, Rotzoll and Fletcher, 2012; Horton et al., 2014). These changes in sea-level can have many adverse effects such as saltwater intrusion, groundwater inundation, and marine inundation.

Saltwater intrusion can deplete freshwater resources by replacing them with saltwater. This results from anthropogenic changes such as groundwater pumping or natural causes such as sea-level rise (Ferguson and Gleeson 2012). When the freshwater-saltwater interface moves landward it can displace groundwater causing groundwater inundation (Rotzoll and Fletcher, 2013).

Groundwater inundation occurs when the water table rises above the land surface which causes permanent flooding (Masterson et al., 2013b; Rotzoll and Fletcher, 2012). This flooding can have many negative impacts on barrier islands including increased land degradation, destruction of infrastructure, and changes to vegetation assemblages (Masterson et al., 2013a, Manda et al., 2014). Sea-level rise also has the potential to cause significant flooding to urban areas (Rotzoll and Fletcher, 2012). Many barrier island systems including Bogue Banks in Eastern North Carolina, are prone to flooding in low lying areas because of a thin vadose zone (Manda et al., 2014). Marine inundation is when sea-level rises and occupies previously dry land. Many coastal communities could experience the effects of groundwater inundation which may be equal to or greater than marine inundation (Rotzoll and Fletcher, 2012, Manda et al., 2014).

The study site for this project is Bogue Banks, a developed barrier island off the coast of North Carolina (Figure 1). This island trends roughly east-west with Bogue Sound to the north and the Atlantic Ocean to the south. The island itself has morphologic variability; the western side of the island is regressive while the eastern side is transgressive (Timmons et al., 2010). Like most coastal communities, this island has seasonal population differences with the off-season population estimated at 7,500 inhabitants (http://www.census.gov) which then increases to ~40,000 people during the peak tourist season in the summer months (https://www.emeraldisle-nc.org/Data/Sites/1/media/pdfs/fast-facts-2020.pdf).

Little is known about how shallow aquifer systems on barrier islands will respond to sea-level rise and the accompanying groundwater inundation and tidal changes. With forecasted climate change and relative sea-level rise expected, knowing how surficial aquifer systems may change will be valuable for future development because some residents rely on these surficial aquifers for potable water and on-site wastewater treatment systems. Another possible change is that the ground surface can become impaired if low-lying areas are inundated by ocean water. Understanding how groundwater will respond to sea-level rise and tidal changes will help water managers forecast future situations and mitigate sunny day flooding.

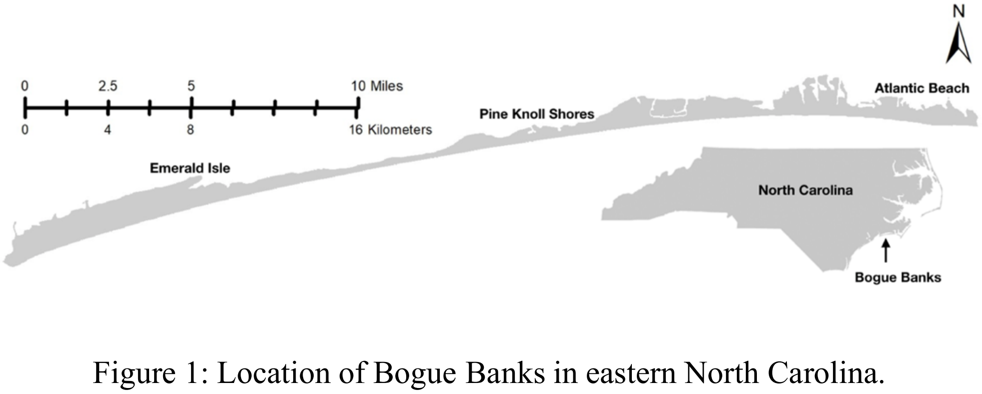

Figure 1: Location of Bogue Banks in eastern North Carolina.

Purpose and scope

The first goal of this study is to evaluate the relative impacts of sea-level rise versus groundwater pumping on saltwater intrusion in the surficial aquifer. This was achieved by evaluating the magnitude of the movement of the freshwater-saltwater interface and computing the change in area occupied by seawater. Knowing which has a greater impact on the movement of the freshwater-saltwater interface can help water managers determine future threats to coastal communities. The second goal of this study was to evaluate how changes in tidal amplitudes caused by sea-level rise may influence groundwater levels in the surficial aquifers on barrier islands. To address this goal, the following objectives were pursued: (1) calculation of the magnitude of the area occupied by seawater in the surficial aquifer as a result of movement of the freshwater-saltwater interface under various sea-level rise scenarios and pumping rates, (2) simulation of tidal amplitudes under different sea-level rise scenarios using an analytical model, and (3) assessment of the effect of sea-level rise and changes in tidal amplitudes on the water table on a barrier island by determining the extent of marine and groundwater inundation.

The hypotheses to be tested in this study are (1) sea-level rise has a greater impact on saltwater intrusion than groundwater pumping when evaluating changes in aquifer area affected by saltwater intrusion, and (2) changes in tidal amplitudes arising from sea-level rise will have a significant impact on marine and groundwater intrusion.

Previous research

Sisco (2013) studied how the groundwater system affects stormwater runoff by determining hydraulic properties and characteristics of the surficial aquifer on the western part of Emerald Isle, North Carolina. This study found that during storm events, storm water runoff increases if the water table crests above the land surface.

Owers (2017) developed a steady state numerical groundwater model of the island to assess the impacts of groundwater inundation on Bogue Banks, North Carolina. He concluded that groundwater inundation is a greater threat to land impairment than marine inundation under various sea-level rise scenarios. Tidal oscillations and how they may change as sea-level rises were not included in his forecasting models.

Ferguson and Gleeson (2012) used an analytical model to assess the impacts of the saltwater wedge under pumping and sea-level rise scenario in various coastal settings. They concluded that groundwater pumping has a greater impact on the movement of the toe of the saltwater wedge than sea-level rise. This model, however, only compared the location of the toe of the saltwater wedge; the location of the leading edge of the freshwater-saltwater interface along the base of the aquifer, instead of the total area lost to saltwater intrusion. The conceptual model (Figure. 2) produced by Ferguson and Gleeson (2012) even shows that the area occupied by saltwater is greater when sea-level rises than when groundwater pumping occurs (for the same distance that the toe (x_t) of the saltwater wedge moves landward)

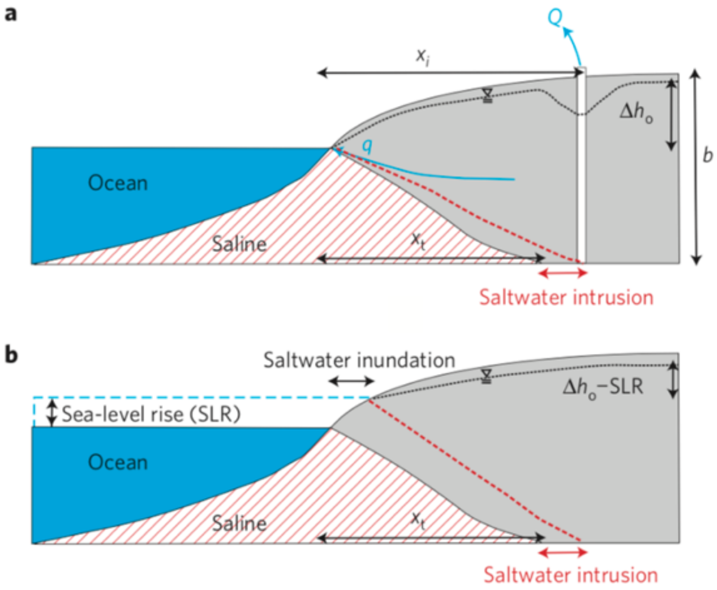

Figure 2: Conceptual model showing influence of groundwater pumping and changes in sea-level (adapted from Ferguson and Gleeson, 2012).

Sukop et al. (2017) and Ross et al. (2017) evaluated how tidal oscillations change with increased sea level. It was determined that tidal amplification may change depending on changes in depth and frictional forces. Areas which use hard beach stabilization techniques may experience an increase in tidal amplitude and inundation. This increase may occur because of increased depth which decreases frictional forces. Soft beach stabilization techniques have adverse effects because they may decrease tidal amplitudes and inundation. This may occur because soft beach stabilization decreases depth which would increase frictional forces. Other factors (e.g., dredging, changes in river discharge, and increased urban runoff) may also change tidal amplitudes (Holleman et al., 2014, Cai et al., 2012).

Carol et al., (2009) studied heterogeneities in an unconfined aquifer in the Samborombon Bay wetland, Argentina. The study conducted by Carol et al. (2009) was to determine how tidal forces change when moving landward. This study provides a useful analytical model to compute amplitudes in water table surfaces due to tidal forces.

Hydrogeologic setting and conceptual model

Bogue Banks is located in the Coastal Plain of North Carolina. Lautier (2001) describes the hydrogeologic framework of the North Carolina Coastal Plain as having eight significant aquifers separated by confining units. The units that make up the Coastal Plain are mostly unconsolidated sediments that thicken and dip eastward at an average rate of 7 m per km (Lautier 2001). This results in a large sediment wedge which varies from 3000 m at its thickest portion under Cape Hatteras to < 30 m in the western Coastal Plain (Bales et al., 2004). Most of the aquifers are predominantly sand with interbedded clays, silts, and shell materials. One notable exception is the Castle Hayne aquifer which consists largely of consolidated limestone. The aquifers range from Early Cretaceous to Holocene. From oldest to youngest, these aquifers are the Lower Cape Fear, the Upper Cape Fear, the Black Creek, the Peedee, the Beaufort, the Castle Hayne, the Yorktown, and the Surficial aquifer (Figure 3). This sediment wedge sits on top of Paleozoic basement rock (Lautier, 2001; Winner and Coble, 1996). This study will focus on the surficial aquifer of Bogue Banks which is not overlain by a confining unit.

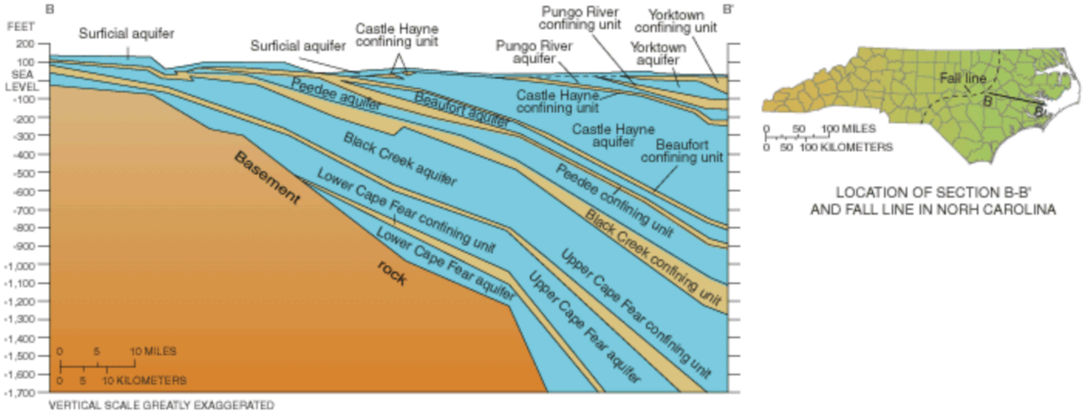

Figure 3: Hydrogeologic cross section of eastern North Carolina's aquifer system (Bales et al., 2004, modified from Winner and Coble, 1996)

The surficial aquifer on Bogue Banks is unconfined, of Quaternary age, and is composed of sandy material with some beds of mud and clay which are common of surficial aquifers throughout the North Carolina Coastal Plain (Lautier, 2001). The inhabitants on the island do not use the surficial aquifer as a source for potable water resources. Potable water is derived from lower confined aquifers such as the Castle Hayne (https://www.ncwater.org/?page=538&quado=1392). Uses for the surficial aquifer include on-site wastewater treatment which may add recharge to the aquifer. The predominant source of recharge into the surficial aquifer is precipitation which is ~130 cm based on data collected from a 10-year period from 1990 to 1999 (Lautier, 2001). About 52 to 92% of this average precipitation is lost to runoff and evapotranspiration which is determined by infiltration capacity, soil types, and local evapotranspiration rates (Lautier, 2001, Masterson et al., 2013-b). Meteorological extremes caused by tropical storms may increase precipitation and associated storm surges which may lead to flooding in low laying areas. In most locations on the island, the water table is usually located a few feet beneath the ground surface. However, there are low-lying swales where the groundwater is close to the land surface that are prone to temporary or permanent groundwater inundation. With forecasted sea-level rise, the magnitude or frequency of groundwater inundation may increase due to rising water table elevations (Rotzoll and Fletcher, 2012, Habel et al, 2017).

The conceptual model given by Ferguson and Gleeson (2012) (Figure 2) is useful for assessing the impacts of sea-level rise and groundwater pumping on the location of the leading edge of the saltwater-freshwater interface at the base of the surficial aquifer (i.e., the toe of the saltwater wedge). This conceptual model shows how the toe of the saltwater wedge moves due to pumping or sea-level rise. The study conducted by Ferguson and Gleeson (2012) only calculated the distance that the toe moved because of pumping and sea-level rise, and not the amount of freshwater lost due to saltwater intrusion. The conceptual model produced by Ferguson and Gleeson (2012) however, shows a greater area lost due to sea level rise (for the same distance that the toe of the saltwater wedge moves landward). This conceptual model seems to suggest that sea-level rise may have a greater impact than pumping when comparing the proportion of aquifer lost due to saltwater intrusion, contrary to Ferguson and Gleeson's (2012) conclusions.

Coastal inundation may not only be affected by rising sea-level, but also by changing tides. Tides are the natural rise and fall of the oceans caused by gravitational forces exerted from the moon, sun, and Earth's rotation. The island of Bogue Banks experiences semi-diurnal tides with two high tides and two low tides within a lunar day. The average amplitude of these tides is ~0.6 m (NOAA tide gage #8656483).

Tidal fluctuations temporarily change groundwater levels in coastal aquifers. To model these changes, an analytical model derived from Carol et al. (2009) was adopted for this study to simulate how tidal influences change as one moves landward (Figure 4). According to the conceptual model, the influence of tidal forces decreases precipitously as one moves inland. The reasons groundwater levels change due to the tides are based on three ideas (Parker and Stringfield, 1950, Freeze and Cherry, 1979). The first idea is that more dense saltwater is forcing the freshwater to rise by wedging beneath it and displacing it. This displaced groundwater has nowhere to go but to rise in the aquifer. The second idea is that gravitational forces that produce the tides also cause the groundwater levels to rise with the tides. The final idea is that both the first and second ideas are both impacting groundwater levels. Tidal oscillations decrease as you move landward so the greatest areas impacted are areas close to shorelines. Barrier islands would experience the effect from both the sound and ocean sides of the island. These tides, however, may change with sea-level rise because increased depth causes a decrease in frictional effects which alters tidal amplification. Mitigation practices for coastal erosion may cause these changes because when soft beach stabilization practices decrease depth, tidal amplitudes decrease. Conversely, when hard beach stabilization practices increase depth, tidal amplitudes increase (Lee et al., 2017).

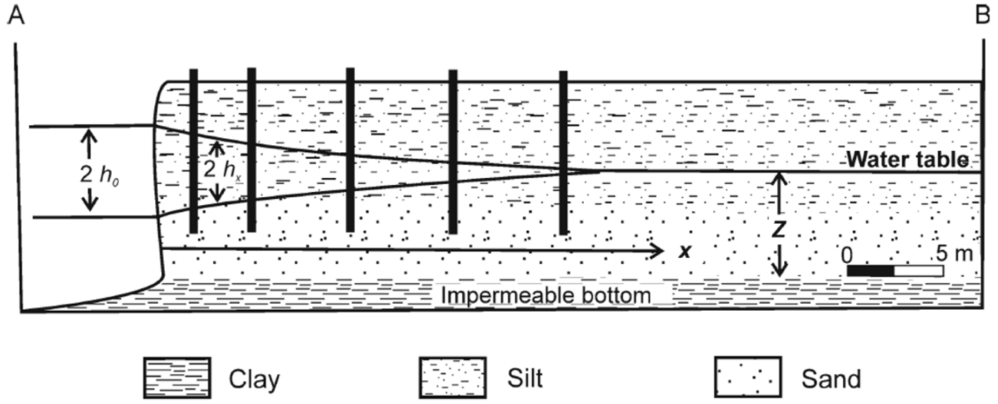

Figure 4: Conceptual model showing how tidal forces interact with groundwater moving landward. Where h_0 = tidal range, h_x = range of water-table fluctuations at distance x, x = distance from tidal source, and z = the thickness of the aquifer (Adapted from Carol et al., 2009).

METHODOLOGY

Sea-level rise versus groundwater pumping

An analytical model derived from Ferguson and Gleeson (2012) was used to determine the location of the toe of the saltwater wedge (Eq.1). The toe is the furthest the freshwater-saltwater interface is located landward. Both sea-level rise and groundwater pumping affect the movement of the freshwater-saltwater interface. This analytical model was used to calculate the location of the toe of the saltwater wedge in response to sea-level rise. The location of the toe was determined using sea-level rise scenarios of 0.2 -1.6 m in increments of 0.2 m. This was chosen because by 2100 sea-level is forecasted to rise 0.2 m -1.5 m (Jevrejeva et al.; 2012, Rotzoll and Fletcher, 2012; Horton et al., 2014). This model was then used to calculate the pumping rate that would be required to move the base of the saltwater wedge an equal amount of distance as sea-level rise (Eq. 2).

(Eq. 1)

$$\frac{\left(\frac{Kb(\Delta H_o - SLR)}{\Delta X}\right)x_t}{K} = s(s-1)d^2/2$$

K= hydraulic conductivity, b= height of the aquifer, H_o = head of observation well, SLR= sea-level rise, x= distance between the shoreline and observation well, s= specific gravity of seawater, d= depth of aquifer, x_t= distance from the shoreline to the base of the saltwater wedge (toe).

(Eq. 2) $$\frac{qx_t}{K} + \frac{Q}{4\pi K} * \ln\left[\frac{(x_t - x_i)^2}{(x_t + x_i)^2}\right] = s(s-1)d^2/2$$

K = hydraulic conductivity, Q = pumping rate, q = flux, x_i = distance between the shoreline and pumping well, s = specific gravity of seawater, d = depth of the saltwater wedge, x_t = distance from the shoreline to the base of the saltwater wedge (toe).

In order to compare changes to area occupied by seawater under sea-level rise and pumping, a baseline from which to make comparisons, was first needed. The baseline is defined here as the area of the aquifer occupied by seawater under no sea-level rise and zero pumping. It is from this baseline that assessments were made on the effect of sea-level rise and pumping on the location of the toe of the saltwater wedge. This was accomplished by comparing the changes in area occupied by saltwater when pumping or sea-level rise caused movement in the location of the toe of the saltwater wedge. Specifically, this was done by subtracting the area occupied by seawater at baseline from the area occupied by seawater after saltwater intrusion occurred either solely from pumping or sea-level rise. To determine whether groundwater pumping or sea-level had the greater impact on saltwater intrusion, comparisons between the area occupied by seawater under the two drivers were made for cases where the toe of the saltwater wedge moved the same distance. Scaled drawings were used to calculate how much area was lost due to sea-level rise and groundwater pumping (figure 5).

The computations of area were based on the following assumptions: The freshwater-saltwater interface and the land surface beneath the ocean were conceptualized as straight lines. The land surface had a plunge of 45 degrees from the horizontal. This angle was chosen to provide vertical exaggeration, this does not interfere with the computation of the location of the base of the saltwater wedge. The Ferguson and Gleeson (2012) model doesn't use shoreline slope to compute the location of the base of the saltwater wedge. This approach simplified the process of computing the area occupied by seawater because triangles could be fitted into that area and used to calculate the total area. This simple two-dimensional model does not consider cones of ascension which may cause more saltwater intrusion due to groundwater pumping. Also recharge and evapotranspiration are assumed to be constant in each scenario.

The well chosen to test this analytical model was OBB07 which is located on the western portion of Bogue Banks (Appendix A). This well was chosen because it is located close to the center of the island (~690 m from the ocean and ~600 m from the sound). For this test, it is assumed that the thickness of the surficial aquifer is uniform, so a thickness of 20 m was chosen. This thickness was chosen based on the average depth to the first confining layer determined by using geophysical logs from the North Carolina Department of Environmental Quality (DEQ) Division of Water Resources.

The areas occupied by seawater were computed from the scaled diagrams using principles of geometry (e.g., finding the area of a right triangle). In the case where the area occupied by sea level was not a right triangle (i.e., for sea level rise scenarios), Herons formula was used because it only requires the lengths of each side of the triangle to compute the area. The areas representing the space occupied by seawater for the same distance moved by the toe of the saltwater wedge for corresponding sea-level rise and pumping scenarios were then compared to one another to determine which driver had a bigger impact on saltwater intrusion. The scenario which had more area lost to saltwater was determined to have the greater impact because it would have had greater amounts of saltwater intrusion.

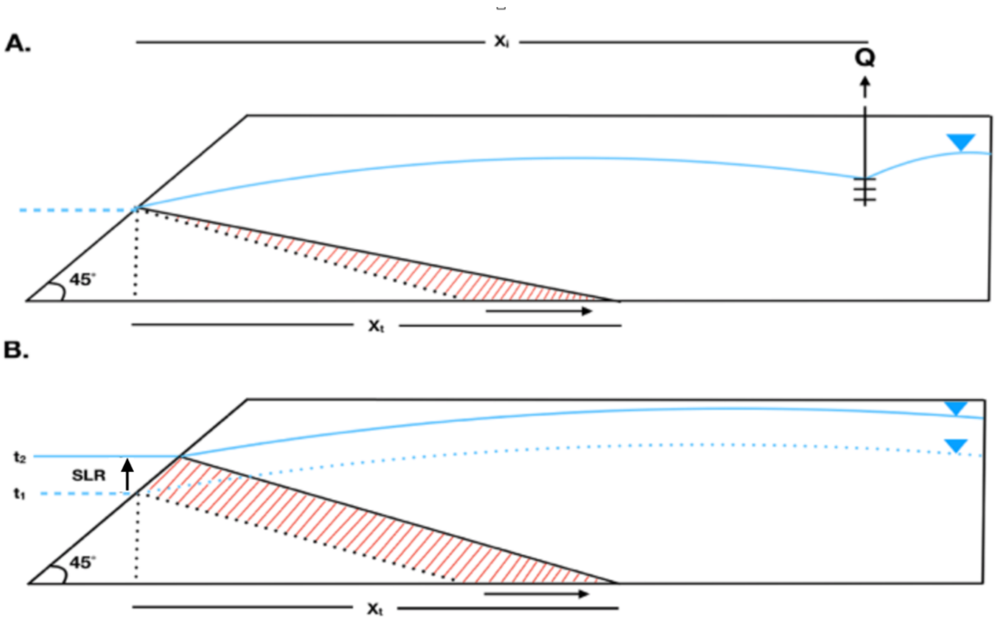

Figure 5: Conceptual model (adapted from Ferguson and Gleeson, 2012) used to compute area occupied by seawater. The shaded area represents the area occupied by seawater as a consequence of saltwater intrusion. A. Movement of the toe of the saltwater wedge by a distance x_t under pumping conditions. B. Movement of the toe of the saltwater wedge by a distance x_t under sea-level rise scenarios.

A sensitivity analysis was also used in this study to understand how hydraulic conductivity affects the amount of saltwater intrusion that would occur due to sea-level rise and pumping. The analytical model given by Ferguson and Gleeson (2012) was used for this purpose. For the sensitivity analysis, hydraulic conductivity was changed by +/- 50% and +/- 30% from a baseline value of 0.003 m/s (this baseline value was determined in a previous study by Owers (2017)). These ranges were used to determine if hydraulic conductivity played a crucial role in the movement of the toe of the saltwater wedge.

Evaluating tidal influence

Groundwater-level data were collected from twenty-nine observation wells located on Bogue Banks which were previously installed in the surficial aquifer by other researchers (Owers, 2017). The location of these wells can be seen in Appendix A. The head data reveal that only ten of these observation wells showed any tidal influence (Appendix B). Typically, the closer the wells were to the ocean or sound, the greater the tidal influence was on groundwater levels. Tidal influence on the water table was generally not seen more than 265 m from the shoreline. However, this was not always observed; some wells close to the shore showed no signs of tidal influence and some wells further inland clearly displayed tidal influence.

To identify which changes in groundwater levels were tidally influenced, it was important to look at time series intervals over a twelve-hour window (due to semi-diurnal tides). A National Oceanographic and Atmospheric Administration (NOAA) tide gage (#8656483) was used to determine the amplitude and period of the tides. The tide gauge, which is located in the town of Beaufort, North Carolina, is the closest tide gauge to the study site (http://tidesandcurrents.noaa.gov). The groundwater data were then broken into shorter segments which showed the tidal oscillations in detail after being detrended using MATLAB. Groundwater levels are constantly increasing and decreasing, any signal processing techniques ought to be performed on detrended time series data. When the time series of water levels are detrended, it is then possible to compute the amplitude of the tidal oscillations. The steps associated with these processes are highlighted in Appendix B.

Using these observed data, an analytical model developed by Carol et al. (2009) was used to determine aquifer properties on Bogue Banks (Eq. 3). Using the detrended data, curve matching techniques were used to find diffusivity (i.e, the ratio of transmissivity to storage) values. Once the curve matching was complete, it was possible to calculate tidal amplitudes from various distances from the sound. Tidal signals from wells on the sound side were used to calibrate the Carol et al. (2009) model because the NOAA tide gauging station was located on the sound side of the island.

(Eq. 3)

$$\boldsymbol{h = h_o e^{-x\sqrt{\pi S/t_o T}} - sin\left(\frac{2\pi t}{t_o} - x\sqrt{\pi S/t_o T}\right)}$$

Where h = amplitude of the water table oscillation, h_0 =tidal amplitude, S = specific yield, T = transmissivity, t_0 = the tidal period, x = distance from the shoreline, and t is the time.

The calibrated models for each well were then used to estimate groundwater levels at different distances from the sound in order to determine tidal influence. Once the tidal oscillations got smaller than 1 mm it was determined that tides were no longer influencing groundwater. Transects were made on the map of Bogue Banks along which changes in tidal influences were evaluated. Assumptions made in this part of the study were that the Surficial aquifer is homogenous and isotropic, and that tidal influences are the same from the Sound as those from the Ocean side (Appendix C). With these assumptions, tidal amplitudes in the ocean would be the same as tidal amplitudes in the sound. The amplitudes along these transects were then increased and decreased by 20% in order to simulate possible changes in depth and frictional forces which may happen with mitigation practices employed to address environmental changes along the coast. These simulations were then used to determine how groundwater levels may respond to tidal fluctuations in future scenarios.

Geospatial procedures to evaluate inundation

In ArcGIS 10.7, a digital elevation model (DEM) of Bogue Banks was used to determine the locations of future shorelines under different sea-level rise scenarios. Using hydraulic head data collected from groundwater monitoring wells on the island, water table contour maps were produced for the island. Head data for the summer as well as the winter were used to highlight seasonal changes of groundwater levels.

The DEM was used to determine the location of shorelines under sea-level rise scenarios of 0.2 m to 1.6 m in 0.2 m increments. This was chosen to represent where the shoreline would be located by 2100 (Jevrejeva et al.; 2012, Rotzoll and Fletcher, 2012; Horton et al., 2014). In order to accomplish this, the DEM of Bogue Banks was used to create shapefile of an outline of the island at mean high water or 0 m of sea-level rise. This process was then repeated for new estimates of sea-level rise to determine what areas would be impaired due to marine inundation. The average tidal amplitude (0.64 m) that would be experienced at the shoreline, computed using the model from Carol et al., (2009), was then added to the mean high-water level (with 0 m of sea-level rise). This average was thereafter used as the baseline for computing potential changes to tidal amplitude. Changes of +/-10% and +/-20% of the tidal amplitude were chosen to represent what may occur in worst case and moderate case scenarios (Cai et al., 2012, Lee et al., 2017). The computed changes for tidal amplitudes were then projected onto groundwater levels under each sea-level rise scenario. The process of creating shapefiles using the DEM was then repeated with tidal amplitude superimposed on increased sea-level. These shapefiles were then used to determine the amount of land that would become impaired due to marine inundation by determining what areas would be under water at each sea-level rise scenario.

In order to compute the area impaired by groundwater inundation, hydraulic head data were used to create a water table surface (Appendix D). The DEM was then subtracted from the resulting water table surface, with positive outcomes representing where the water table is above the land surface and negative values representing where water tables were below the land surface.

In order to include tidal amplification due to shoreline mitigation and sea-level rise on groundwater levels, computed changes were added to baseline tidal amplitudes. Baseline tidal amplitudes were based on observed head values from each well which showed tidal influence (Appendix B). These were considered baseline because they were calculated under 0 m of sea-level rise. Changes to the baseline condition would be the result of implementation strategies to mitigate shoreline erosion under sea-level rise scenarios because hard stabilization would increase tidal amplitudes while soft stabilization would cause a decrease in tidal amplitudes (Lee et al., 2017). Tidal amplitudes were therefore changed by +/-10% and +/-20% from the baseline to account for implementation of mitigation strategies for shoreline erosion (Cai et al 2012, Lee et al., 2017).

These changes in amplitude were then incorporated into water table surfaces to evaluate how changes in tidal amplitude would impact groundwater inundation. This was achieved by subtracting the DEM from the water table surface to calculate the amount of land which becomes impaired due to the water table rising above the ground surface. The resulting layers which showed groundwater inundation were then combined with the other layers that showed marine inundation. When combined, the layers showed which areas were unimpaired, impaired by marine inundation, and impaired by groundwater inundation. These steps were then repeated under (a) each sea-level rise scenario and (b) each potential tidal amplitude change to produce ‘inundation maps’.

ArcGIS was also used to determine the thickness of the surficial aquifer across the island in order to understand the differences in diffusivity values that were determined during the calibration process. This was done by using well logs collected by Bogue Banks Water Corporation and using elevations of units and depths to the first confining layer to determine thickness. Understanding the thicknesses of the surficial aquifer can help explain extreme differences in diffusivity values because transmissivity is influenced by aquifer thickness and hydraulic conductivity. Also, contour maps showing the extent of tidal influence were produced in order to understand how groundwater levels would be impacted by tidal influence across the island (Appendix E).

RESULTS AND DISCUSSION

Sea-level rise versus groundwater pumping results

The results show that sea-level rise has a greater impact on saltwater intrusion than groundwater pumping (for equal movement of the toe of the saltwater wedge) (Figure 6). It should be noted that with each increment in sea-level rise, the area that is lost to the sea is due to both marine inundation and saltwater intrusion. Groundwater pumping, however, does not induce any marine inundation. So, when we compare the area lost due to sea-level rise to the area lost due to pumping, it is evident that sea-level rise has a greater impact because there is a 96% increase in area occupied by seawater from the baseline for the worst case scenario (i.e., sea-level rise of 1.6 m) (Table 1).

When pumping rates are 370,000 gallons per day, the toe of the saltwater wedge is in the same position as the case where sea-level rise is equal to 1.6 m. Under this pumping rate scenario, there is an increase in the area of the aquifer occupied by seawater by 65% from the baseline (Table 2). These results indicate that ~30% more aquifer becomes occupied with seawater due to 1.6 m of sea-level rise compared to the area occupied by seawater due to pumping at 370,000 gallons per day (Table 3).

According to data from the Central Coastal Plain Capacity Use Area (CCPCUA), a pumping rate of 400,000 gallons per day is equivalent to a small town’s water usage. An example of a small town that has this type of water usage is Washington, NC, with a population of ~10,000 residents (Census 2017). Areas with greater populations are expected to have higher demand for water, thus increased pumping rates to meet water demand would likely induce a greater movement of the toe of the saltwater wedge. This increased pumping rate would move the toe farther than that under a 1.6 m rise of sea-level. Appendix F shows the impacts of sea level rise from 0.2 m to 2 m.

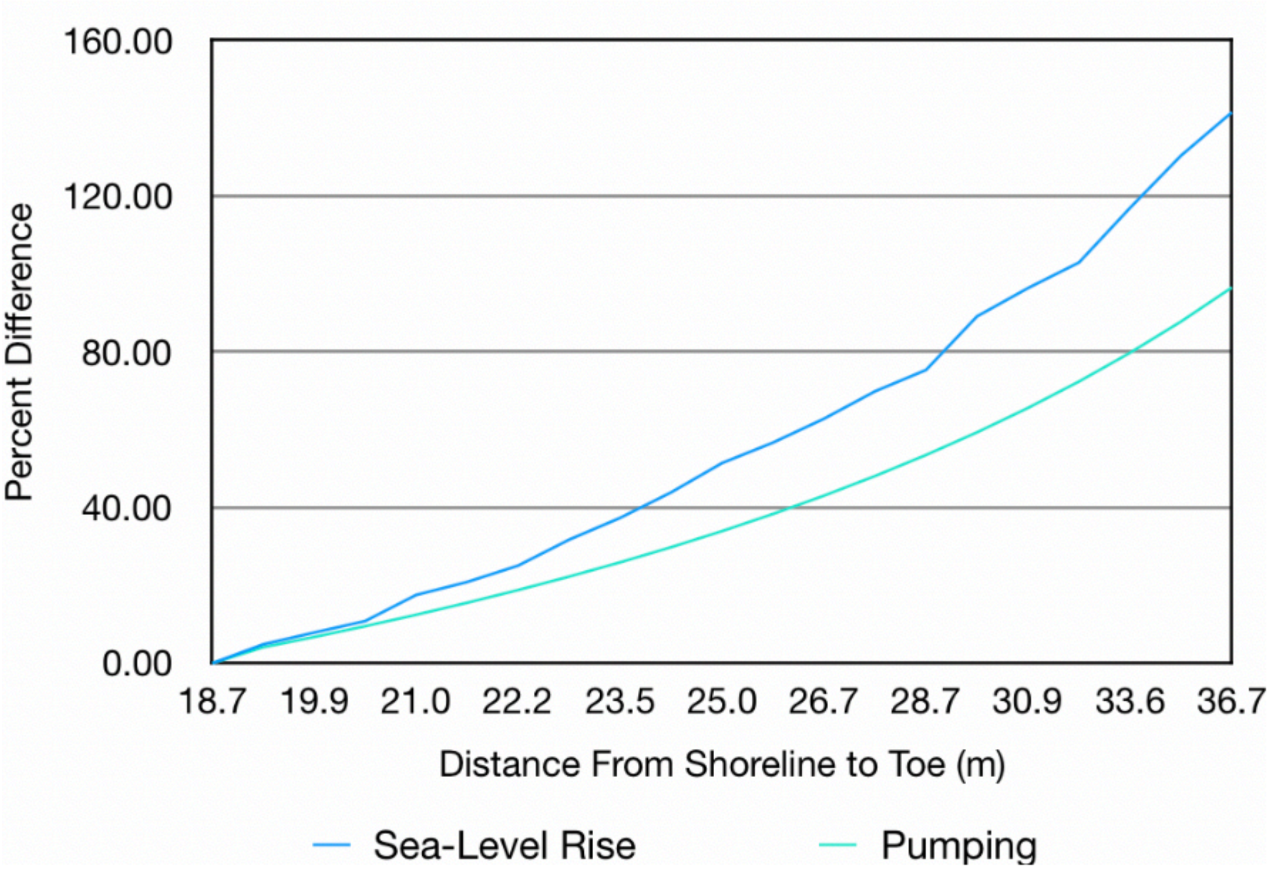

Figure 6: Percent difference in area occupied by seawater as a result of sea-level rise and groundwater pumping for equivalent distances of movement of the toe of the saltwater wedge.

Table 1: Changes in the area occupied by seawater as a result of sea-level rise (SLR).

SLR (m)	Distance from shoreline to toe (m)	Total area occupied by seawater (m^2)	Percent change in area occupied by seawater
0	18.7	102.71	0.00
0.2	19.9	110.81	7.88
0.4	21.0	120.73	17.54
0.6	22.2	128.47	25.07
0.8	23.5	141.06	37.33
1	25.0	155.53	51.42
1.2	26.7	167.23	62.81
1.4	28.7	180.08	75.33
1.6	30.9	201.68	96.35

Table 2: Changes in the area occupied by seawater as a result of groundwater pumping (GPD = gallons per day).

Distance from shoreline to toe (m)	Pumping rate (GPD)	Total area occupied by seawater (m^2)	Percent change in area occupied by seawater
18.7	0.00	*102.71*	*0.00*
19.9	45649	109.64	6.74
21.0	91298	115.50	12.45
22.2	136947	122.03	18.80
23.5	187160	129.33	25.92
25.0	228244	137.57	33.94
26.7	273893	146.93	43.05
28.7	319542	157.65	53.49
30.9	374321	170.07	65.58

The area of the of the saltwater wedge with no groundwater pumping

Table 3: Comparing impacts of sea-level rise and pumping on area occupied by seawater.

Distance from shoreline to toe (m)	Percent change in area occupied by seawater (SLR)	Percent change in area occupied by seawater (pumping)	Difference in area (SLR - pumping)
18.7	0.0	0.0	0.0
19.9	7.9	6.7	1.1
21	17.5	12.5	5.1
22.2	25.1	18.8	6.3
23.5	37.3	25.9	11.4
25	51.4	33.9	17.5
26.7	62.8	43.1	19.8
28.7	75.3	53.5	21.8
30.9	96.4	65.6	30.8

Sensitivity

Sensitivity analyses were performed to determine how varying the parameters of the Ferguson and Gleeson (2012) analytical model (Eq. 2) would change the results. This was necessary since there is a large range of possible values for each of the input parameters that would produce the same result. The conclusion from the sensitivity analysis is that with an increase in hydraulic conductivity, pumping rates would need to increase in order to move the toe of the saltwater wedge the same distance. An aquifer with higher hydraulic conductivity would require greater pumping rates to move the toe of the saltwater wedge the same distance because higher hydraulic conductivities would allow for greater amounts of freshwater to replace the pumped water. If the hydraulic conductivity value is lowered, it takes less pumping to move the base of the saltwater wedge because the lower hydraulic conductivity means there’s less flow of water replacing the freshwater that was removed.

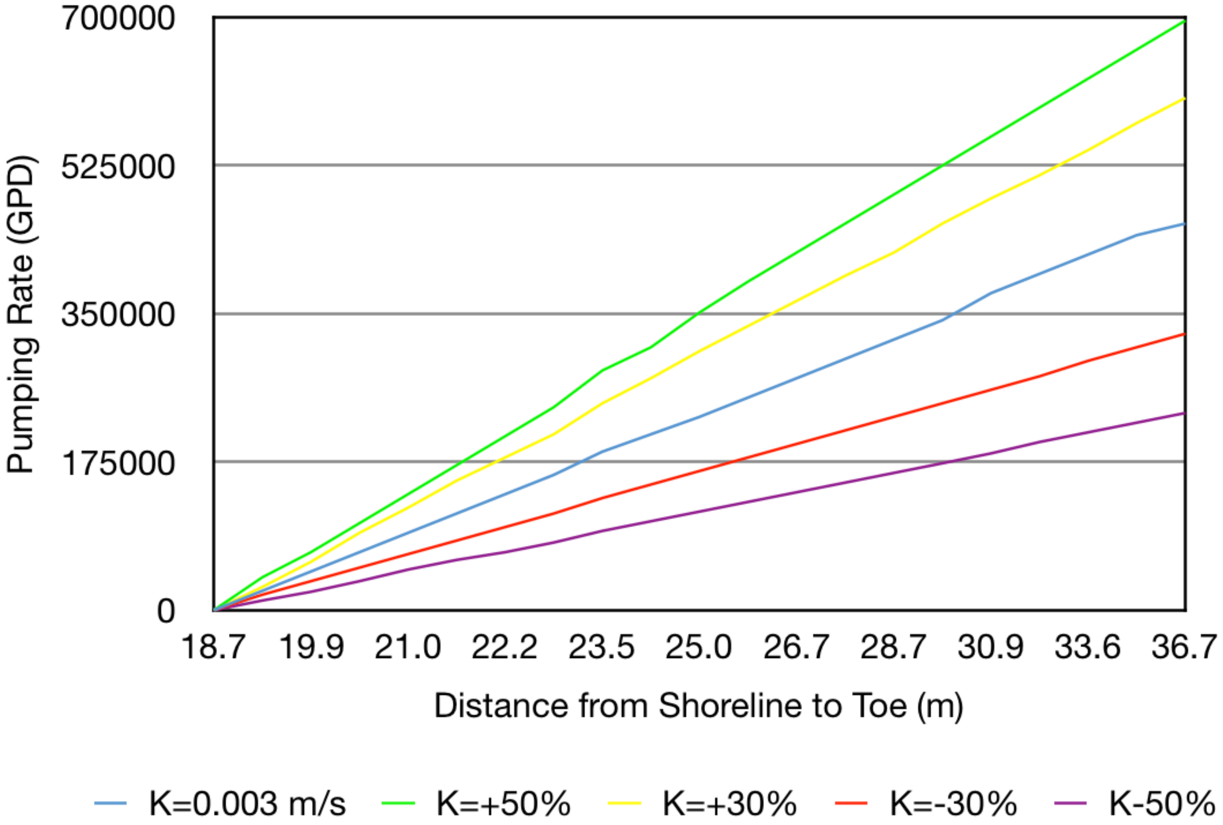

Figure 7: Results from sensitivity analysis showing rates of groundwater pumping required to move the toe of the saltwater wedge the same distance with different hydraulic conductivity

Evaluation of tidal influence results

The results also indicate that, as expected, tidal amplitudes in groundwater decrease in wells that are farther away from the shoreline. However, this observation is not always valid; water levels in some wells close to the shoreline did not exhibit any tidal influences whatsoever. Results from the calibration process reveal that tidal amplitudes in groundwater are no larger than 6 cm. At a distance of ~265 m from the shoreline, changes in groundwater levels in all wells due to tidal influence are not seen. More than half of the wells that did not show water table oscillations were farther than 200 meters from the shoreline. The wells located between 65 m and 200 m away from large water bodies experienced a mix of both large and small water table fluctuations in tidally influenced amplitudes. These results suggest that heterogeneities in the Surficial aquifer may affect the extent of tidal fluctuations in the aquifer (Figure 8).

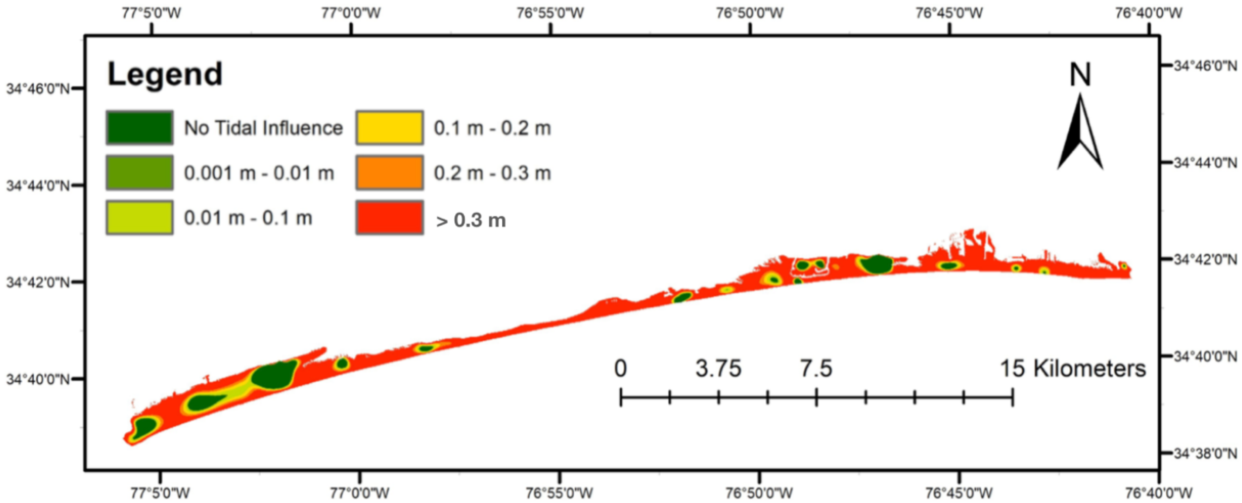

Figure 8: Observed tidal amplitudes on Bogue Banks, NC.

Several wells had significantly low diffusivity values and were located very close to the shoreline (wells OBB 04, 27, and 29) (Appendix A). This is because these wells had a greater abundance of clays and peat. This would greatly lower the hydraulic conductivity which in turn would lower transmissivity (assuming no change in the thickness of the aquifer) making diffusivity much lower. Another factor that would yield different diffusivity values is the thickness of the Surficial aquifer, which varies throughout the island. Logs from wells drilled by Bogue Banks Water Corporation showed that the thickness of the Surficial aquifer can vary from 10 to ~50 m. This difference in thickness would impact transmissivity values which would impact diffusivity values (Figure 9).

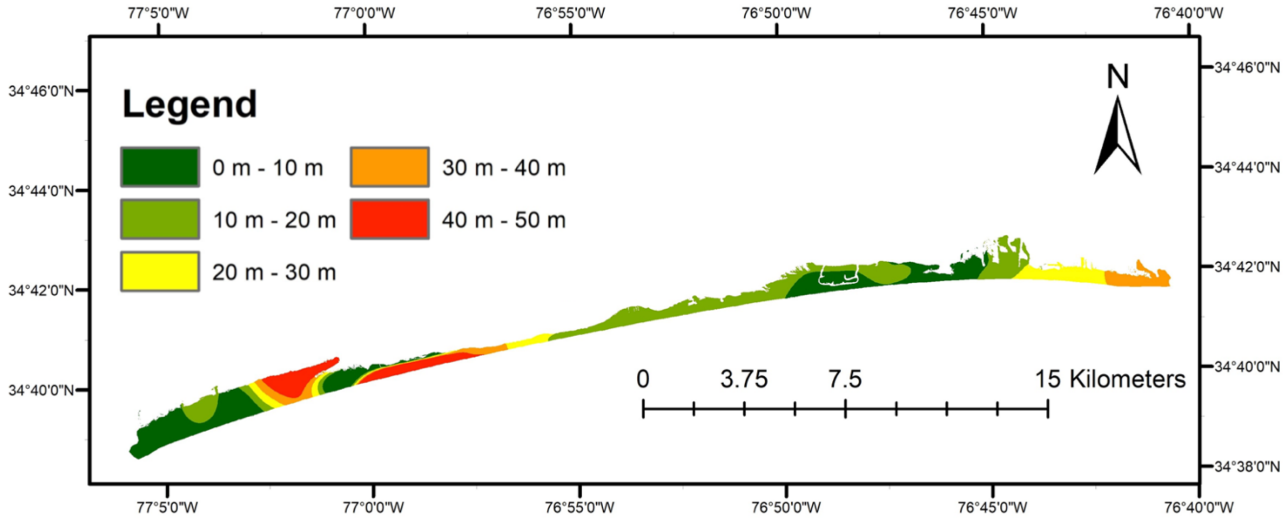

Figure 9: Map showing surficial aquifer thickness on Bogue Banks, NC.

Uncertainty

Due to inherent uncertainty in future conditions, all models should include estimates of uncertainty (Tartakovsky, 2013). One method of portraying uncertainty is a process called scenario modeling in which multiple forecasts are made to represent a range of possible outcomes (Anderson et al., 2015). Hard stabilization techniques would increase tidal amplitudes while soft stabilization techniques would cause a decrease. In this study, analysis of uncertainty is accomplished by performing forecasts from 0.2 m to 1.6 m of sea-level rise above the baseline (Jevrejeva et al., 2012, Rotzoll and Fletcher, 2012, Horton et al., 2014). To accommodate change due to mitigation techniques, tidal amplitudes were changed by +/-10% and +/- 20%. These changes would accompany each sea-level rise scenario depending on shoreline stabilization techniques to calculate marine and groundwater inundation. Uncertainty relating to pumping was modeled by using differences that the toe of the saltwater wedge would move at the base of the aquifer (Table 2).

Impact of changes in tidal amplitudes on groundwater and marine inundation

Marine inundation increases in severity as sea-level rises (Table 4). Marine inundation accounts for 57.2% of impaired land at 0.2 m of sea-level rise and 31.9% at 1.6 m of sea-level rise (Table 5). Tidal amplitudes may change with shoreline mitigation techniques by +/- 20%. Depending on the mitigation technique, this can impact the severity of marine inundation. With increased tidal amplitude, marine inundation becomes more severe and with a decrease, less severe (Figure 10). For the most severe sea-level rise scenario of 1.6 m, tidal amplitudes can change the amount of impaired land due to marine inundation by 5%. With a change in tidal amplitude of 10%, marine inundation would only change by 2-3%. Tidal amplitudes, however, don’t start impacting marine inundation until 0.6 m of sea level rise if tidal amplitudes are increased by 20%. If tidal amplitudes are increased by 10%, tidal amplitudes don’t measurably impact the amount of marine inundation until 0.8 m of sea-level rise. If there is a negative tidal amplitude change, it is not observed to make an impact until 0.8 m of sea-level rise (Figure 10). Tidal amplitude changes increase the severity of marine inundation because tidal forces are in direct contact with the shoreline, so any changes in amplitude would have a direct impact on the amount of land impaired by marine inundation.

Table 4: Surface area impaired by marine inundation under different sea-level and tidal amplitude scenarios.

Sea-level rise (m)	Area impaired by marine inundation (Km^2)	Area impaired by marine inundation if tidal amplitudes are increased 20% (Km^2)	Area impaired by marine inundation if tidal amplitudes are decreased 20% (Km^2)	Area impaired by marine inundation if tidal amplitudes are increased 10% (Km^2)	Area impaired by marine inundation if tidal amplitudes are decreased - 10% (Km^2)
0.2	2.03	2.03	2.03	2.03	2.03
0.4	3.35	3.35	3.35	3.35	3.35
0.6	3.88	4.41	3.88	3.88	3.88
0.8	4.41	5.67	4.41	5.04	4.41
1.0	5.67	6.51	5.04	5.67	5.04
1.2	6.51	7.34	5.67	6.51	5.67
1.4	7.34	9.00	6.51	8.17	6.51
1.6	9.00	10.32	7.34	9.66	8.17

Table 5: Percent of surface area impaired by marine inundation under different sea-level and tidal amplitude scenarios.

Sea-level rise (m)	Percent of area impaired due to marine inundation	Percent of area impaired by marine Inundation if tidal amplitudes are increased 20%	Percent of area impaired by marine inundation if tidal amplitudes are decreased - 20%	Percent of area impaired by marine inundation if tidal amplitudes are increased 10%	Percent of area impaired by marine inundation if tidal amplitudes are decreased 10%
0.2	7.2%	7.2%	7.2%	7.2%	7.2%
0.4	11.9%	11.9%	11.9%	11.9%	11.9%
0.6	13.8%	15.6%	13.8%	13.8%	13.8%
0.8	15.6%	20.1%	15.6%	17.9%	15.6%
1.0	20.1%	23.1%	17.9%	20.1%	17.9%
1.2	23.1%	26.0%	20.1%	23.1%	20.1%
1.4	26.0%	31.9%	23.1%	29.0%	23.1%
1.6	31.9%	36.6%	26.0%	34.3%	29.0%

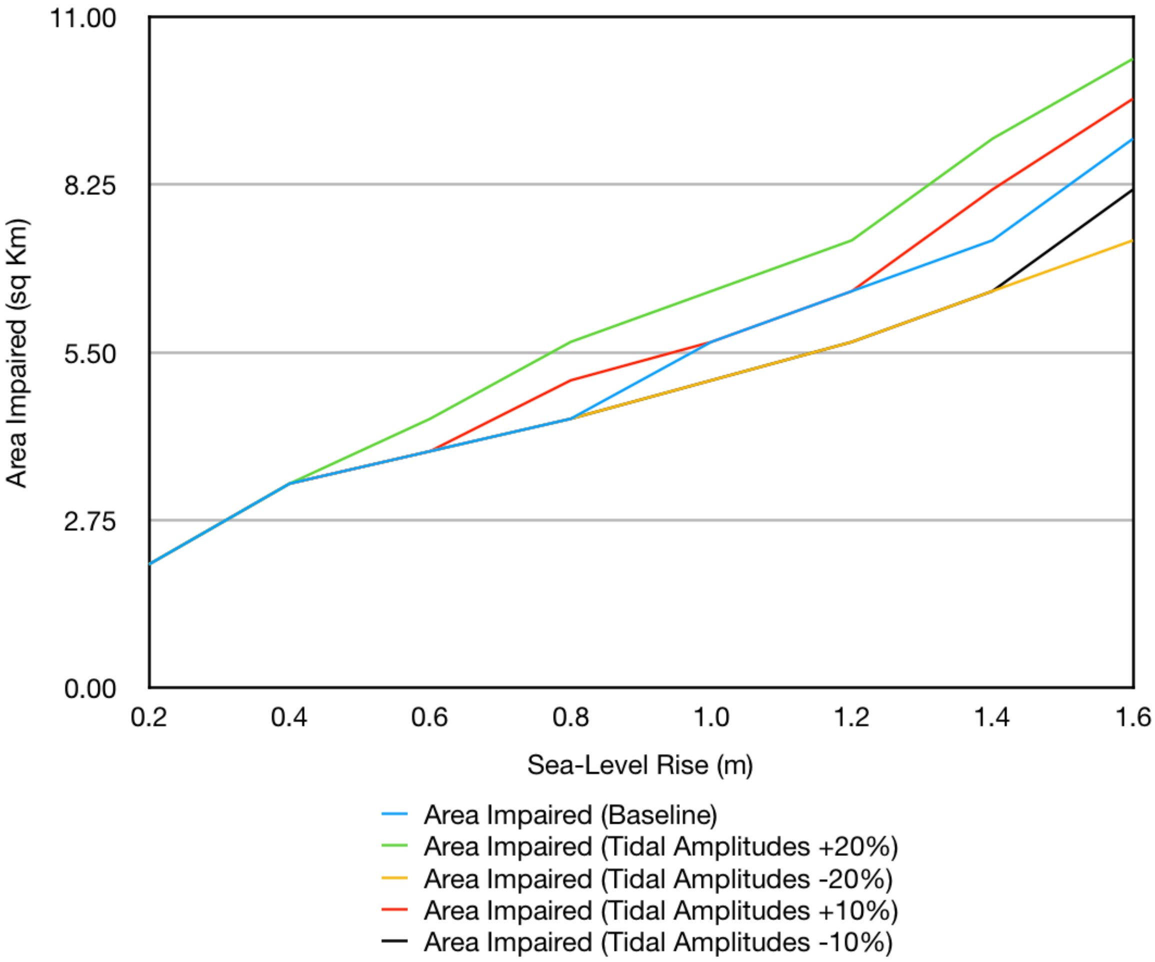

Figure 10: The amount of land impaired by marine inundation under different sea-level rise scenarios and tidal amplitudes.

Groundwater inundation would cause greater impairment of land on Bogue Banks than marine inundation in all SLR scenarios (Table 6). At 0.2 m of sea-level rise groundwater impairment makes up 36.8% of total impairment while marine inundation only makes up 7% (Table 7). Changes in tidal amplitudes do not appear to cause a lot of change in the amount of land impaired by groundwater inundation. At the most extreme scenario of 1.6 m of sea-level rise and tidal amplitude change at plus or minus 20%, groundwater impairment only changes by 2%. This is because only 10 of the 29 wells experienced changes in tidal amplitude so parts of the island would not experience amplitude changes in the groundwater because after 260 m from the shoreline, changes in tidal amplitudes are not seen. Also, if changes in tidal amplitudes are equal to 10% or less, they do not appear to change the amount of groundwater impairment (Figure 11). This can be because observed amplitudes were very small, being no bigger than 6 cm, so changes of only 10% would not be significant. At the most extreme sea-level rise scenario of 1.6 m, groundwater inundation makes up 50% of all impaired land.

Table 6: Surface area impaired by groundwater inundation under different sea-level rise scenarios and tidal amplitudes.

Sea-level rise (m)	Area impaired by groundwater inundation (km^2)	Area impaired by groundwater inundation if tidal amplitudes are increased 20% (km^2)	Area impaired by groundwater inundation if tidal amplitudes are decreased 20% (km^2)	Area impaired by groundwater inundation if tidal amplitudes are increased 10% (km^2)	Area impaired by groundwater inundation if tidal amplitudes are decreased 10% (km^2)
0.2	10.38	11.13	10.18	11.05	10.28
0.4	11.43	11.59	11.29	11.43	11.36
0.6	11.87	12.16	11.59	11.87	11.73
0.8	12.35	12.70	11.97	12.35	12.16
1.0	12.79	13.24	12.35	12.79	12.79
1.2	13.24	13.75	12.69	13.24	13.24
1.4	13.67	14.24	13.08	13.67	13.67
1.6	14.09	14.66	13.42	14.09	14.09

Table 7: Percent of surface area impaired by groundwater inundation under different sea-level rise scenarios and tidal amplitudes.

Sea-level rise (m)	Percent of area impaired due to groundwater inundation	Percent of area impaired by groundwater inundation if tidal amplitudes are increased 20%	Percent of area impaired by groundwater inundation if tidal amplitudes are decreased 20%	Percent of area impaired by groundwater inundation if tidal amplitudes are increased 10%	Percent of area impaired by groundwater inundation if tidal amplitudes are decreased 10%
0.2	36.8%	39.5%	36.1%	39.2%	36.5%
0.4	40.5%	41.1%	40.0%	40.5%	40.3%
0.6	42.1%	43.1%	41.1%	42.1%	41.6%
0.8	43.8%	45.0%	42.4%	43.8%	43.1%
1.0	45.4%	46.9%	43.8%	45.4%	45.4%
1.2	46.9%	48.8%	45.0%	46.9%	46.9%
1.4	48.5%	50.5%	46.4%	48.5%	48.5%
1.6	50.0%	52.0%	47.6%	50.0%	50.0%

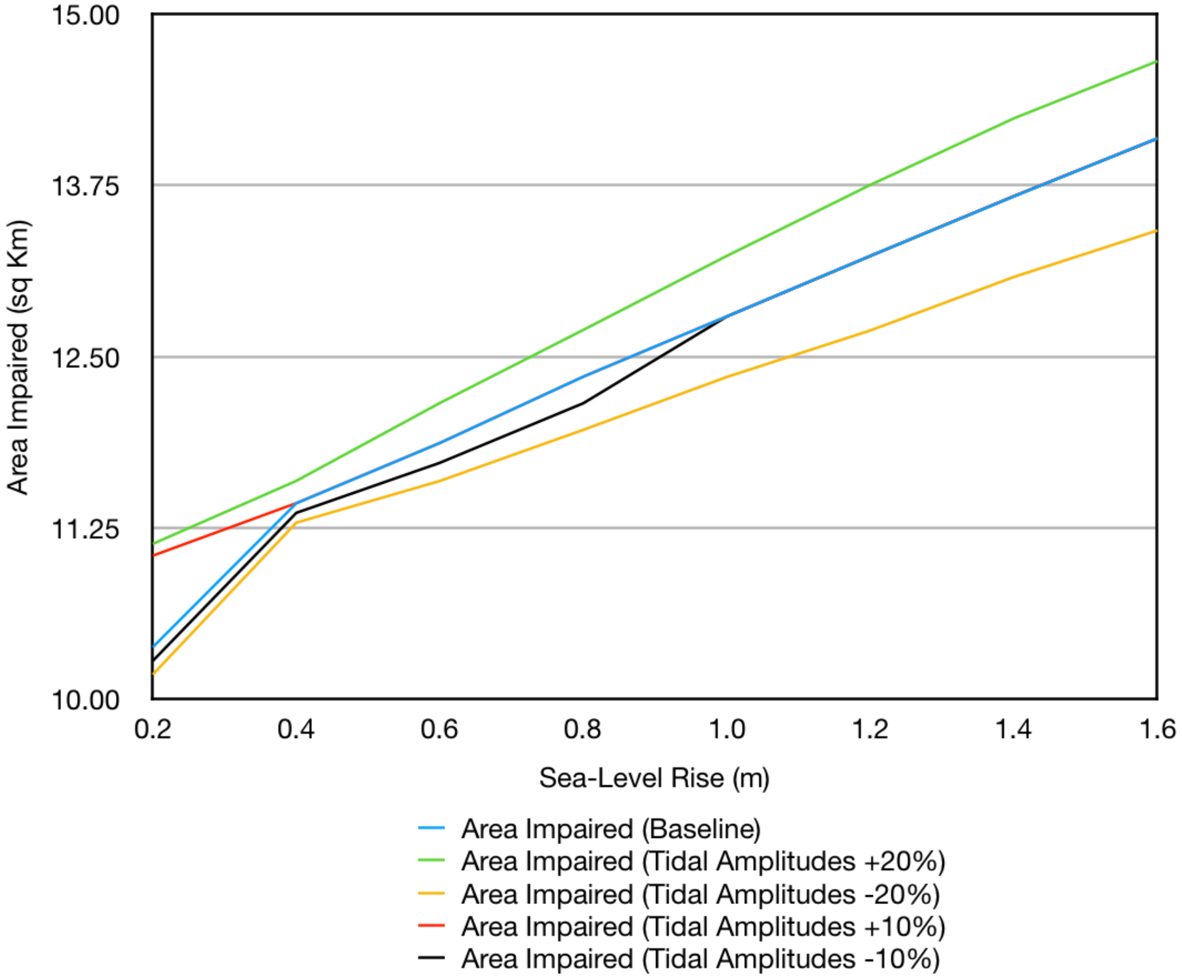

Figure 11: The amount of land impaired by groundwater inundation under different sea-level rise scenarios and tidal amplitudes.

Impairment due to marine plus groundwater inundation will become an issue with sea-level rise (Table 8). Under ideal scenarios of 0.2 m of sea-level rise, impairment is at 44%. At the most severe scenarios with 1.6 m of sea-level rise, the total amount of impaired land rises to 82% (Table 9). Most of the impairment in both of these scenarios is due to groundwater inundation. Changes in tidal amplitudes can also increase or decrease the amount of impaired land (Figure 12). With changes of 20% to tidal amplitudes, there is an increase or decrease of 7% of the amount of land impaired; 5% contributed from marine inundation and 2% from groundwater inundation. With changes of 10% to tidal amplitudes there is an increase or decrease of 2-5%; with most of it contributed by Groundwater inundation.

Table 8: Total surface area impaired by both marine and groundwater inundation under different sea-level rise scenarios and tidal amplitudes.

Sea-level rise (m)	Total impaired due to inundation (km^2)	Total area impaired by Inundation if tidal amplitudes are increased 20% (km^2)	Total area impaired by inundation if tidal amplitudes are decreased 20% (km^2)	Total area impaired by inundation if tidal amplitudes are increased 10% (km^2)	Total area impaired by inundation if tidal amplitudes are decreased 10% (km^2)
0.2	12.41	13.16	12.21	13.07	12.31
0.4	14.78	14.94	14.64	14.78	14.71
0.6	15.75	16.57	15.47	15.75	15.61
0.8	16.77	18.37	16.38	17.40	16.57
1.0	18.47	19.74	17.39	18.47	17.84
1.2	19.74	21.09	18.36	19.74	18.91
1.4	21.01	23.24	19.59	21.41	20.18
1.6	23.10	24.97	20.76	23.75	21.84

Table 9: Percent of total surface area impaired by both marine and groundwater inundation under different sea-level rise scenarios and tidal amplitudes.

Sea-level rise (m)	Percent of area impaired due to inundation	Percent of area impaired by inundation if tidal amplitudes are increased 20%	Percent of area impaired by inundation if tidal amplitudes are decreased 20%	Percent of area impaired by Inundation if tidal amplitudes are increased 10%	Percent of area impaired by inundation if tidal amplitudes are decreased 10%
0.2	44.0%	46.7%	43.3%	46.4%	43.6%
0.4	52.4%	53.0%	51.9%	52.4%	52.2%
0.6	55.9%	58.8%	54.9%	55.9%	55.3%
0.8	59.5%	65.1%	58.1%	61.7%	58.8%
1.0	65.5%	70.0%	61.7%	65.5%	63.2%
1.2	70.0%	74.8%	65.1%	70.0%	67.0%
1.4	74.5%	82.4%	69.5%	75.9%	71.5%
1.6	81.9%	88.5%	73.6%	84.2%	77.5%

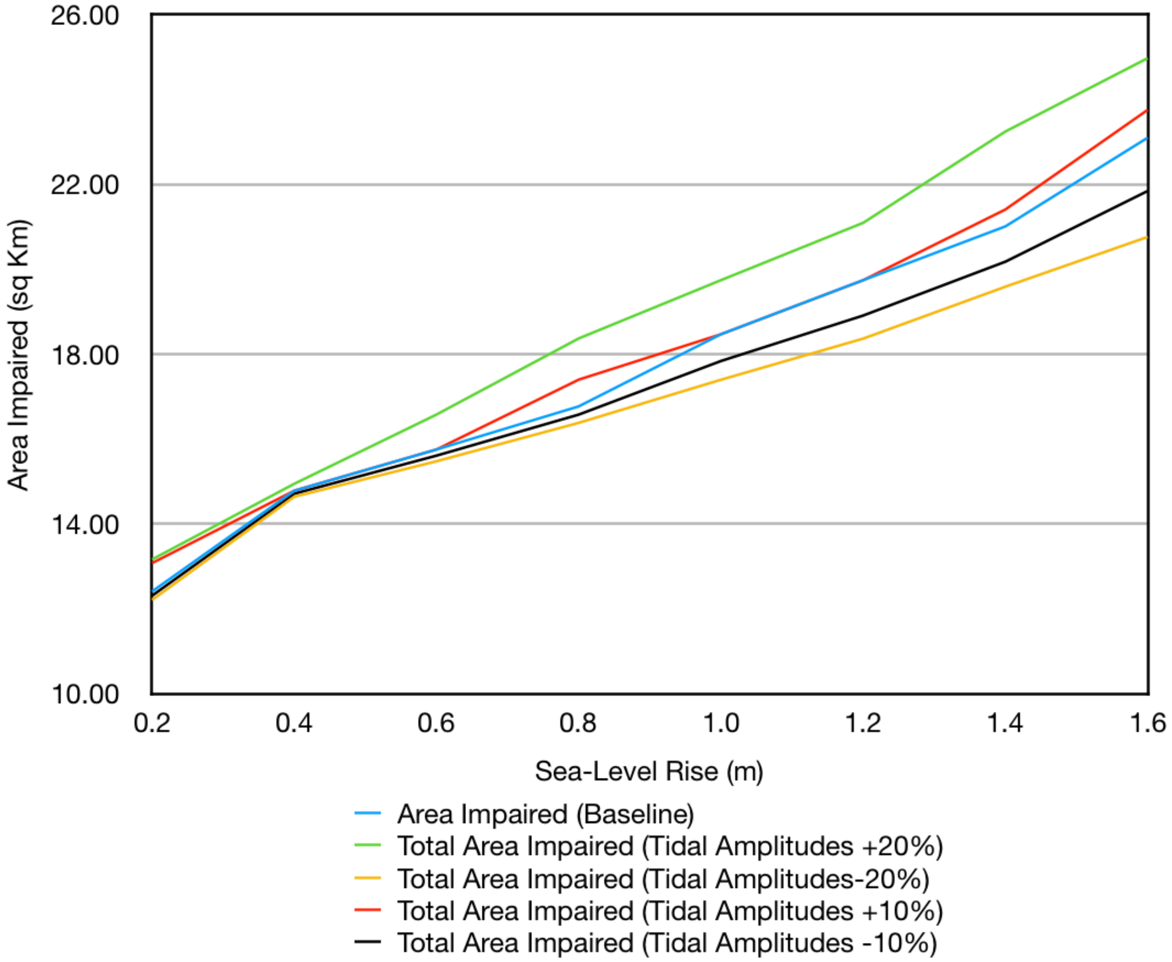

Figure 12: The total amount of land impaired by groundwater and marine inundation under different sea-level rise scenarios and tidal amplitudes.

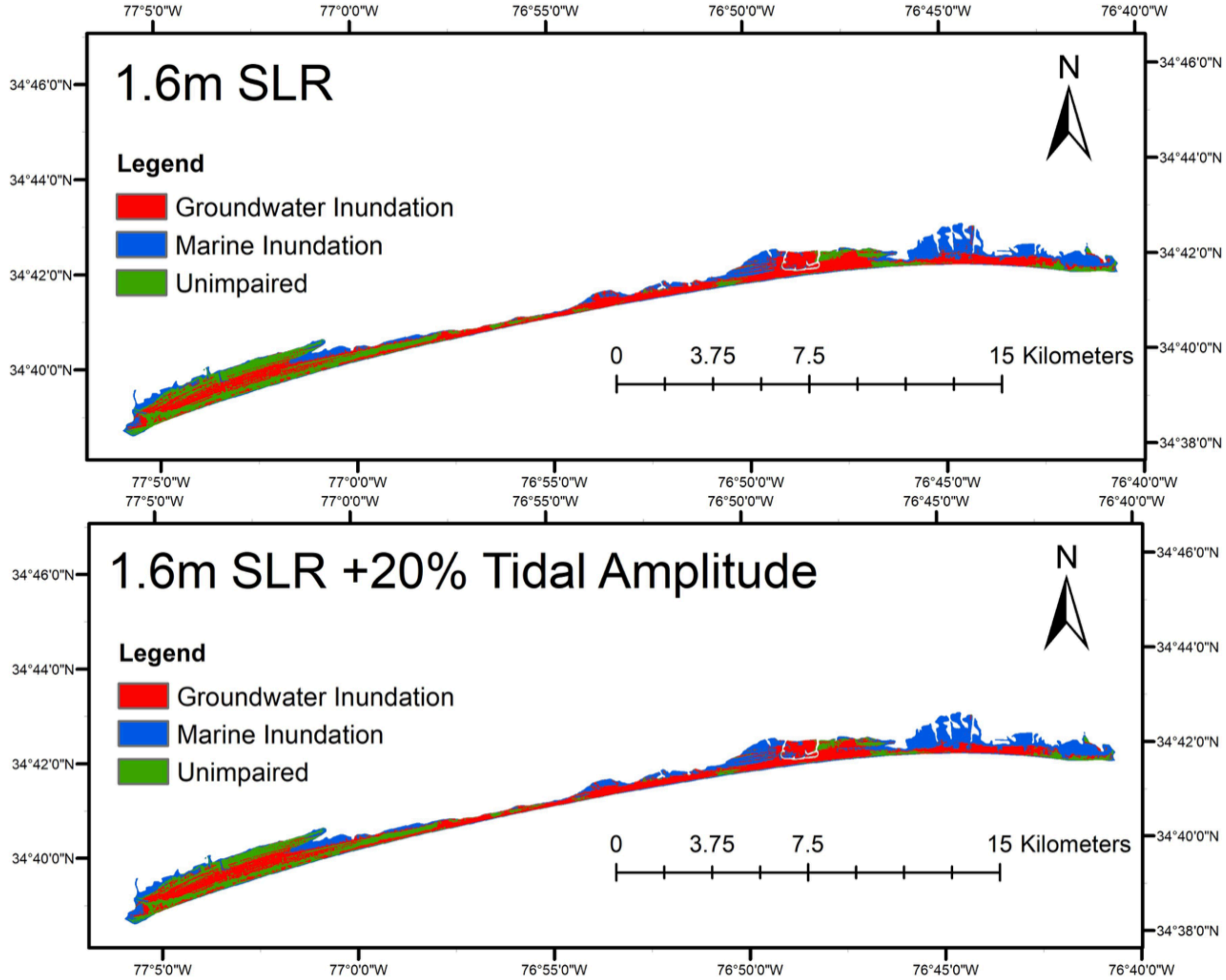

Figure 13: Examples of inundation maps comparing 1.6 m of sea-level rise and 1.6 m of sea-level rise +20% tidal amplitude. There is only a 5% increase in marine inundation and 2% groundwater inundation when increasing tidal amplitude. All other maps can be seen in Appendix G.

Marine inundation causes less land impairment but is most susceptible to tidal amplitude changes. Groundwater inundation causes more land impairment but is least susceptible to tidal amplitude changes (Figure 13). This research is important in understanding how future mitigation practices will affect how tides may change inundation amount. Understanding how different coastal mitigation techniques may change tidal amplitudes by up to 20% can help city managers understand possible outcomes for certain mitigation techniques (Cai et al., 2012, Lee et al., 2017). This study can also help environmental managers understand the threat of sea-level rise and how it may impact coastal communities.

Assumptions and limitations

One assumption made during this study is that sea-level will rise consistently even though rates have changed in the past (Dean and Huston, 2013, Lavelle-Levinson et al., 2017). Climate change may influence these rates in the next 100 years. Another assumption is that the island of Bogue Banks is assumed to remain in its current location due to anthropogenic actions. Barrier islands in a natural system, would move 1000 feet landward for 1 foot of sea-level rise (Pilkey et al., 1980). The surficial aquifer is assumed to be a flux controlled system meaning that the hydraulic gradient for the groundwater system remains constant with sea-level rise, i.e., the water table is translated upwards (Ketabchi et al., 2016). Several parameters are assumed to be constant over the duration of the 100-year simulation period (e.g., evapotranspiration, recharge, wind speed, temperature etc.). However, these attributes may change as a result of climate change. Another possible consequence of climate change is a change in precipitation rates as well as possible meteorological extremes. These meteorological extremes can cause greater or more frequent storm surges which can increase saltwater intrusion as well as marine and groundwater inundation. A decrease in precipitation due to droughts may decrease groundwater inundation if evapotranspiration can be maintained.

The pumping well location to evaluate sea-level rise and groundwater pumping was chosen because it was close to the center of the island. Wells that are placed close to the shoreline or clustered closely together can increase the amount of saltwater intrusion. Thus, the simulated pumping well is assumed to not have any influence from other pumping wells.

Furthermore, the aquifer in which this simulated well is screened is assumed to not receive any recharge from lower leaky confining units, or recharge from on-site wastewater treatment systems.

SUMMARY AND CONCLUSIONS

This study is one of a few that seeks to understand the impacts of sea-level rise on the groundwater system on a barrier island. Sea-level rise will be a significant threat to coastal communities over the next century, so it is important to assess the impacts to mitigate future problems. Changes in depth and friction caused by different mitigation techniques can cause changes in tidal amplitudes. Hard stabilization techniques would increase tidal amplitudes while soft stabilization techniques would cause a decrease in tidal amplitudes (Cai at al., 2012, Lee et al., 2017).

The results of this study show that sea-level rise has the potential to pose a major threat to coastal communities. Sea-level rise has a bigger impact on saltwater intrusion than groundwater pumping for equal distance that the saltwater toe moves inland (when one compares the area occupied in the subsurface by seawater due to sea level rise). Sea-level rise induces a greater amount of saltwater intrusion as shown by the area in the subsurface which was occupied by seawater (40% higher than due to pumping when the toe of the saltwater wedge moved the same distance). However, because a pumping rate of 370,000 gallons per day would move the toe of the saltwater wedge the same distance as 1.6 m of sea-level rise, areas with greater populations would have different results because water demand would be much higher. Also 1.6 m sea-level rise is an extreme case of sea-level rise and is less likely to occur than a pumping rate of 370,000 gallons per day.

Tidal amplitudes influence groundwater levels. Data collected from twenty-three wells were examined for tidal influence. Tidal influence tends to decrease farther from the shoreline but several wells which were close to the shoreline didn’t show any tidal influence. This may have occurred because of clay and peat layers which were observed in logs of cores. Tidal amplitudes can vary with changes in sea-level depending on shoreline mitigation techniques. Mitigation techniques may change tidal amplitudes because tidal amplification occurs with change in water depth which in turn influence frictional forces. Soft beach stabilization can potentially lower tidal amplitudes because this stabilization practice decreases water depth which would increase frictional forces. In contrast, hard beach stabilization practices increase water depth which decreases frictional forces thereby increasing tidal amplification.

Groundwater inundation causes greater land impairment than marine inundation. Under a sea-level rise of 1.6 m, groundwater inundation causes 50% of land impairment while marine impairment causes 30%. Different studies indicate a change of plus or minus twenty percent of tidal amplification with an increase in sea-level of two meters (e.g., Hollman and Stacey, 2014., Cai et al, 2012). Tidal amplitudes can change the amount of land impaired by both marine and groundwater inundation. Tidal amplitudes have a larger impact on the amount of land impaired by marine inundation because with 1.6 m of sea-level rise, there can be a change of impaired land by up to 5%. Tidal amplitudes, however, don't have much of an impact on the amount of land impaired due to groundwater inundation. With the most severe scenarios, tidal amplitudes only change the amount of impaired land due to groundwater inundation by up to 2%. However, both groundwater and marine inundation can change the amount of impaired land by up to 7%. Mitigation techniques such as soft beach stabilization would decrease the amount of impaired land significantly (7% less impairment or 2.34 Km^2). Mitigation techniques such as hard beach stabilization my increase impairment by 6% (1.87 Km^2). Knowing how tidal amplitudes may change with sea-level rise allows city planners to better understand what land may become impaired due to inundation and how to better protect coastal communities from environmental changes. Local and state governments should implement strategies including public outreach, adapting to changing conditions, migration, preserving undeveloped land, and financial incentives to be proactive in flood management.

Soft beach stabilization practices (e.g., beach nourishment) should be considered by coastal communities to reduce inundation caused by tidal amplitudes. Reducing tidal amplitudes would decrease the likelihood of both marine and groundwater inundation. Soft beach stabilization practices would reduce tidal amplitudes by decreasing depth. Hard beach stabilization practices (e.g., seawalls) would increase tidal amplitudes increasing the likelihood of both marine and groundwater inundation. Seawalls, depending on material and extent in coastal environments may impact tidal influence observed in groundwater. understanding how seawalls impact tidal influence in groundwater can expand this study.

Future work to build off this study would be to address the constrains placed on the analysis by the assumptions made in this study. For example, seasonal changes in the water table, temperature, precipitation, and evapotranspiration should be incorporate in the model. Because precipitation rates in the North Carolina coastal plain vary seasonally (Sayemuzzaman and Jha, 2014), preforming this experiment using various recharge rates will provide a better understanding of the hydrodynamics of Bogue Banks.

REFERENCES

Anderson, M. P., Woessner, W.H., and Randall J., 2015, Applied groundwater modeling: Simulation of flow and advective transport. Academic Press: San Diego, 2015, 384 p.

Bales, J.D., Chapman, M.J., Oblinger, C.J., Robbins, J.C., 2004, North Carolina District Science Plan Science Goals for 2003-2008, U.S. Geological Survey OFR 2004-1025, https://nc.water.usgs.gov/reports/ofr041025/report.html.

Cai, H., Savenije, H. G., Toffolon, M., 2012, A new analytical framework for assessing the effect of sea-level rise and dredging on tidal damping in estuaries: Journal of geophysical research vol 117, C09023, doi:10:10.1029/2012JC008000, 2012.

Carol, E. S., Kruse, E. E., Pousa, J. L., Roig, A. R., 2008, Determination of heterogeneities in hydraulic properties of a phreatic aquifer from tidal level fluctuations: a case in Argentina. Hydrology Journal (2009) 17: 1727-1732

Dean, R. G., Houston, J. R., 2013, Recent sea level trends and accelerations: Comparison of tide gauge and satellite results: Coastal Engineering 75 (2013) pg4-9

Ferguson, G., and Gleeson, T., 2012, Vulnerability of coastal aquifers to groundwater use and climate change: Nature Climate Change, v. 2, p. 342-345.

Freeze, A. R., Cherry, A. J, 1979, Groundwater: Prentice-Hall Inc, Englewood Cliffs, New Jersey 07632.

Habel, S., Fletcher, C. H., Rotzoll, K., El-Kadi, A. I., 2017, Development of a model to simulate groundwater inundation induced by sea-level rise and high tides in Honolulu, Hawaii: water research 114 (2017) 122-134.

Heath, R.C., 1983, Basic Ground-Water Hydrology: USGS Water-Supply Paper 2220, 86p.

Holleman, R. C., Stacey, M. T., 2014, Coupling of Sea Level Rise, Tidal Amplification, and Inundation: Journal of Physical Oceanography; Boston Vol. 44, Iss 5, (May 2014)

Horton B.P., Rahmstorf, S., Engelhart, S.E., and Kemp, A.C., 2014, Expert assessment of sea-level rise by AD 2100 and AD 2300: Quaternary Science Reviews, v. 84, p. 1–6.

Jevrejeva, S., Moore, J.C., and Grinsted, A., 2012, Sea level projections to AD2500 with a new generation of climate change scenarios, Global and Planetary Change, v. 80–81. p. 14–20.

Ketabchi, H., Mahmoodzadeh, D., Ataie-Ashtiani, B., Simmons, C. T., 2016, Sea-level rise impacts on seawater intrusion in coastal aquifers: Review and integration: Journal of Hydrology 535 (2016) 235-255

Lavelle-Levinson, A., Dutton, A., Martin, J.B., 2017, Spatial and temporal variability of sea level rise hot spots over the eastern United States: Geophysical Research Letters, v.44, p. 7876-7882, doi: 10.1002/2017GLO73926.

Lautier, J. C., 2001, Hydrogeologic framework and ground water condition in the North Carolina Central Coastal Plain: North Carolina Department of Environment and Natural Resources, Division of Water Resources.

Lee, S. B., Li, M., Zhang, F., 2017, Impact of sea level rise on tidal range in Chesapeake and Delaware Bays: Journal of Geophysical Research: Oceans, AGU Publications.

Manda, A.K., Sisco, M.S., Mallinson, D.J., Griffin, M.T., 2014, Relative role and extent of marine and groundwater inundation on a dune-dominated barrier island under sea-level rise scenarios: Hydrological Processes, 11p. doi: 10.1002/hyp.10303.

Masterson, J.P., and Garabedian, S.P., 2007, Effects of sea-level rise on ground water flow in a coastal aquifer system: Ground Water, v. 45, p. 20,209-217.

Masterson, J.P., Fienen, M.N., Thieler, E.R., Gesch, D. B., Gutierrez, B.T., and Plaint, N.G., 2013a, Effects of sea level rise on barrier island groundwater system dynamics-Ecohydrological implications: Ecohydrology, v.7, 1064–1071. doi: 10.1002/eco.1442

Masterson, J.P, Fienen, M.N., Gesch, D.B., and Carlson, C.S., 2013b, Development of a numerical model to simulate groundwater flow in the shallow aquifer system of Assateague Island, Maryland and Virginia, U.S. Geological Open-File Report 2013-1111. http://pubs.usgs.gov/of/2013/1111/.

National Oceanographic and Atmospheric Administration, NOAA Tides and Currents Station Selection: 8656483 Beaufort, Duke Marine Lab, NC https://tidesandcurrents.noaa.gov/datums.html?units=1&epoch=0&id=8656483&name=Beaufort&state=NC (accessed October, 2019).

Owers M.S., 2017, Modeling Groundwater Inundation Under Climate Change Scenarios In the Surficial Aquifer Of Bogue Banks, North Carolina, [M.S. Thesis]: Greenville, NC, East Carolina University.

Parker, G. G., Stringfield, V. T., 1950, Effects of Earthquakes, Trains, Tides, Winds, and Atmospheric Pressure Changes on Water in the Geologic Formations of Southern Florida: Economic Geology, v. 45, pg. 441-460, Society of Economic Geologists Inc.

Pilkey Jr., O.H., Neal, W.J., Pilkey Sr., Orrin H., and Riggs, S.R., 1980, From Currituck to Calabash: Living with North Carolina's barrier islands, Second Edition. North Carolina Science and Technology Research Center.

Ross, A. C., Najjar, R. G., Li, M., Lee, S. B., Zhang, F., Liu, W., 2017, Fingerprints of Sea Level Rise on Changing Tides in the Chesapeake and Delaware Bays: Journal of Geophysical Research: Oceans, AGU Publications.

Rotzoll, K., and Fletcher, C.H., 2012, Assessment of groundwater inundation as a consequence of sea-level rise: Nature Climate Change. doi: 10.1038/NCLIMATE1725.

Sayemuzzaman, M., Jha, M.K., 2014, Seasonal and annual precipitation time series trend analysis in North Carolina, United States: Atmospheric Research, v. 137, p.183-194, https://doi.org/10.1016/j.atmosres.2013.10.012

Sisco, M.S., 2013, Assessing the shallow groundwater system as a potential factor in generating storm-water runoff on a North Carolina barrier island [M.S. thesis]: Greenville, NC, East Carolina University.

Sukop, M. C., Rodgers, M., Guannel, G., Infanti, J. M., Hagemann, K., 2017, High temporal resolution modeling of the impact of rain, tides, and sea level rise on water table flooding in the Arch Creek basin, Miami-Dade County Florida USA: Science of the Total Enviornment.

Tartakovsky, D.M., 2013. Assessment and management of risk in subsurface hydrology: A review and perspective: Advances in Water Resources, v. 51, p.247-260. http://dx.doi.org/10/1016/j.advwatres.2012.04.007.

Timmons, E.A., Rodriguez, A.B., Mattheus, C.R., and Dewitt, R., 2010, Transition of a regressive to a transgressive barrier island due to back-barrier erosion, increased storminess, and low sediment supply: Bogue Banks, North Carolina, USA: Marine Geology, v. 278, p. 100-114.

Winner Jr, M.D., and Coble, R.W., 1996. Hydrogeologic framework of the North Carolina coastal plain. U.S. Geological Survey Professional Paper 1401-1.

APPENDICES

A- Location of observations wells on Bogue Banks, NC

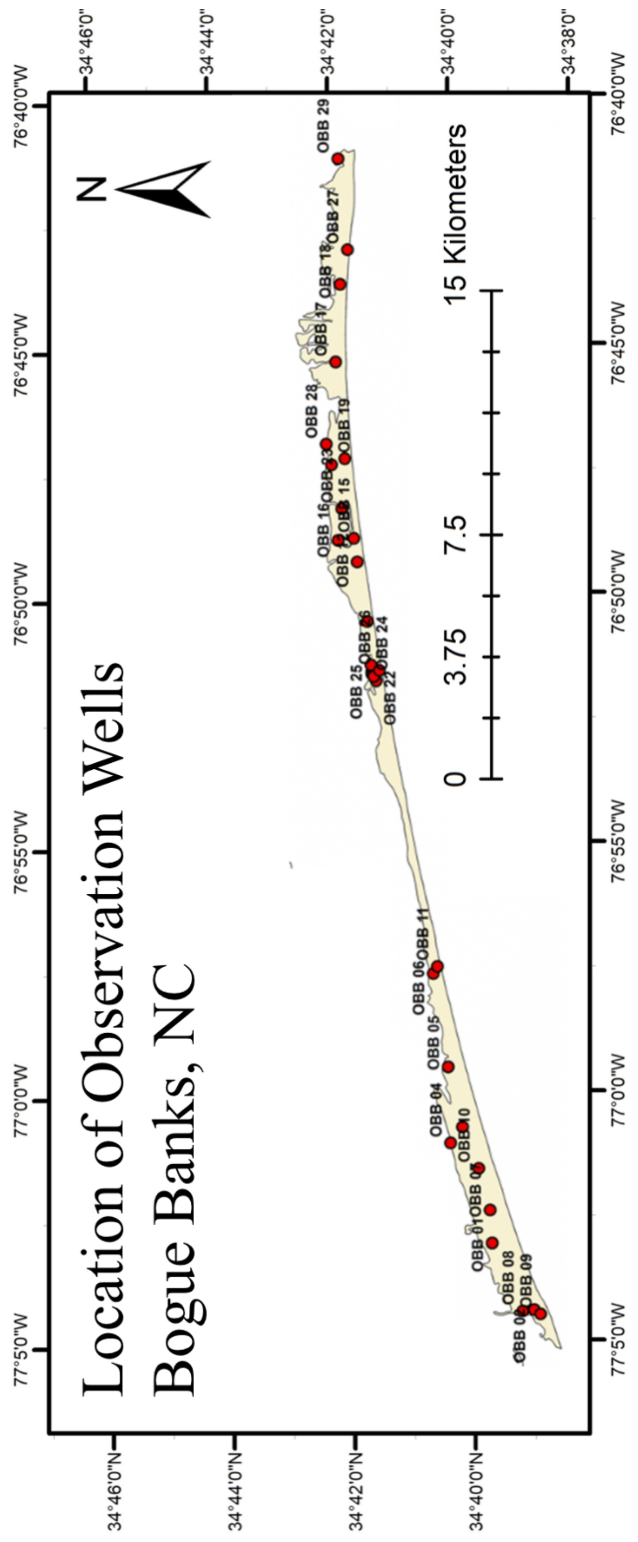

B - Well segments which show tidal influence

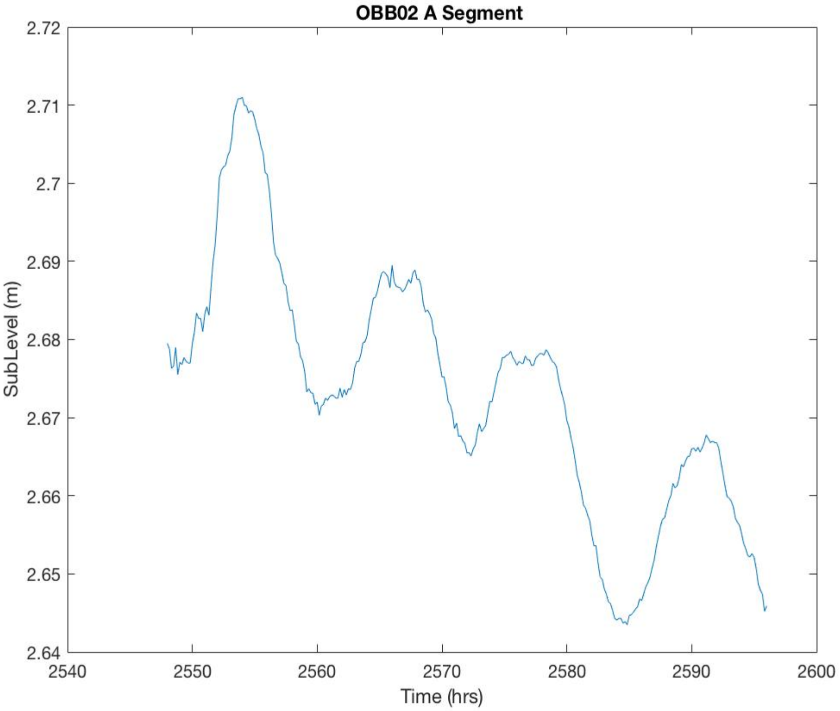

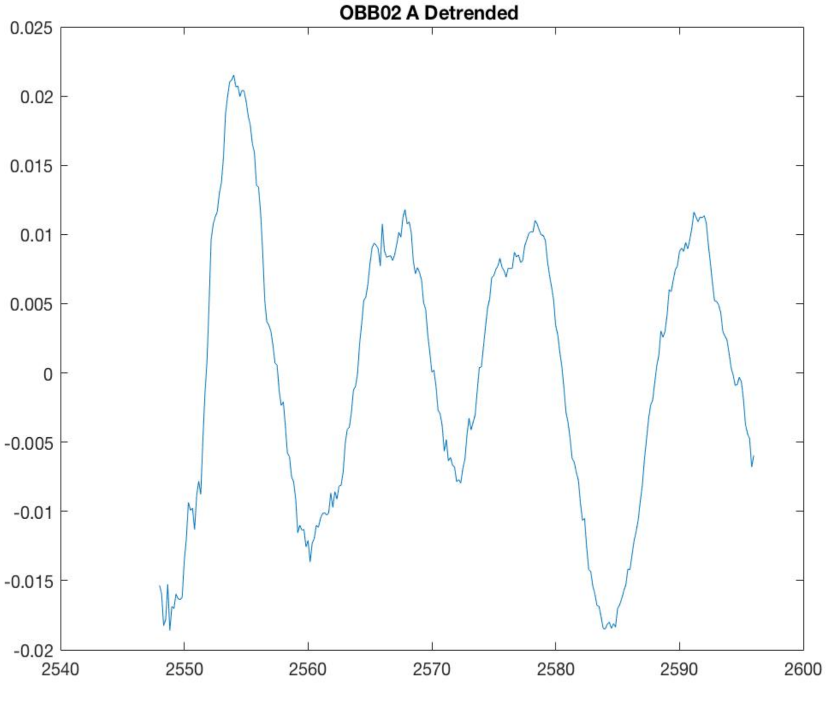

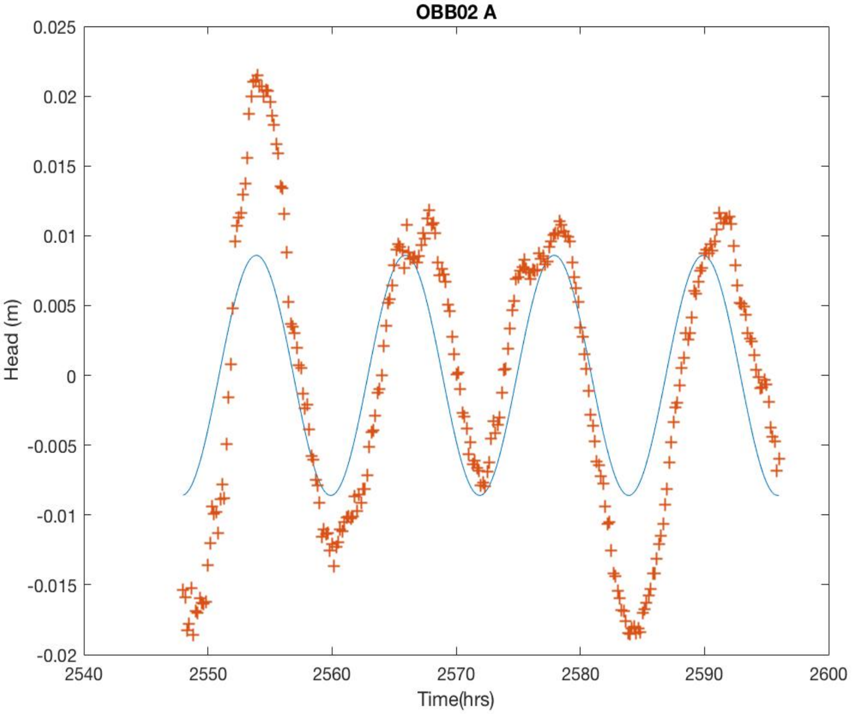
OBB02 A
Head (m)
Time(hrs)
0.025
0.02
0.015
0.01
0.005
0
-0.005
-0.01
-0.015
-0.02
2540
2550
2560
2570
2580
2590
2600

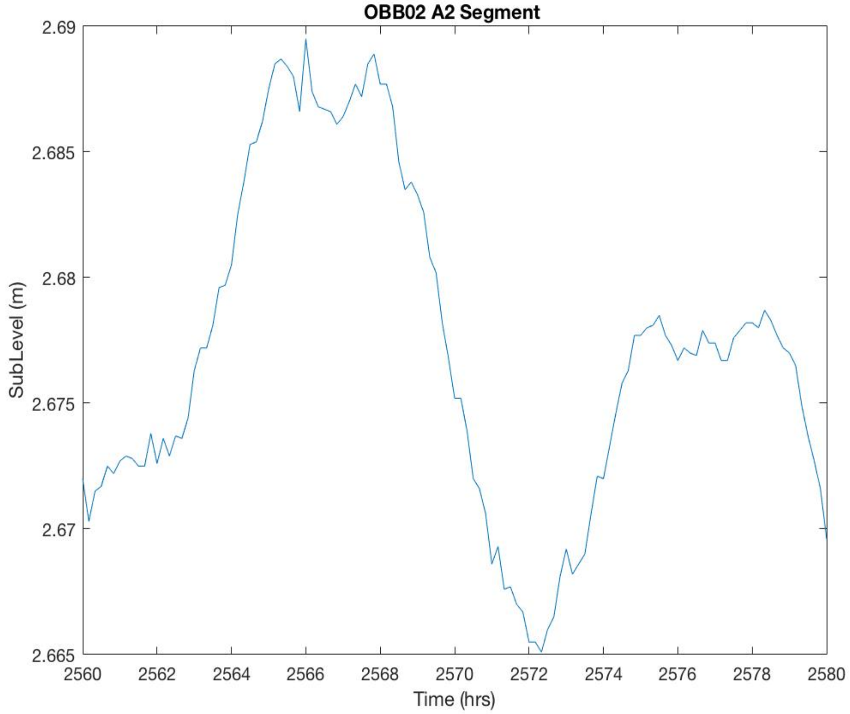
OBB02 A2 Segment
SubLevel (m)
Time (hrs)
2.69
2.685
2.68
2.675
2.67
2.665
2560
2562
2564
2566
2568
2570
2572
2574
2576
2578
2580

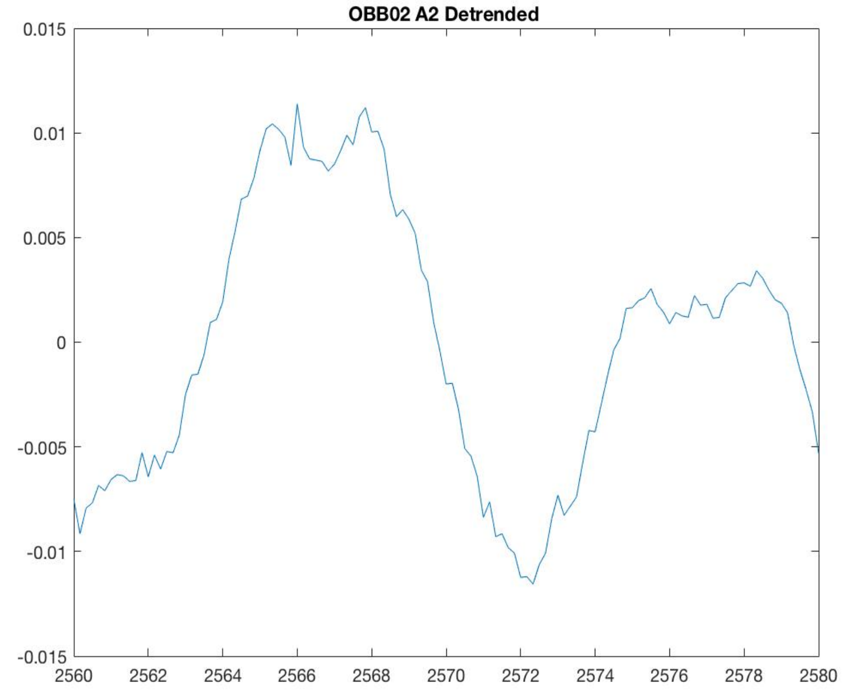
OBB02 A2 Detrended
0.015
0.01
0.005
0
-0.005
-0.01
-0.015
2560
2562
2564
2566
2568
2570
2572
2574
2576
2578
2580

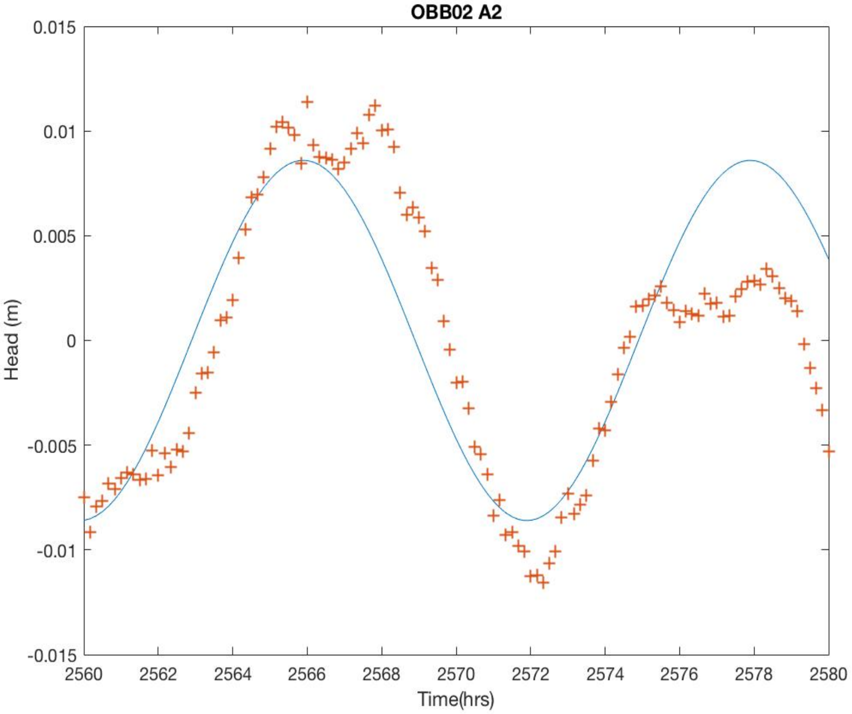
OBB02 A2
Head (m)
0.015
0.01
0.005
0
-0.005
-0.01
-0.015
2560
2562
2564
2566
2568
2570
2572
2574
2576
2578
2580
Time(hrs)

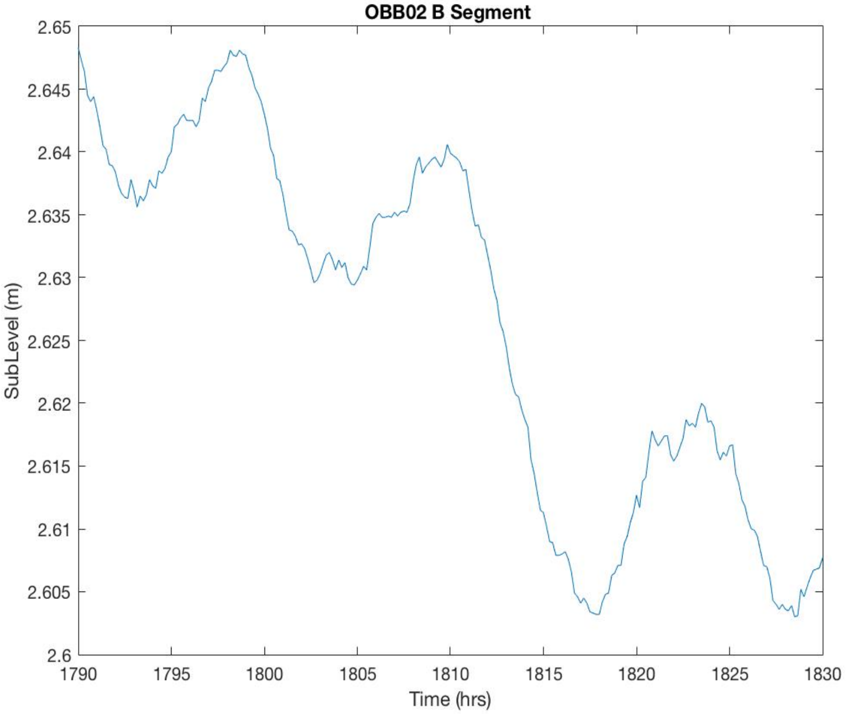
OBB02 B Segment
SubLevel (m)
Time (hrs)
2.65
2.645
2.64
2.635
2.63
2.625
2.62
2.615
2.61
2.605
2.6
1790
1795
1800
1805
1810
1815
1820
1825
1830

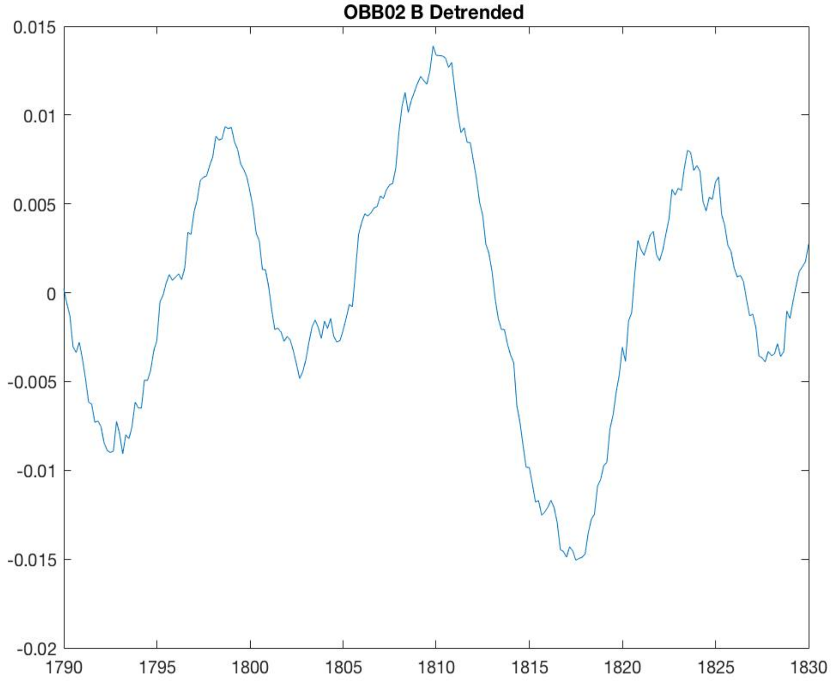
OBB02 B Detrended
0.015
0.01
0.005
0
-0.005
-0.01
-0.015
-0.02
1790
1795
1800
1805
1810
1815
1820
1825
1830

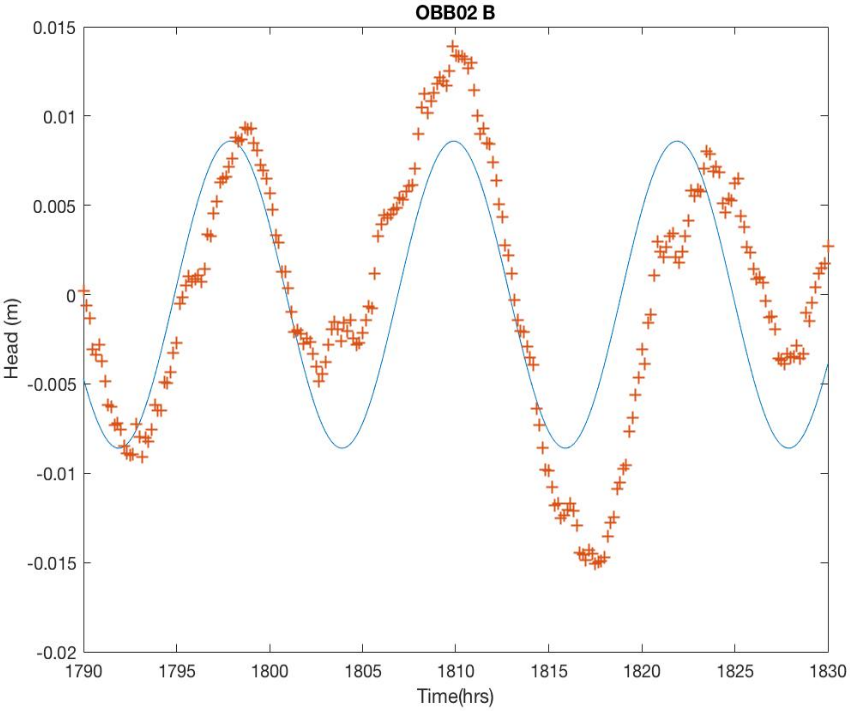
OBB02 B
Head (m)
0.015
0.01
0.005
0
-0.005
-0.01
-0.015
-0.02
1790
1795
1800
1805
1810
1815
1820
1825
1830
Time(hrs)

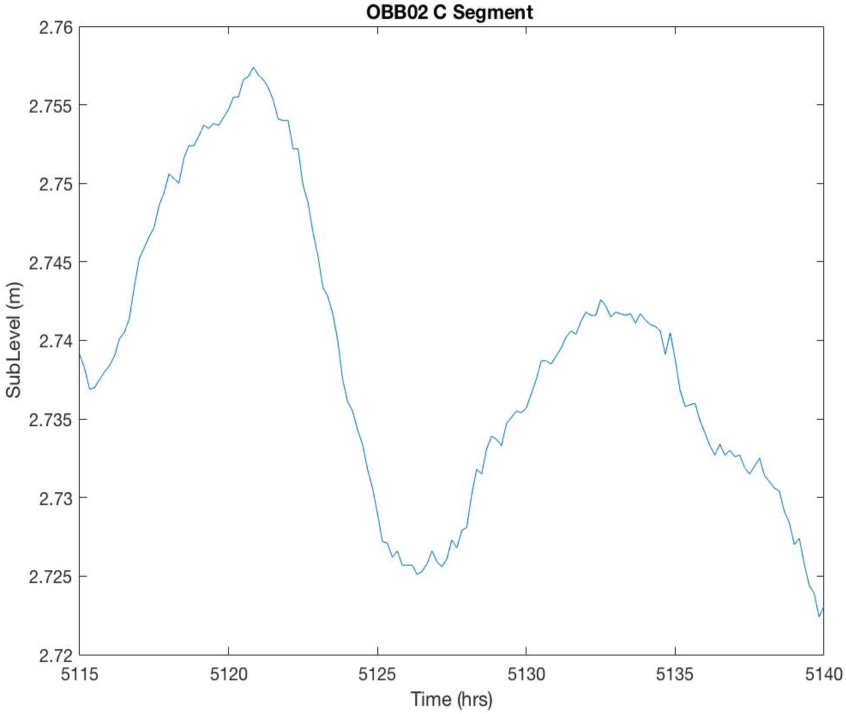
OBB02 C Segment
SubLevel (m)
2.76
2.755
2.75
2.745
2.74
2.735
2.73
2.725
2.72
5115
5120
5125
5130
5135
5140
Time (hrs)

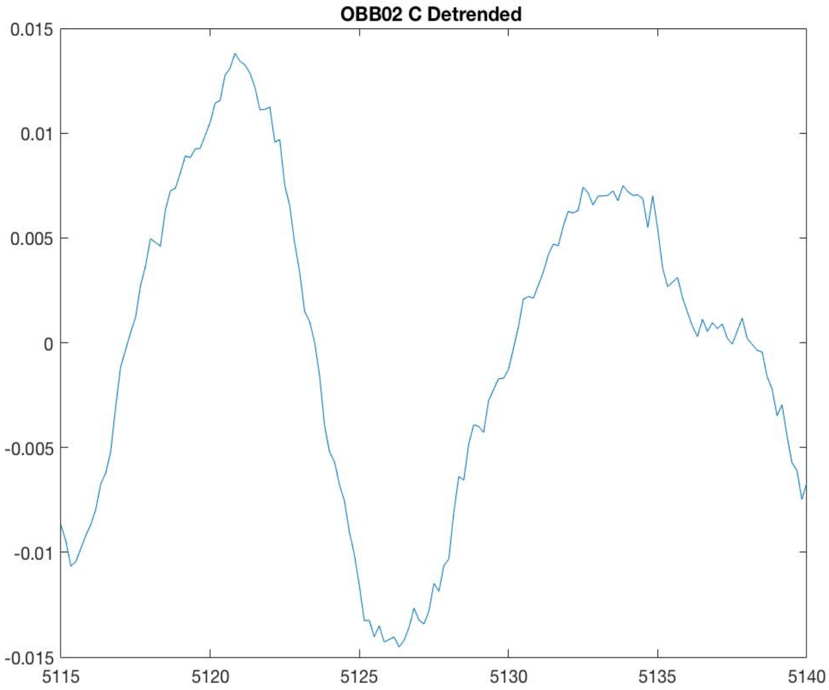
OBB02 C Detrended
0.015
0.01
0.005
0
-0.005
-0.01
-0.015
5115
5120
5125
5130
5135
5140

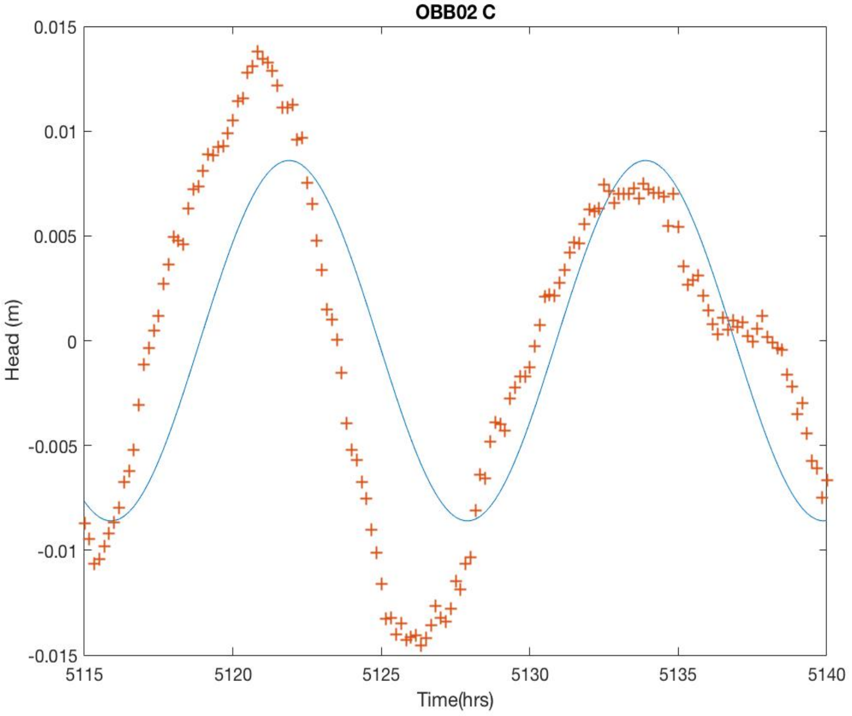
OBB02 C
Head (m)
0.015
0.01
0.005
0
-0.005
-0.01
-0.015
5115
5120
5125
5130
5135
5140
Time(hrs)

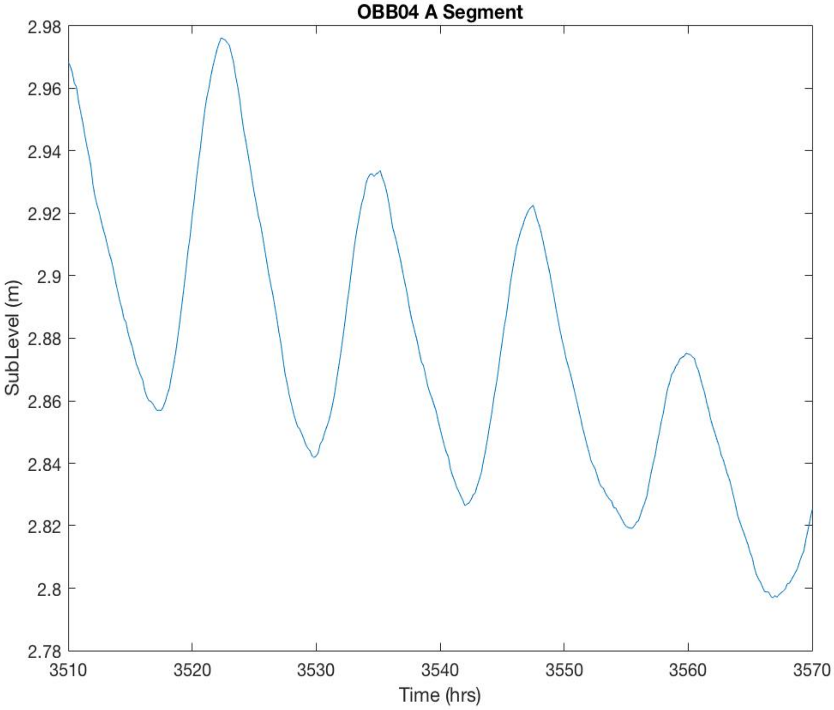
OBB04 A Segment

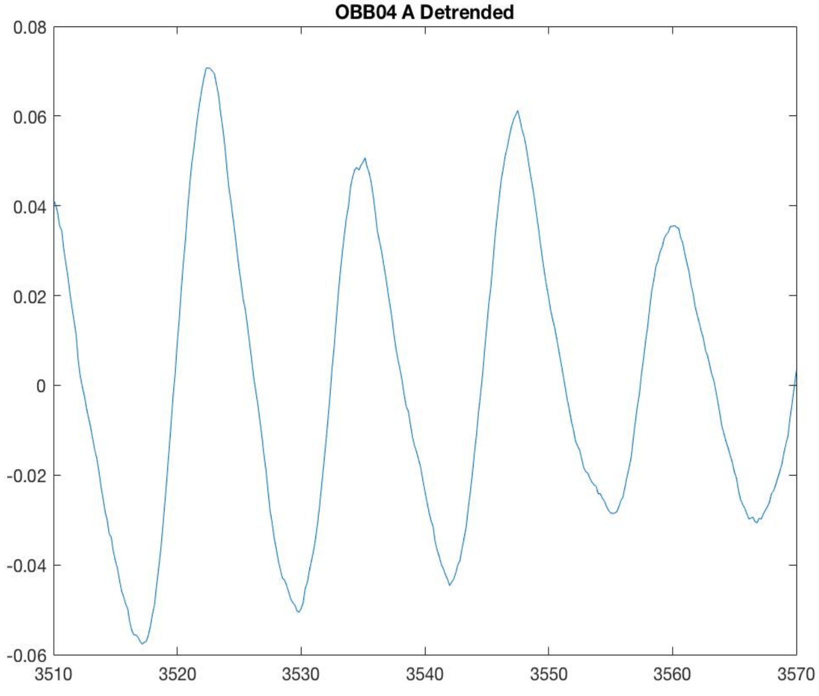
OBB04 A Detrended

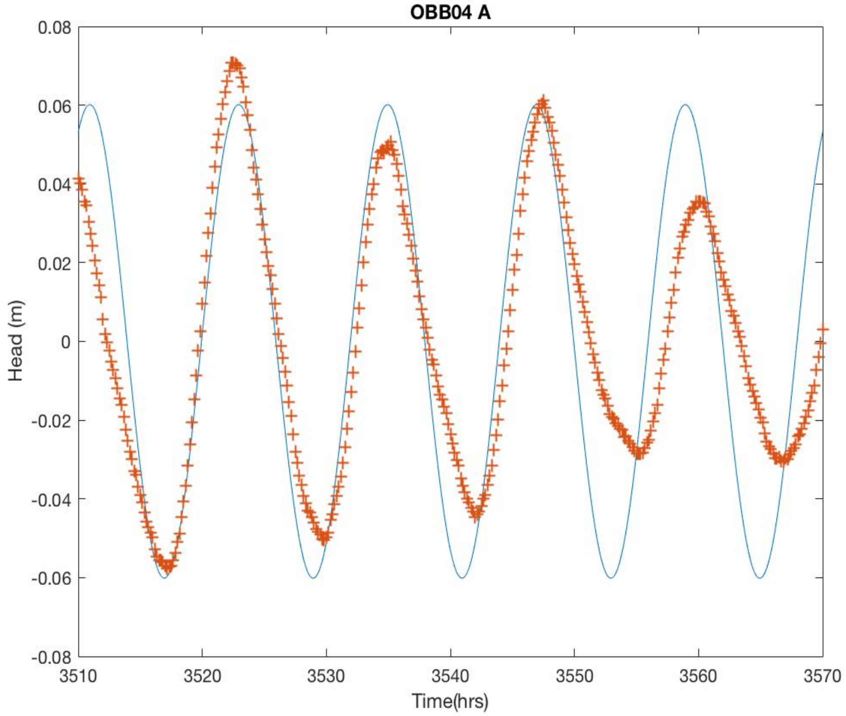
OBB04 A
Head (m)
Time(hrs)
0.08
0.06
0.04
0.02
0
-0.02
-0.04
-0.06
-0.08
3510
3520
3530
3540
3550
3560
3570

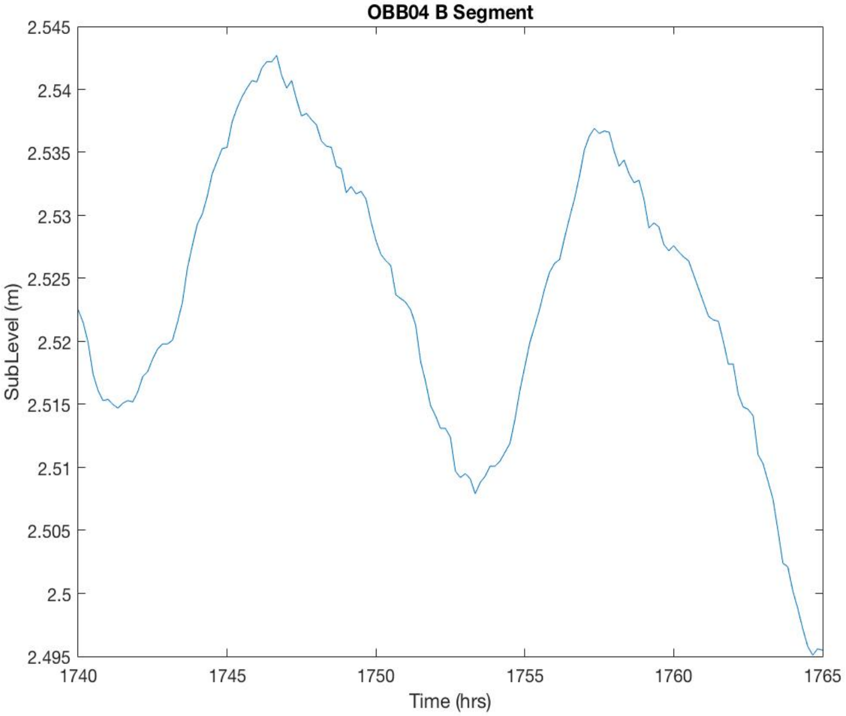
OBB04 B Segment
SubLevel (m)
Time (hrs)
2.545
2.54
2.535
2.53
2.525
2.52
2.515
2.51
2.505
2.5
2.495
1740
1745
1750
1755
1760
1765

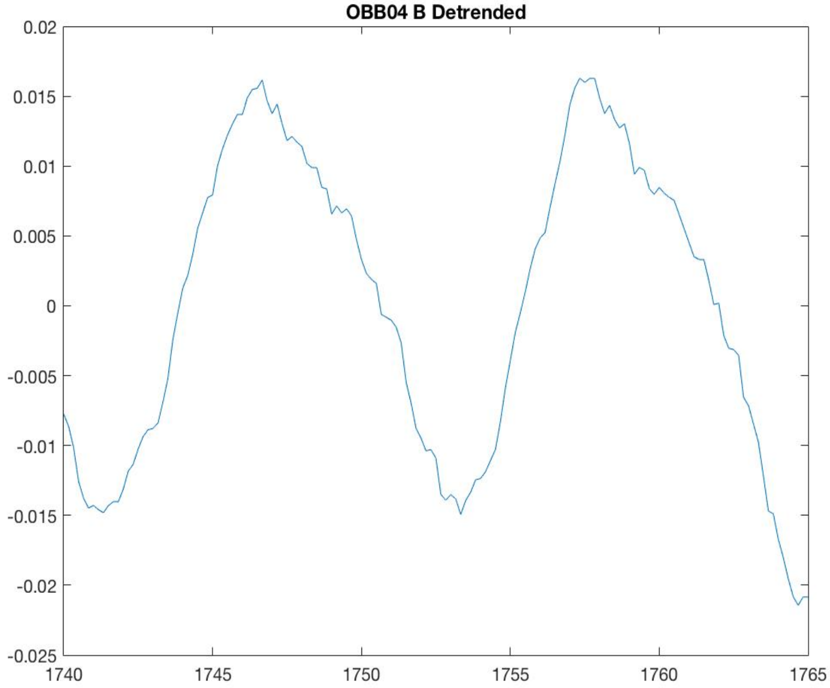
OBB04 B Detrended
0.02
0.015
0.01
0.005
0
-0.005
-0.01
-0.015
-0.02
-0.025
1740
1745
1750
1755
1760
1765

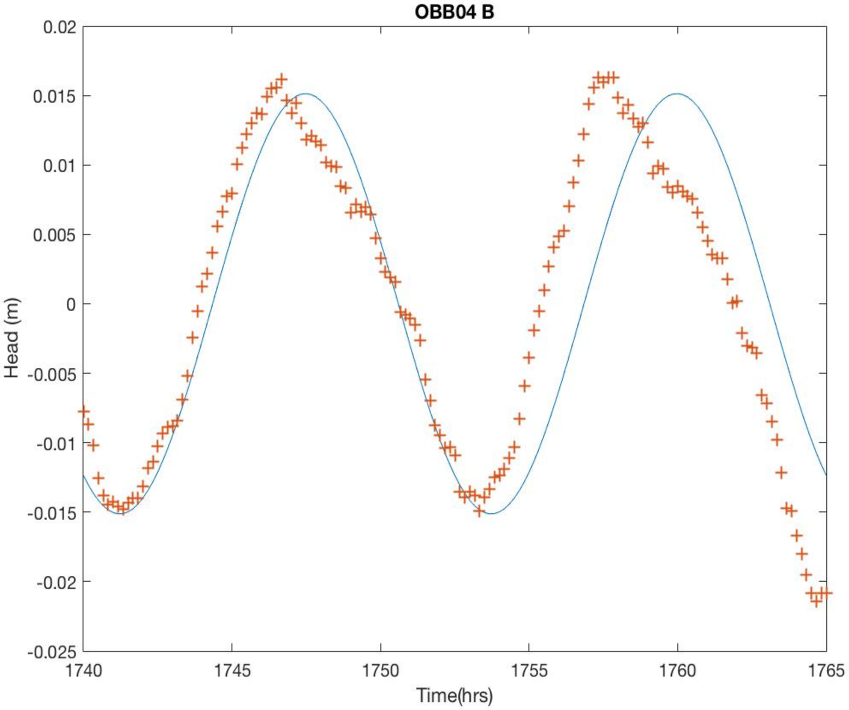
OBB04 B
Head (m)
0.02
0.015
0.01
0.005
0
-0.005
-0.01
-0.015
-0.02
-0.025
1740
1745
1750
1755
1760
1765
Time(hrs)

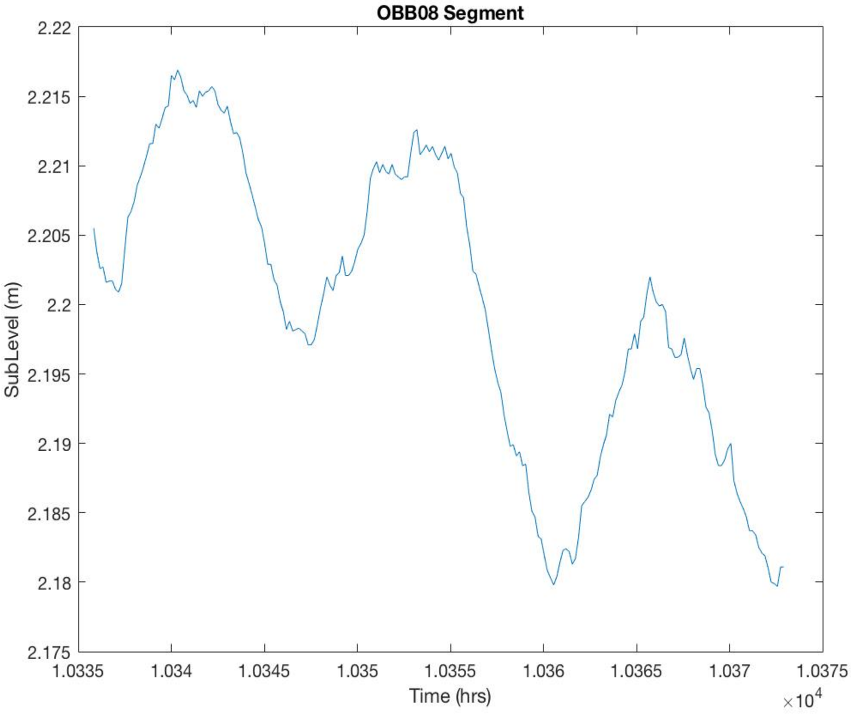

OBB08 Segment
SubLevel (m)
2.22
2.215
2.21
2.205
2.2
2.195
2.19
2.185
2.18
2.175
1.0335
1.034
1.0345
1.035
1.0355
1.036
1.0365
1.037
1.0375
Time (hrs)
$\times 10^4$

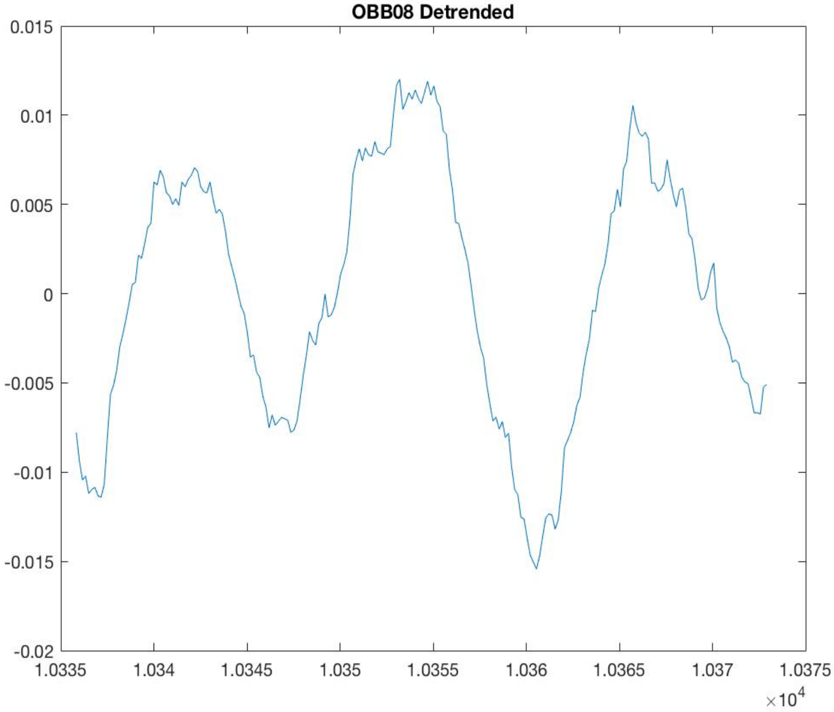

OBB08 Detrended
0.015
0.01
0.005
0
-0.005
-0.01
-0.015
-0.02
1.0335
1.034
1.0345
1.035
1.0355
1.036
1.0365
1.037
1.0375
$\times 10^4$

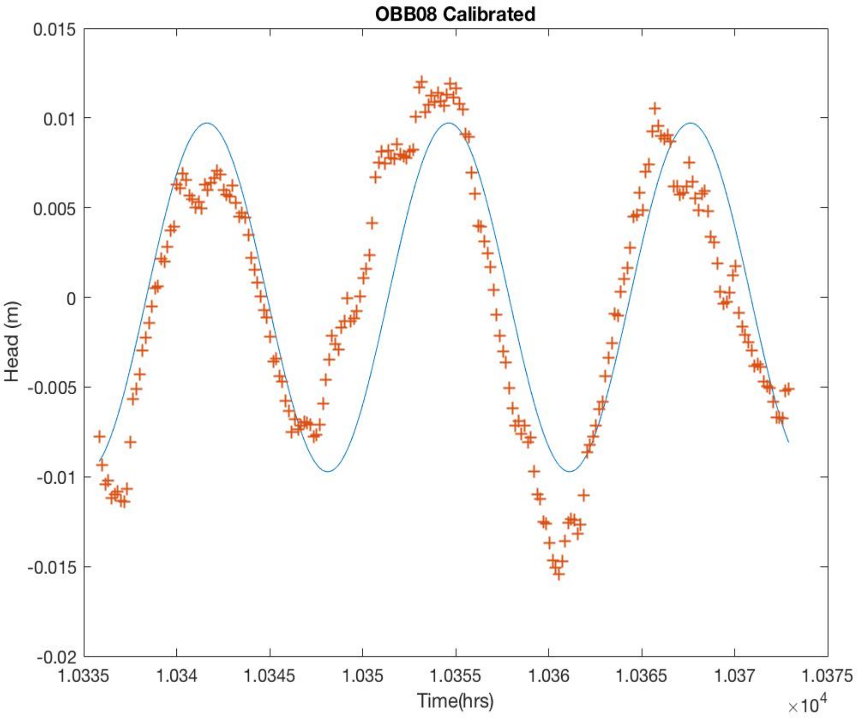
OBB08 Calibrated
Head (m)
0.015
0.01
0.005
0
-0.005
-0.01
-0.015
-0.02
1.0335
1.034
1.0345
1.035
1.0355
1.036
1.0365
1.037
1.0375
Time(hrs)
×10^4

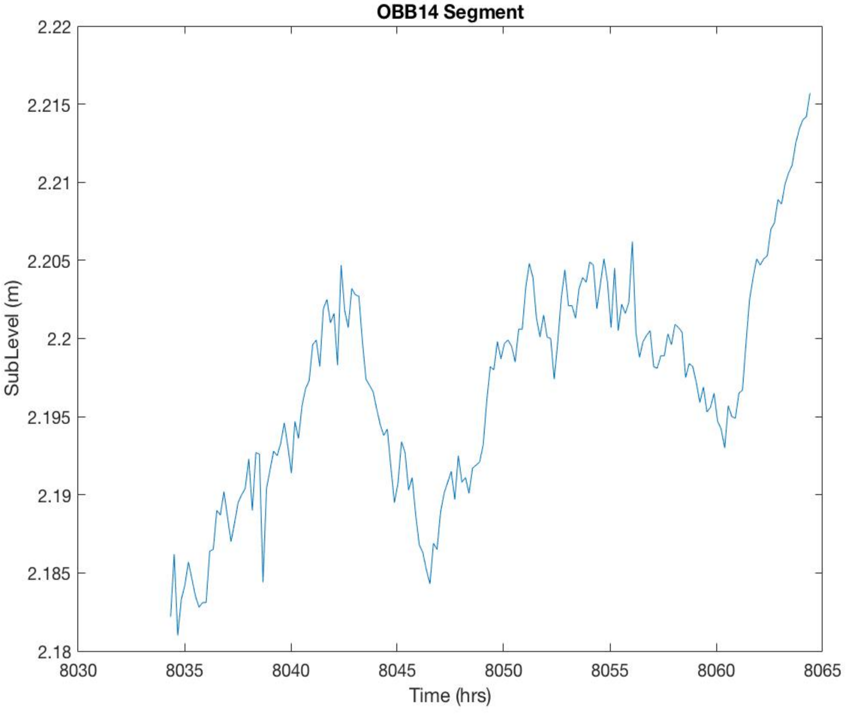
OBB14 Segment
SubLevel (m)
2.22
2.215
2.21
2.205
2.2
2.195
2.19
2.185
2.18
8030
8035
8040
8045
8050
8055
8060
8065
Time (hrs)

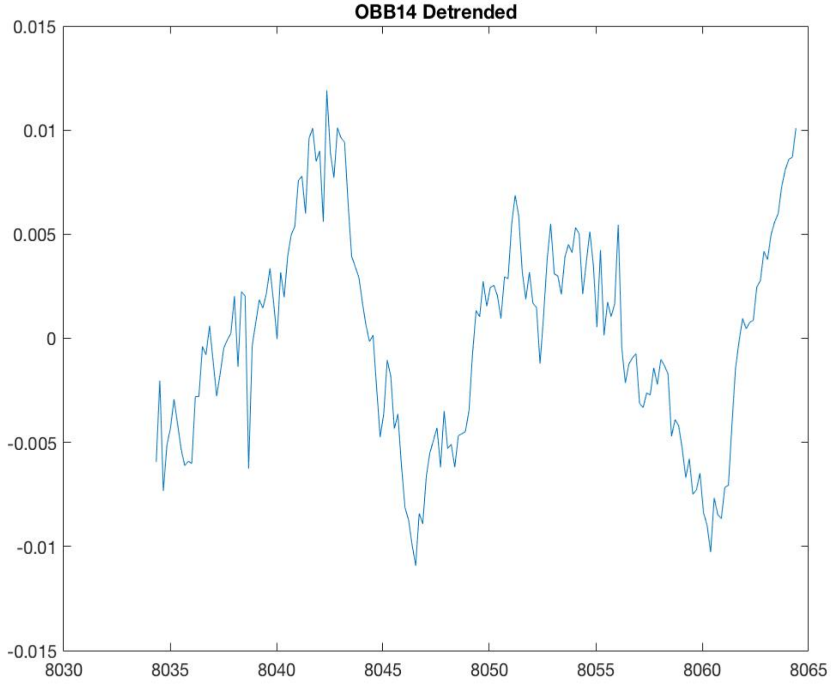

OBB14 Detrended

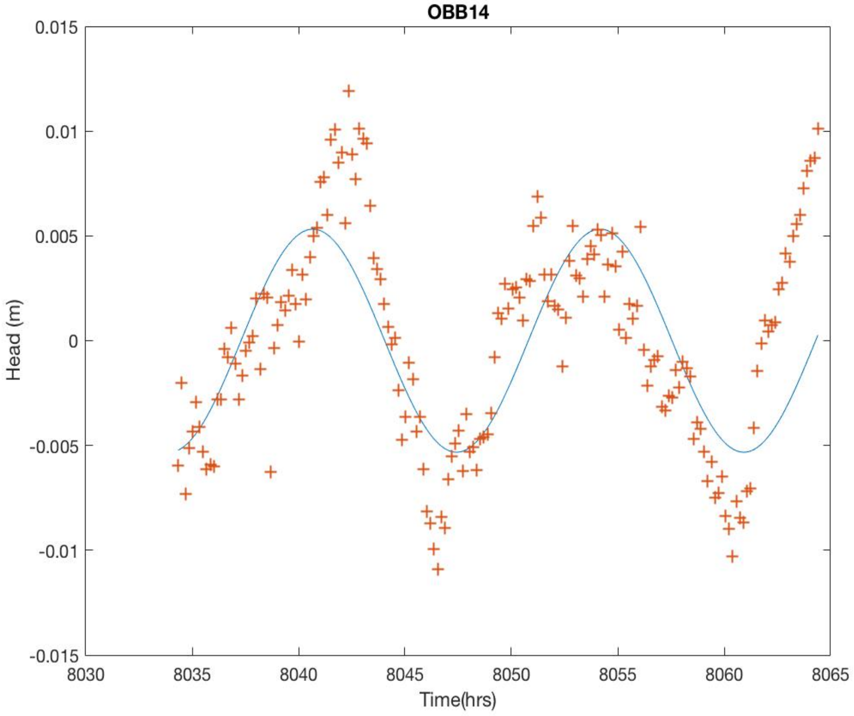

OBB14

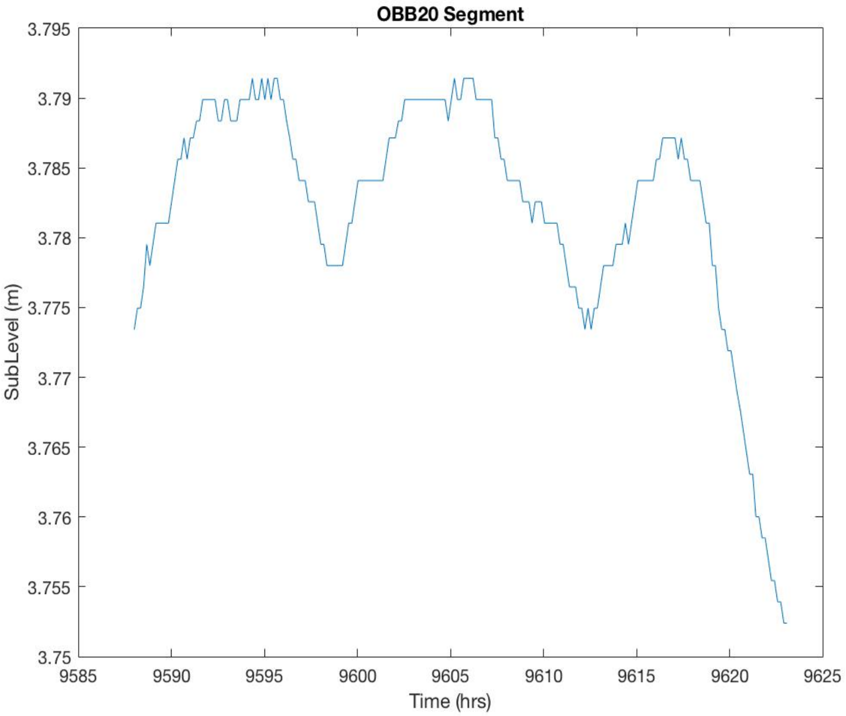
OBB20 Segment
SubLevel (m)
3.795
3.79
3.785
3.78
3.775
3.77
3.765
3.76
3.755
3.75
9585
9590
9595
9600
9605
9610
9615
9620
9625
Time (hrs)

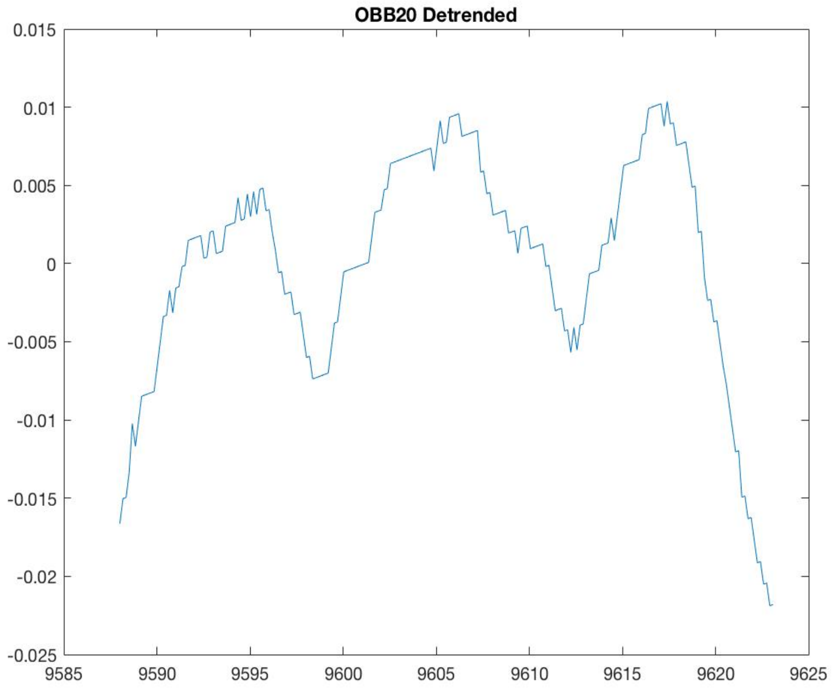
OBB20 Detrended
0.015
0.01
0.005
0
-0.005
-0.01
-0.015
-0.02
-0.025
9585
9590
9595
9600
9605
9610
9615
9620
9625

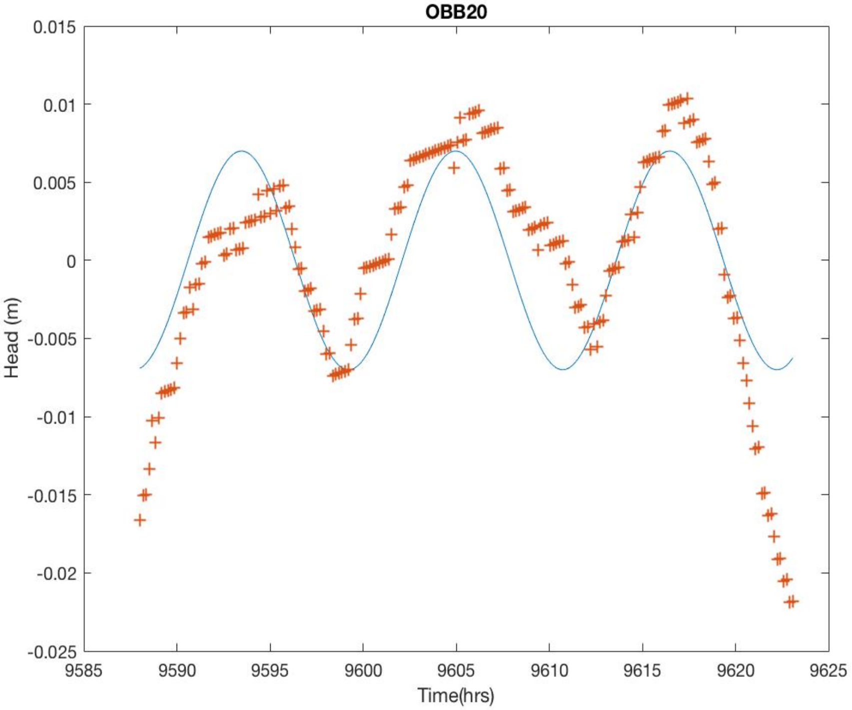
OBB20
Head (m)
0.015
0.01
0.005
0
-0.005
-0.01
-0.015
-0.02
-0.025
9585
9590
9595
9600
9605
9610
9615
9620
9625
Time(hrs)

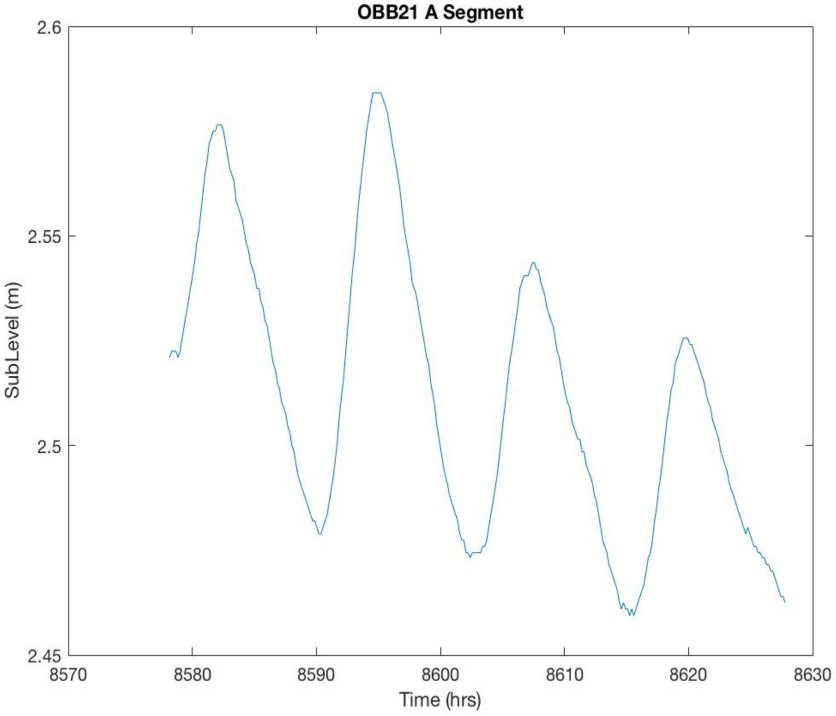
OBB21 A Segment
SubLevel (m)
2.6
2.55
2.5
2.45
8570
8580
8590
8600
8610
8620
8630
Time (hrs)

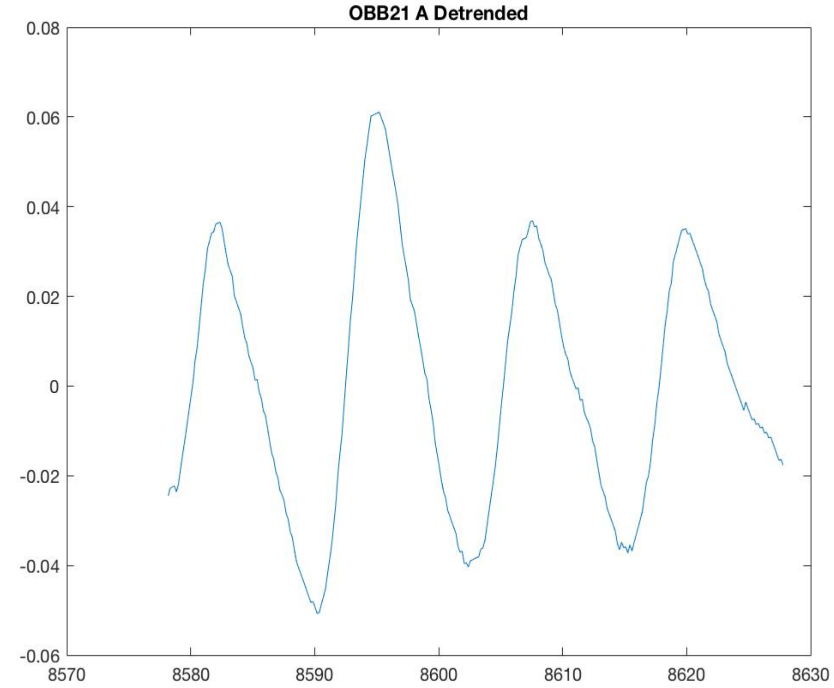
OBB21 A Detrended
0.08
0.06
0.04
0.02
0
-0.02
-0.04
-0.06
8570
8580
8590
8600
8610
8620
8630

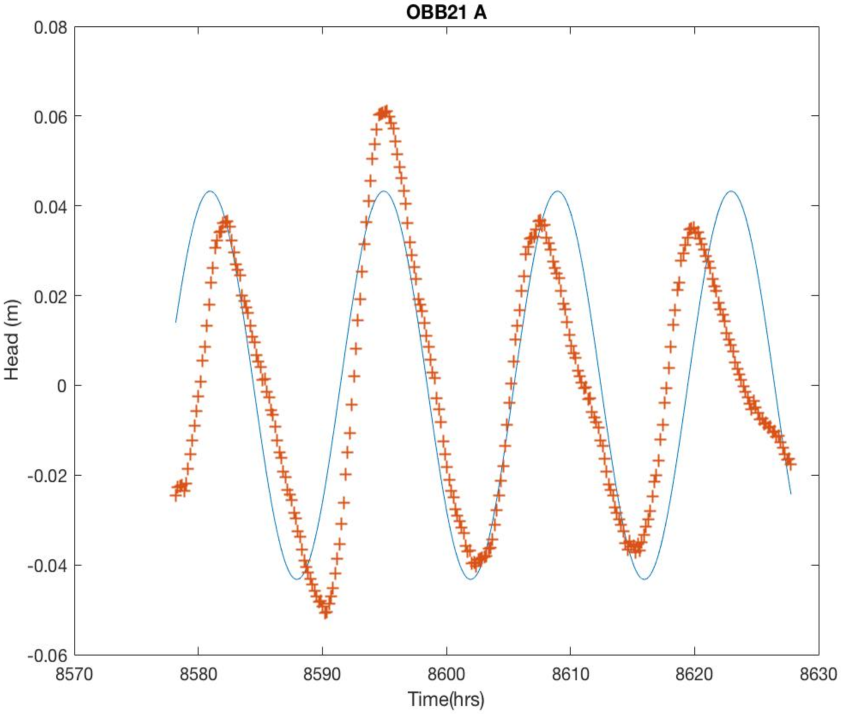
OBB21 A
Head (m)
0.08
0.06
0.04
0.02
0
-0.02
-0.04
-0.06
8570
8580
8590
8600
8610
8620
8630
Time(hrs)

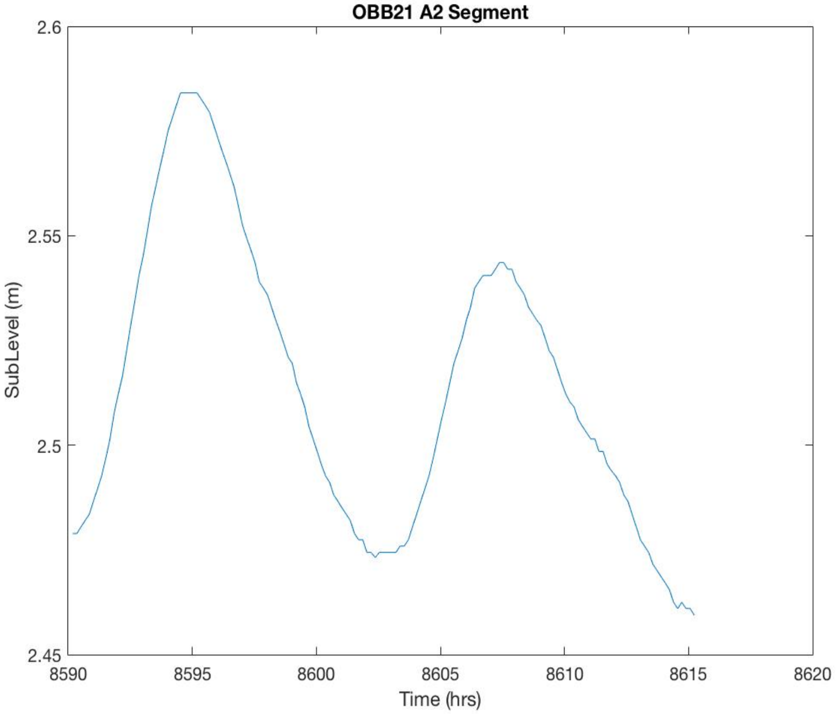
OBB21 A2 Segment
SubLevel (m)
2.6
2.55
2.5
2.45
8590
8595
8600
8605
8610
8615
8620
Time (hrs)

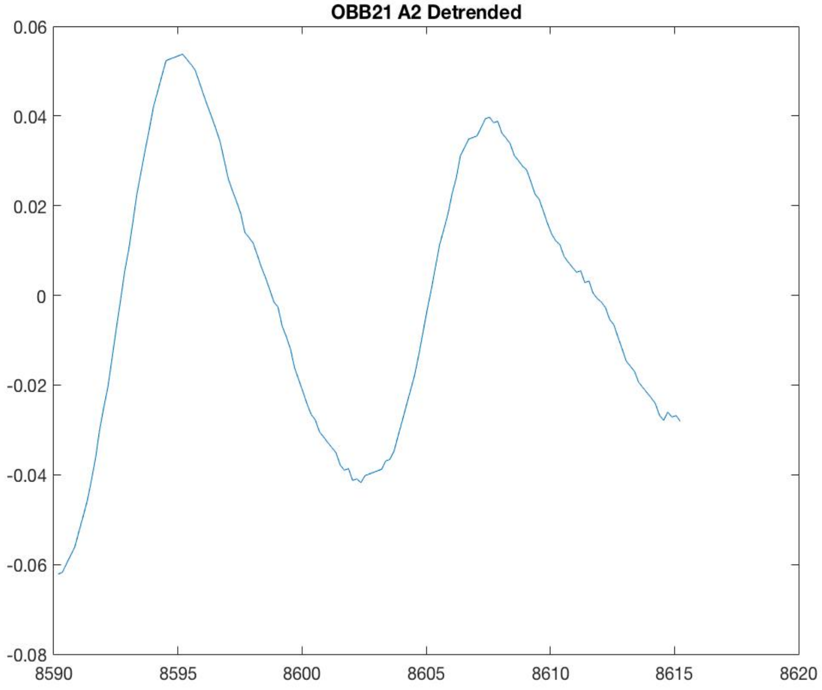
OBB21 A2 Detrended
0.06
0.04
0.02
0
-0.02
-0.04
-0.06
-0.08
8590
8595
8600
8605
8610
8615
8620

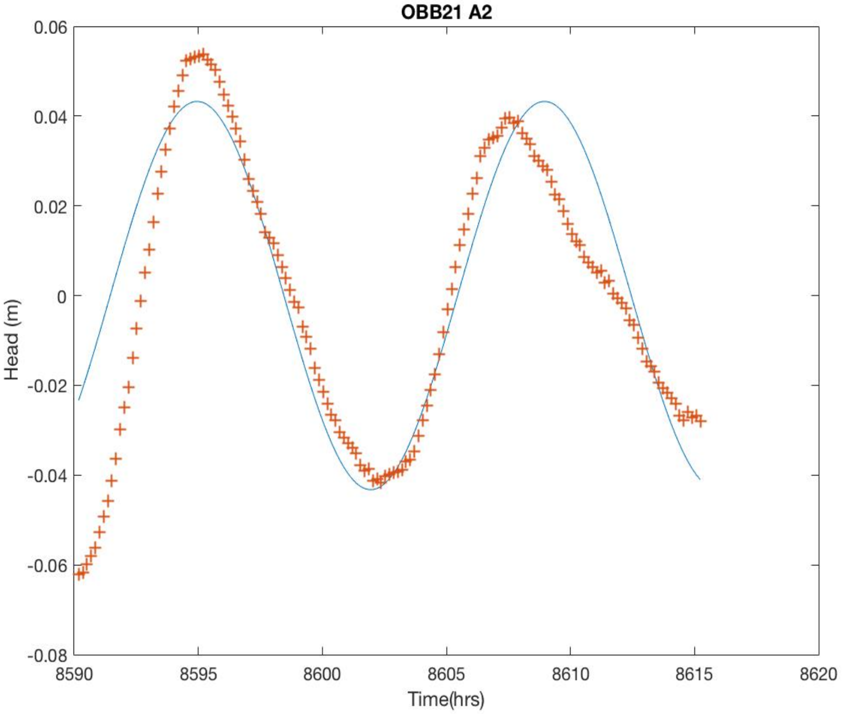

OBB21 A2
Head (m)
Time(hrs)
0.06
0.04
0.02
0
-0.02
-0.04
-0.06
-0.08
8590
8595
8600
8605
8610
8615
8620

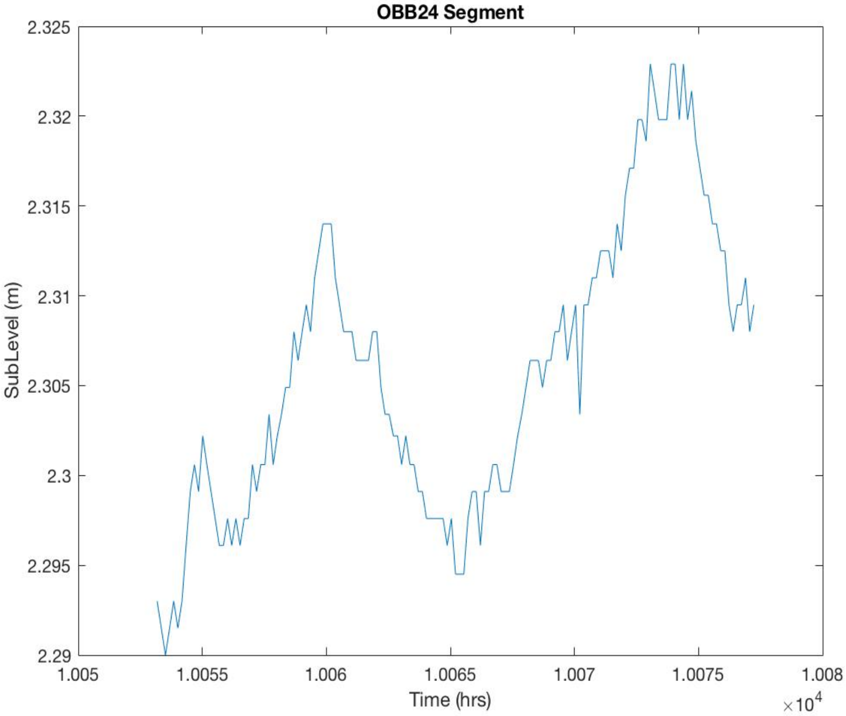

OBB24 Segment
SubLevel (m)
Time (hrs)
2.325
2.32
2.315
2.31
2.305
2.3
2.295
2.29
1.005
1.0055
1.006
1.0065
1.007
1.0075
1.008
×10^4

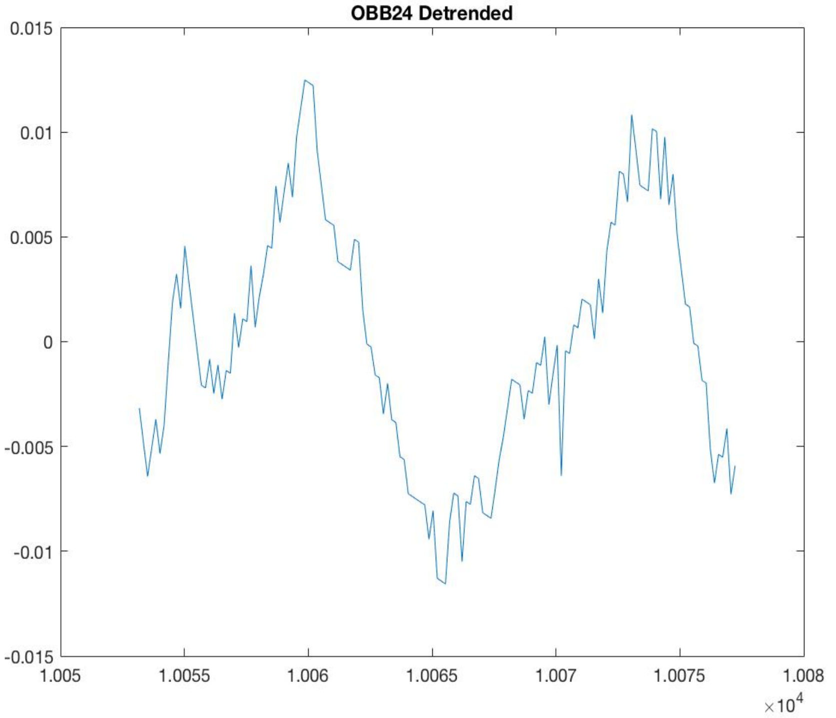
OBB24 Detrended
0.015
0.01
0.005
0
-0.005
-0.01
-0.015
1.005
1.0055
1.006
1.0065
1.007
1.0075
1.008
×10^4

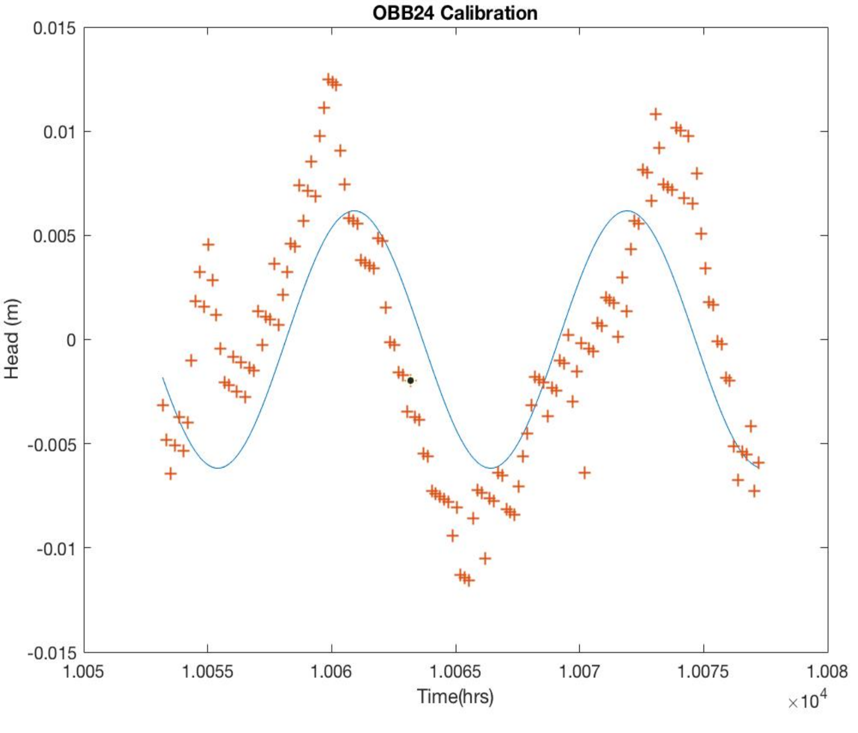
OBB24 Calibration
Head (m)
0.015
0.01
0.005
0
-0.005
-0.01
-0.015
1.005
1.0055
1.006
1.0065
1.007
1.0075
1.008
Time(hrs)
×10^4

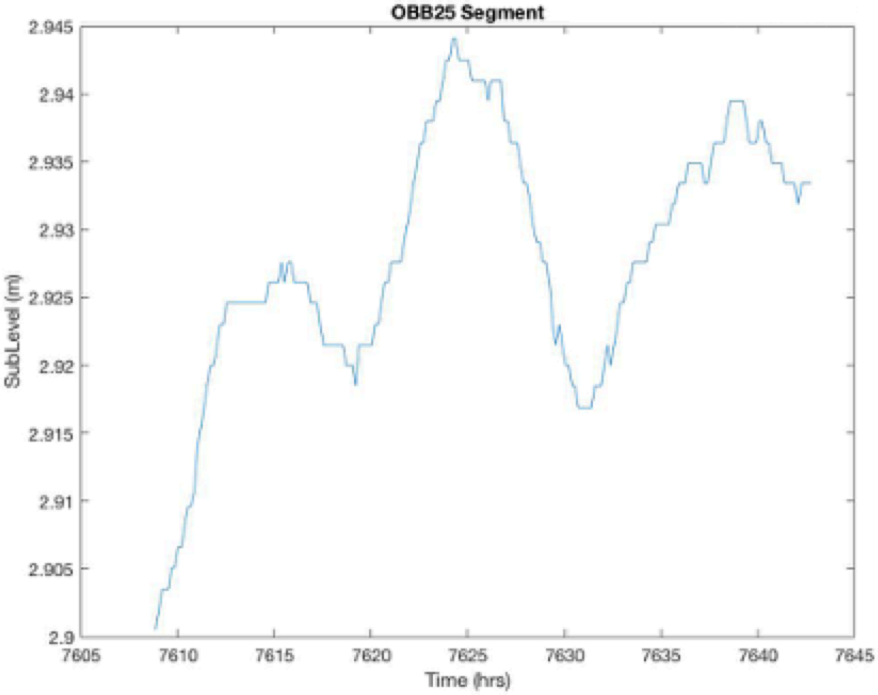
OBB25 Segment
SubLevel (m)
Time (hrs)
2.945
2.94
2.935
2.93
2.925
2.92
2.915
2.91
2.905
2.9
7605
7610
7615
7620
7625
7630
7635
7640
7645

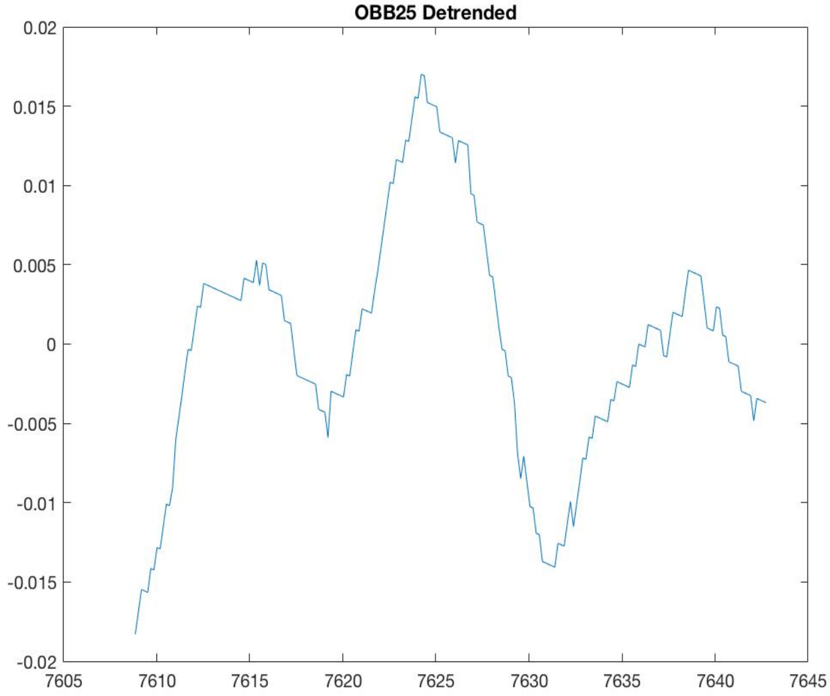
OBB25 Detrended
0.02
0.015
0.01
0.005
0
-0.005
-0.01
-0.015
-0.02
7605
7610
7615
7620
7625
7630
7635
7640
7645

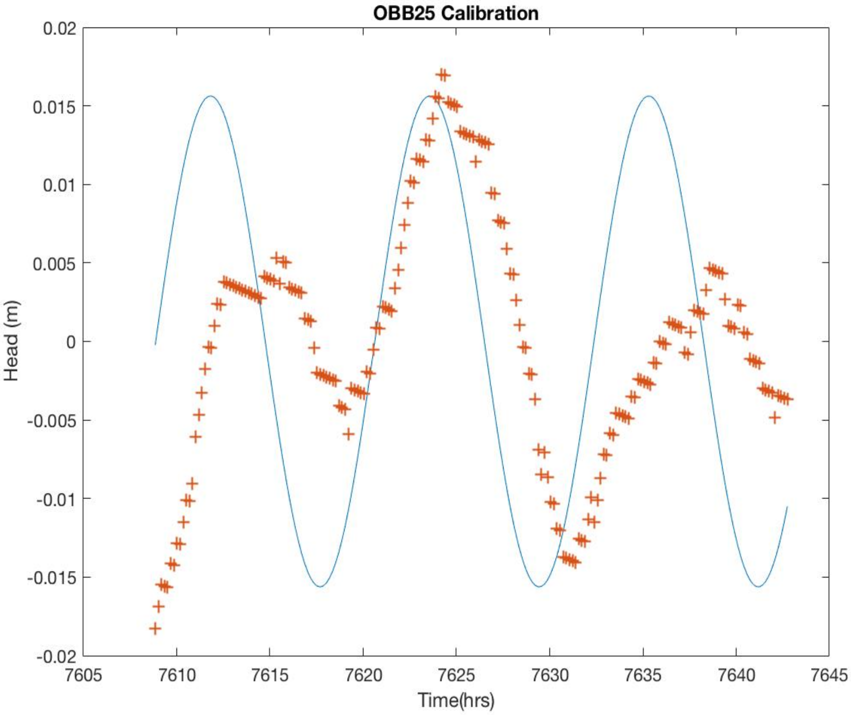
OBB25 Calibration
Head (m)
Time(hrs)
0.02
0.015
0.01
0.005
0
-0.005
-0.01
-0.015
-0.02
7605
7610
7615
7620
7625
7630
7635
7640
7645

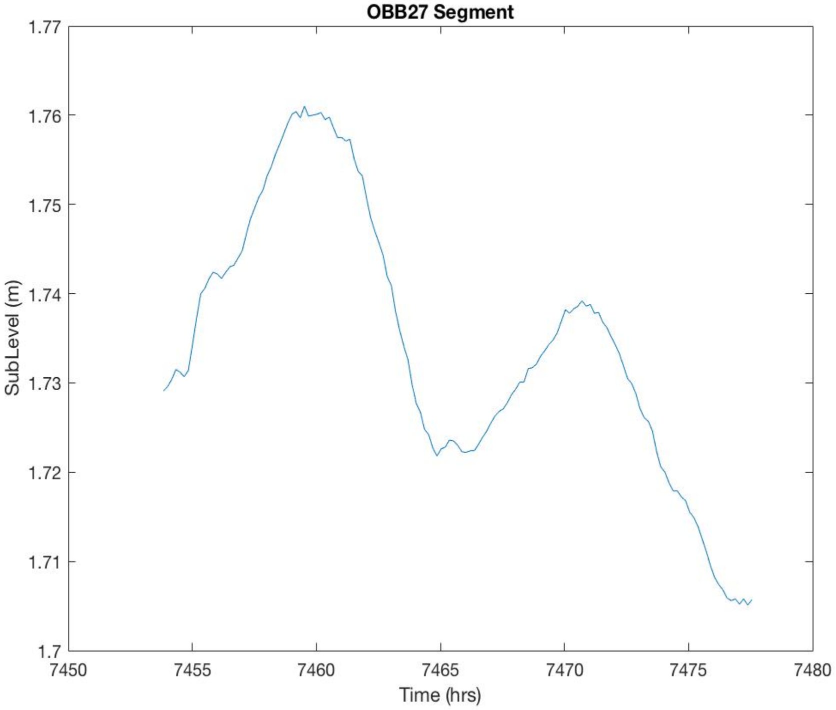
OBB27 Segment
SubLevel (m)
Time (hrs)
1.77
1.76
1.75
1.74
1.73
1.72
1.71
1.7
7450
7455
7460
7465
7470
7475
7480

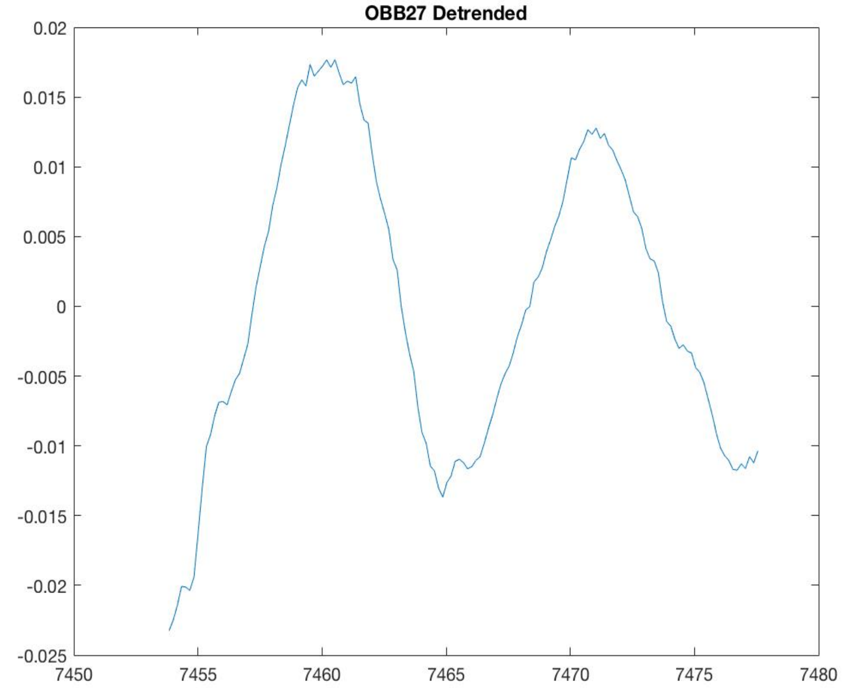
OBB27 Detrended
0.02
0.015
0.01
0.005
0
-0.005
-0.01
-0.015
-0.02
-0.025
7450
7455
7460
7465
7470
7475
7480

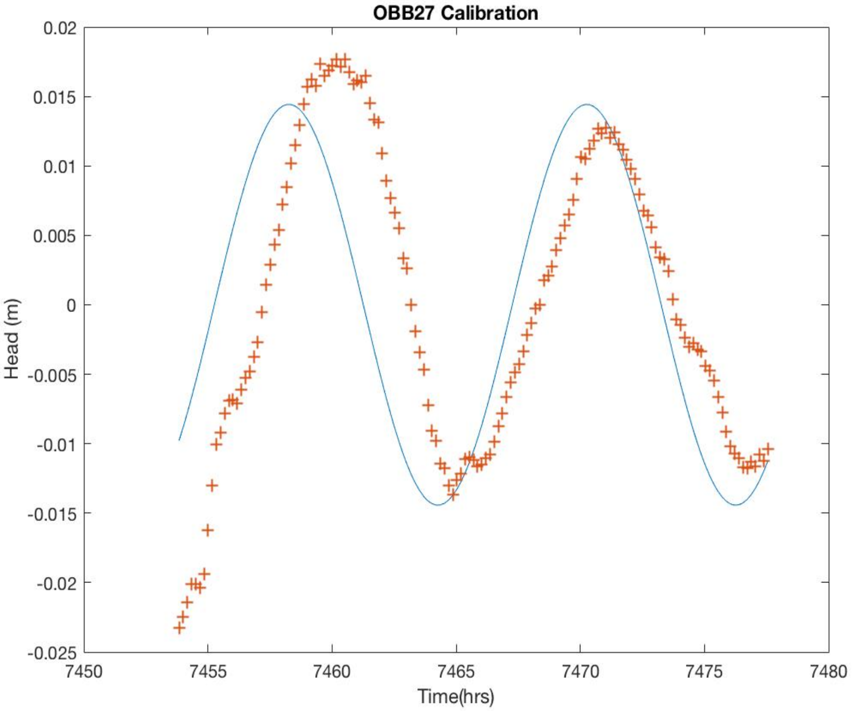
OBB27 Calibration
Head (m)
0.02
0.015
0.01
0.005
0
-0.005
-0.01
-0.015
-0.02
-0.025
7450
7455
7460
7465
7470
7475
7480
Time(hrs)

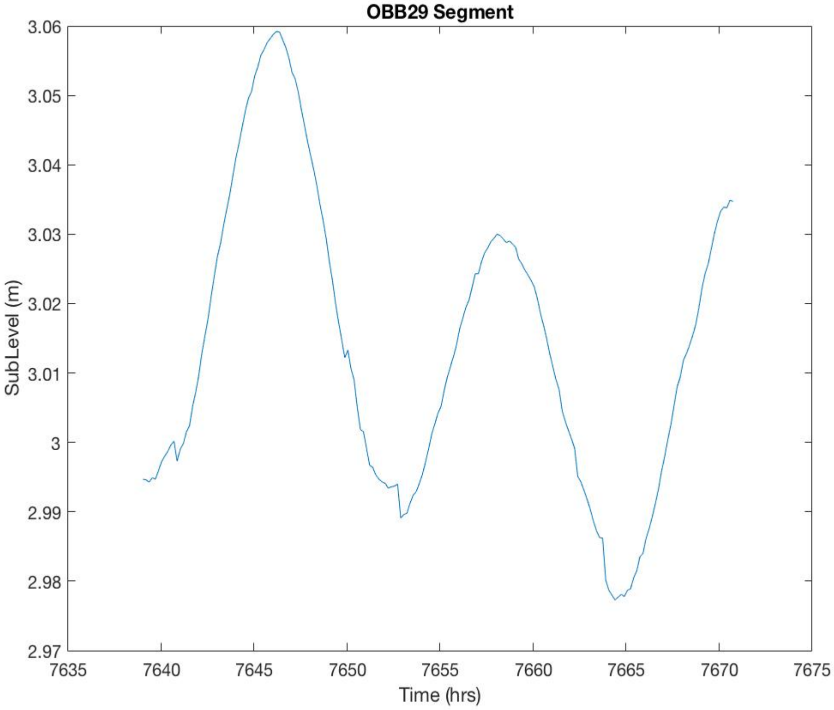
OBB29 Segment
SubLevel (m)
3.06
3.05
3.04
3.03
3.02
3.01
3
2.99
2.98
2.97
7635
7640
7645
7650
7655
7660
7665
7670
7675
Time (hrs)

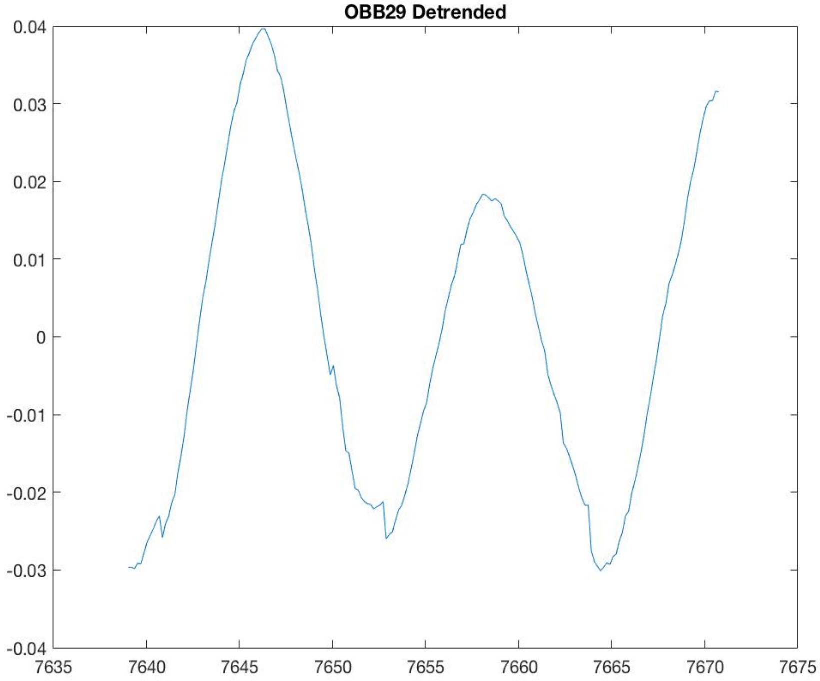
OBB29 Detrended
0.04
0.03
0.02
0.01
0
-0.01
-0.02
-0.03
-0.04
7635
7640
7645
7650
7655
7660
7665
7670
7675

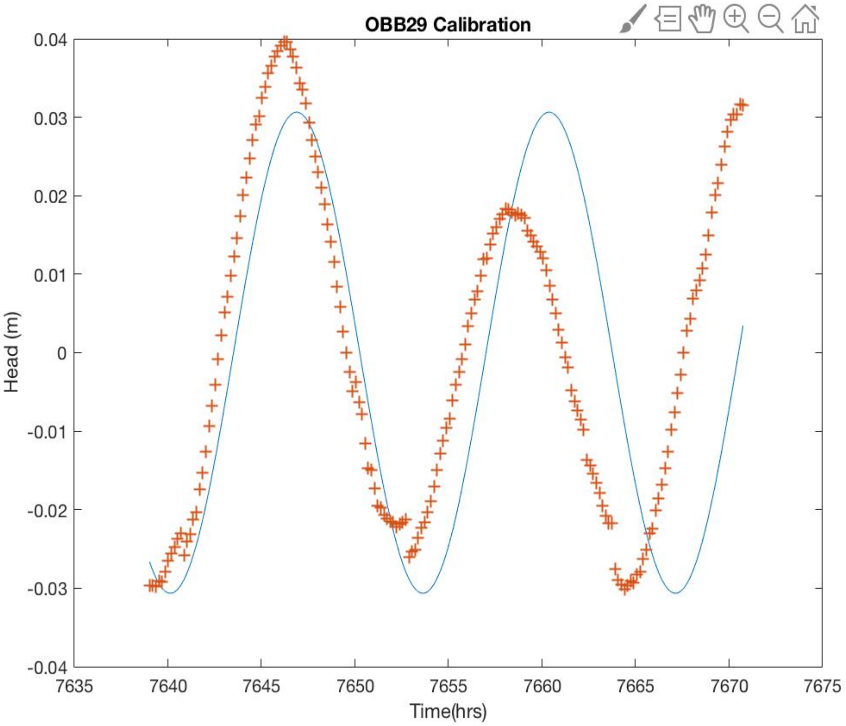
OBB29 Calibration
Head (m)
0.04
0.03
0.02
0.01
0
-0.01
-0.02
-0.03
-0.04
7635
7640
7645
7650
7655
7660
7665
7670
7675
Time(hrs)

C- Amplitude data

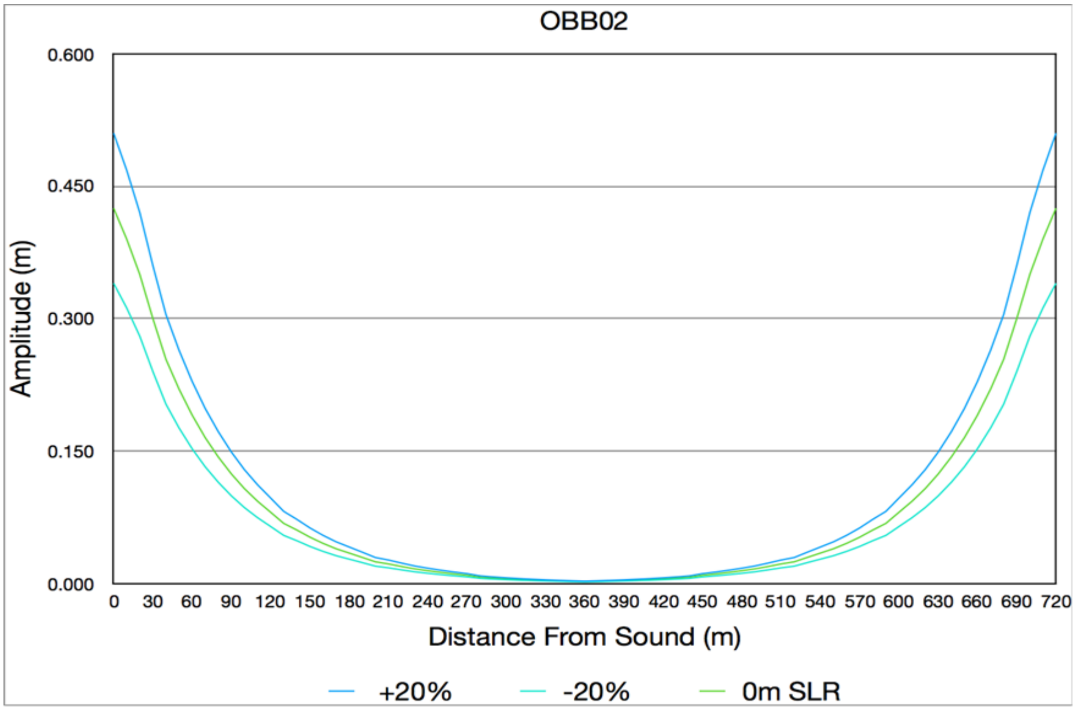

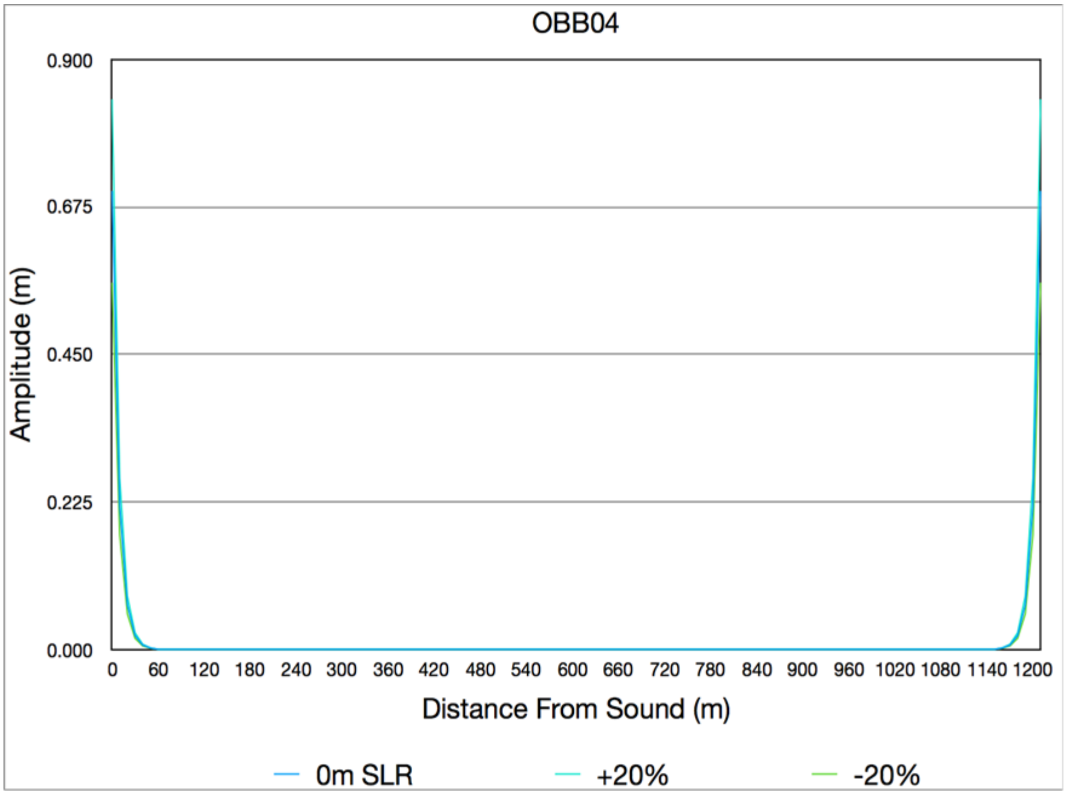

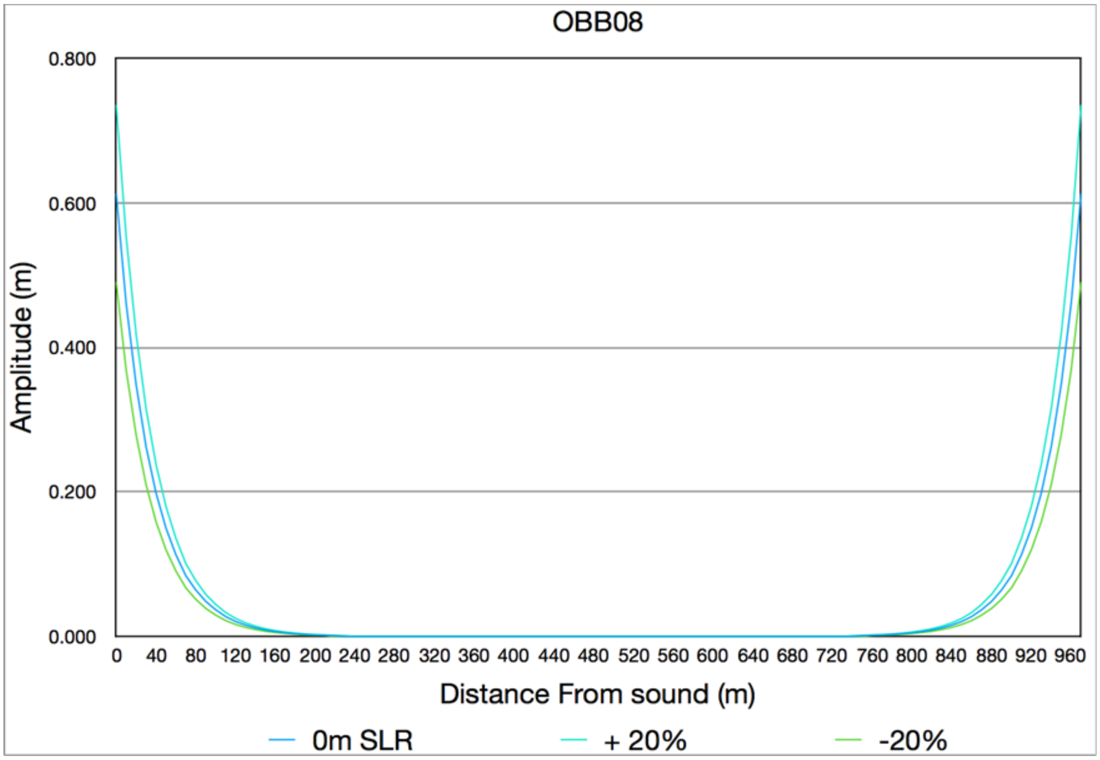
OBB08
0.800
0.600
0.400
0.200
0.000
Amplitude (m)
0
40
80
120
160
200
240
280
320
360
400
440
480
520
560
600
640
680
720
760
800
840
880
920
960
Distance From sound (m)
0m SLR
+ 20%
-20%

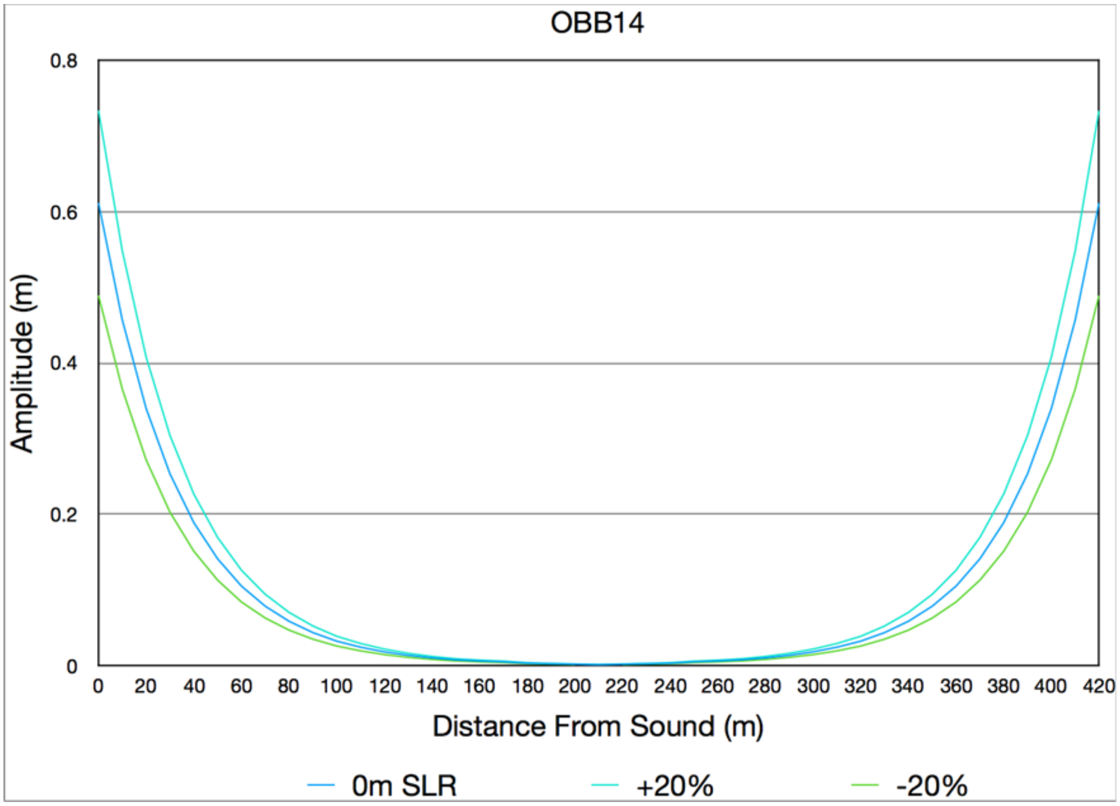
OBB14
0.8
0.6
0.4
0.2
0
Amplitude (m)
0
20
40
60
80
100
120
140
160
180
200
220
240
260
280
300
320
340
360
380
400
420
Distance From Sound (m)
0m SLR
+20%
-20%

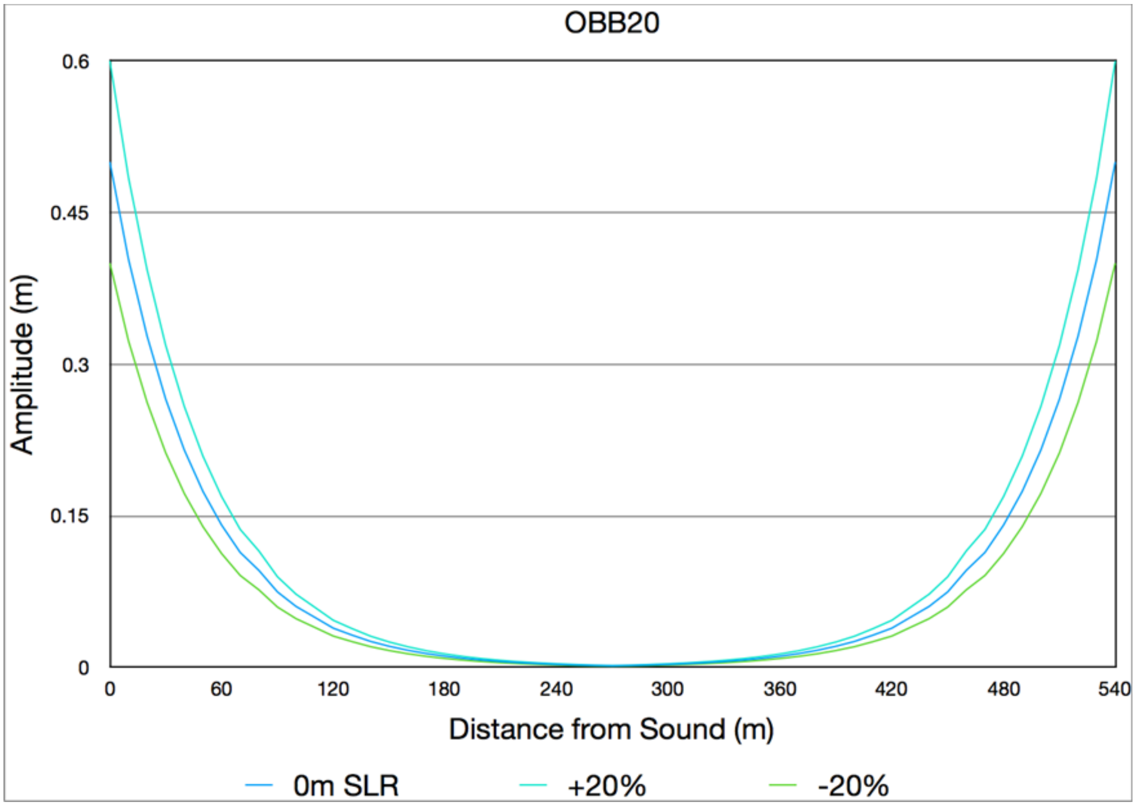
OBB20
Amplitude (m)
0.6
0.45
0.3
0.15
0
0
60
120
180
240
300
360
420
480
540
Distance from Sound (m)
0m SLR
+20%
-20%

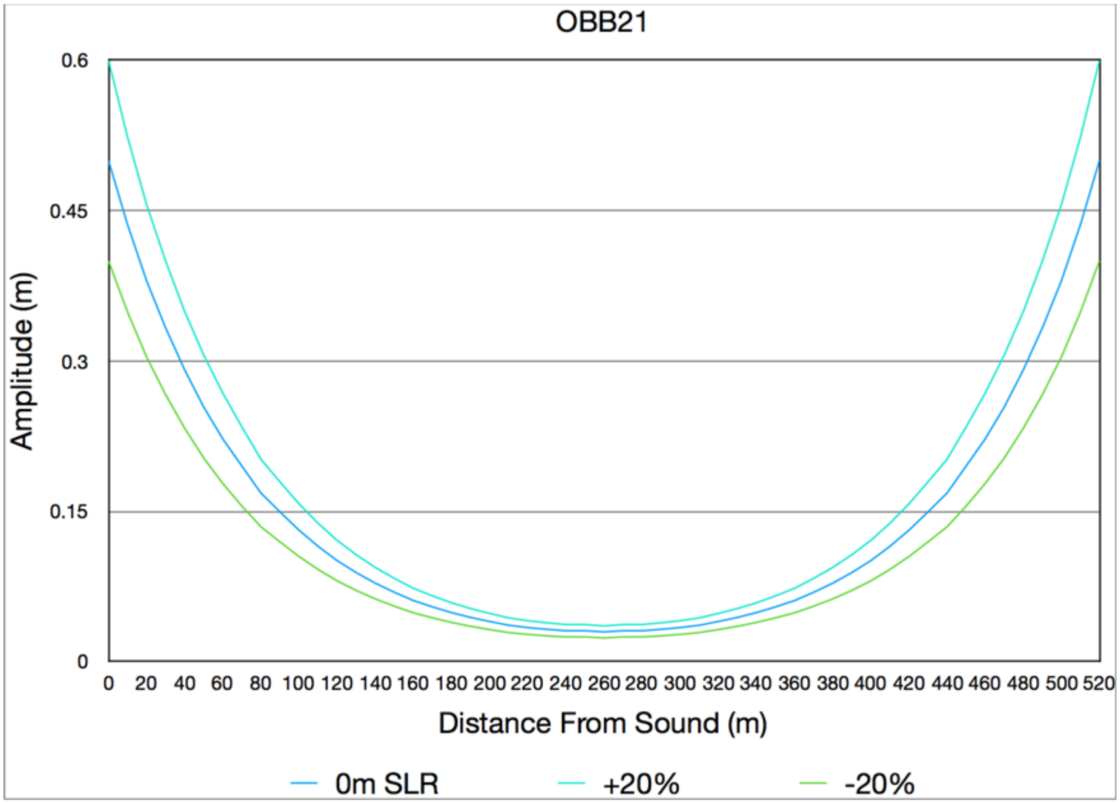
OBB21
Amplitude (m)
0.6
0.45
0.3
0.15
0
0
20
40
60
80
100
120
140
160
180
200
220
240
260
280
300
320
340
360
380
400
420
440
460
480
500
520
Distance From Sound (m)
0m SLR
+20%
-20%

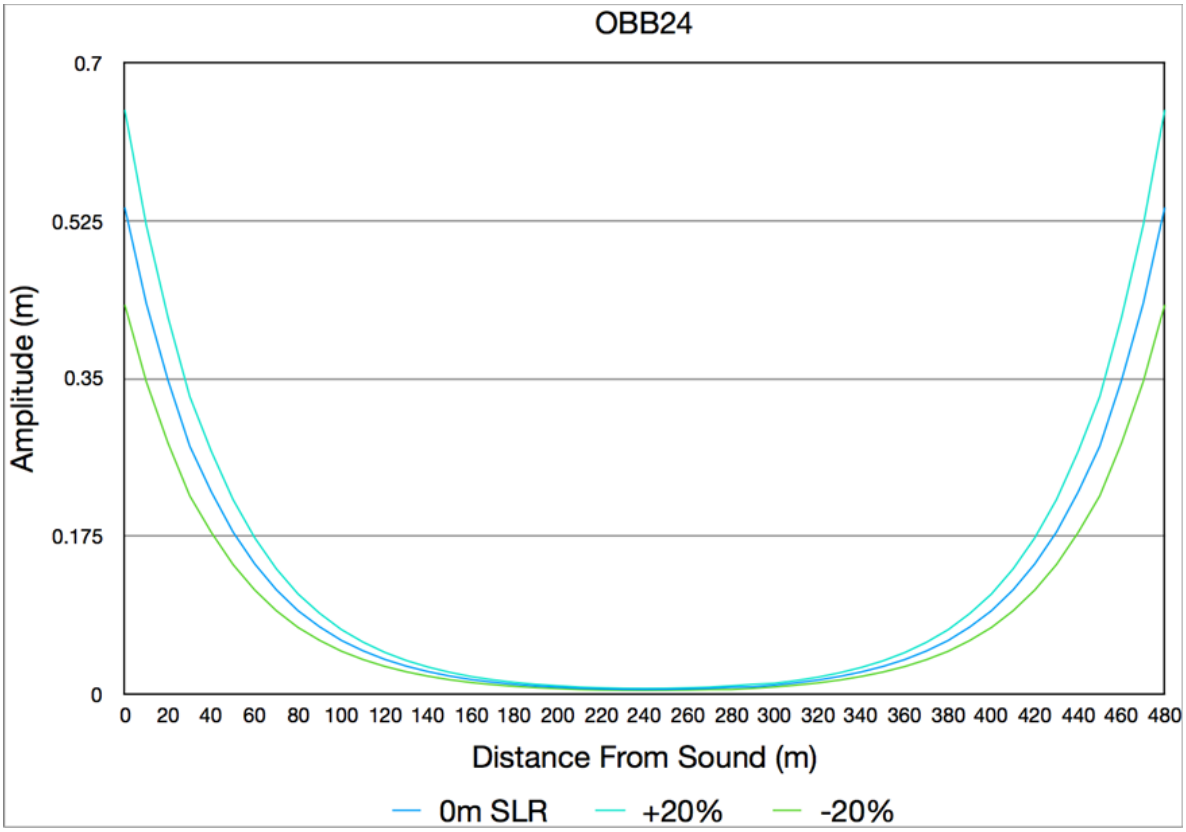
OBB24
0.7
0.525
0.35
0.175
0
Amplitude (m)
0 20 40 60 80 100 120 140 160 180 200 220 240 260 280 300 320 340 360 380 400 420 440 460 480
Distance From Sound (m)
0m SLR
+20%
-20%

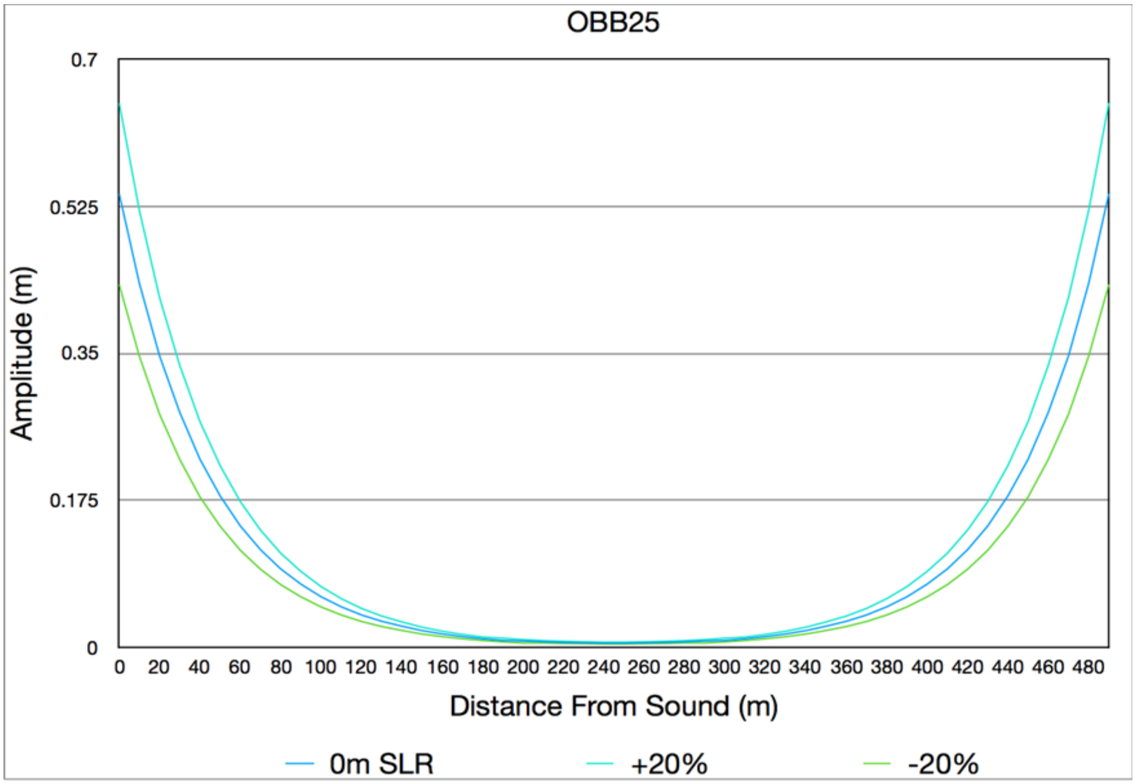
OBB25
0.7
0.525
0.35
0.175
0
Amplitude (m)
0 20 40 60 80 100 120 140 160 180 200 220 240 260 280 300 320 340 360 380 400 420 440 460 480
Distance From Sound (m)
0m SLR
+20%
-20%

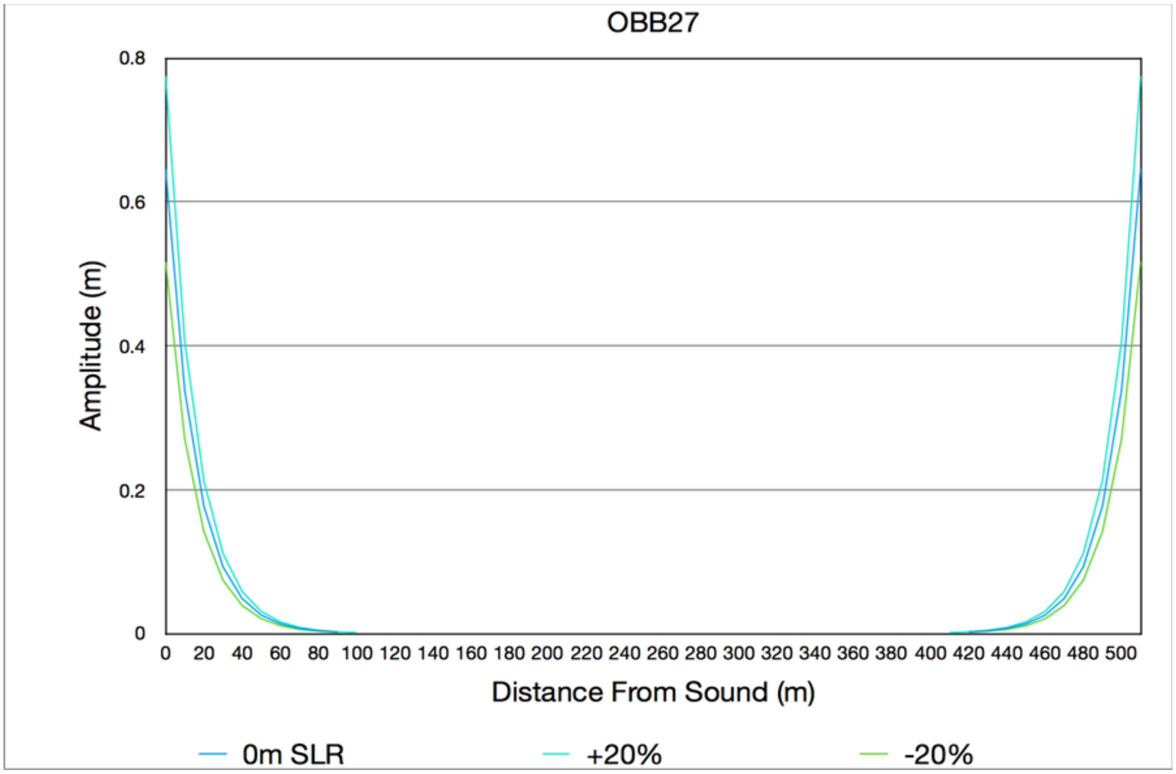
OBB27
Amplitude (m)
0.8
0.6
0.4
0.2
0
0 20 40 60 80 100 120 140 160 180 200 220 240 260 280 300 320 340 360 380 400 420 440 460 480 500
Distance From Sound (m)
0m SLR
+20%
-20%

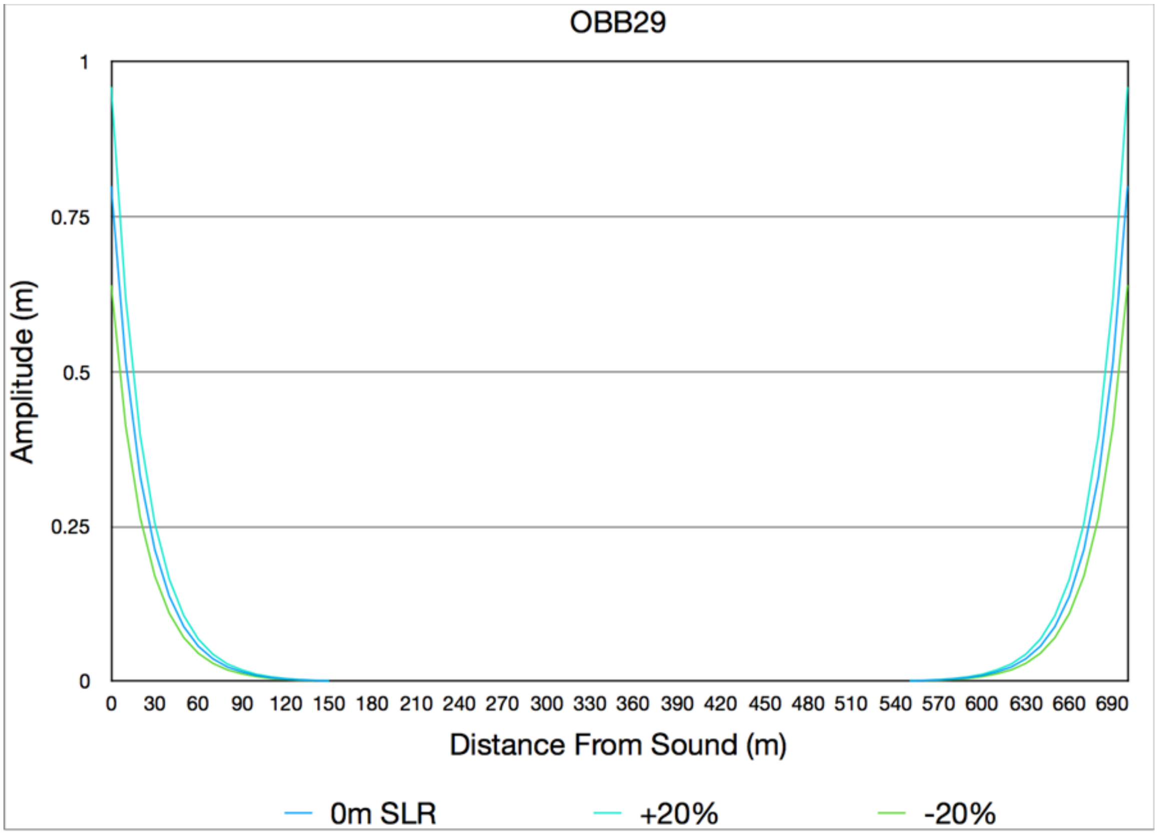
OBB29
Amplitude (m)
1
0.75
0.5
0.25
0
0 30 60 90 120 150 180 210 240 270 300 330 360 390 420 450 480 510 540 570 600 630 660 690
Distance From Sound (m)
0m SLR
+20%
-20%

D- Well head data

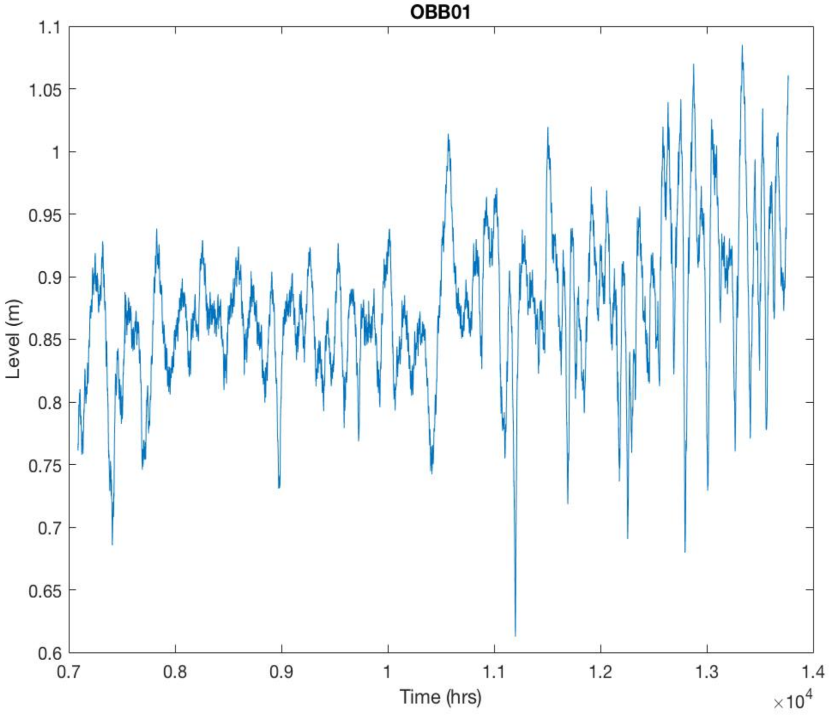

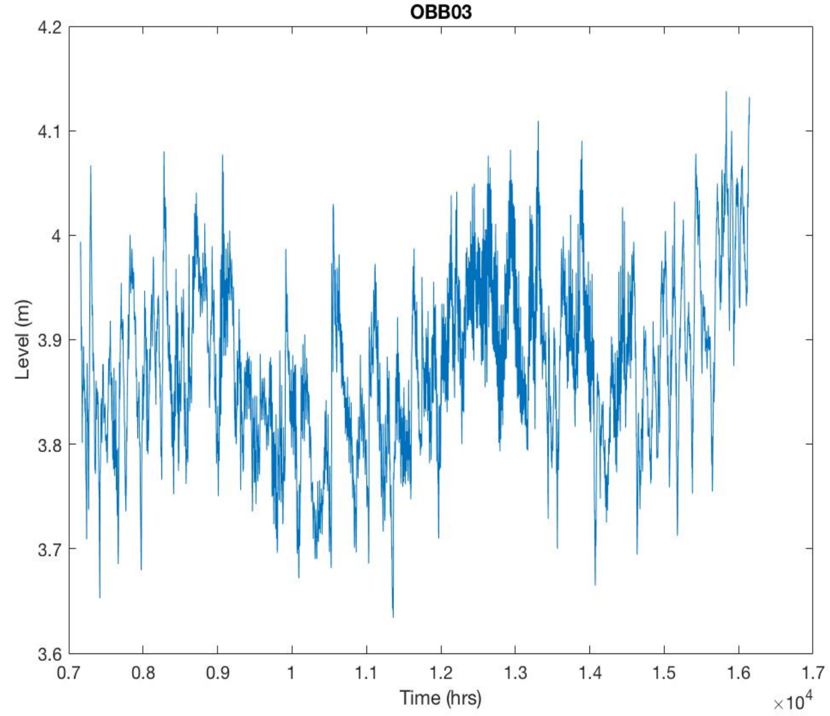

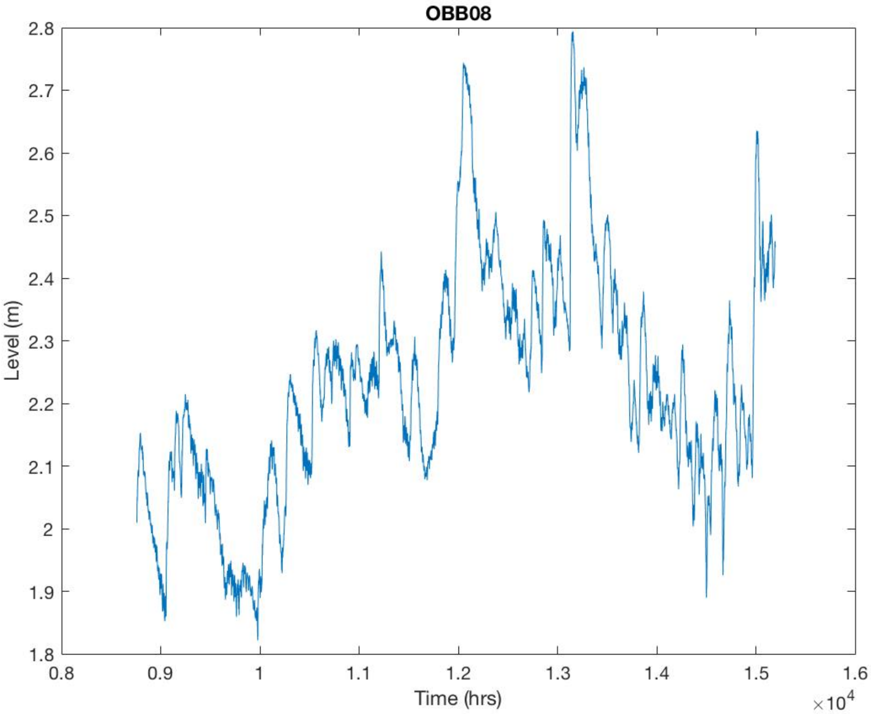
OBB08
Level (m)
2.8
2.7
2.6
2.5
2.4
2.3
2.2
2.1
2
1.9
1.8
0.8
0.9
1
1.1
1.2
1.3
1.4
1.5
1.6
Time (hrs)
×10^4

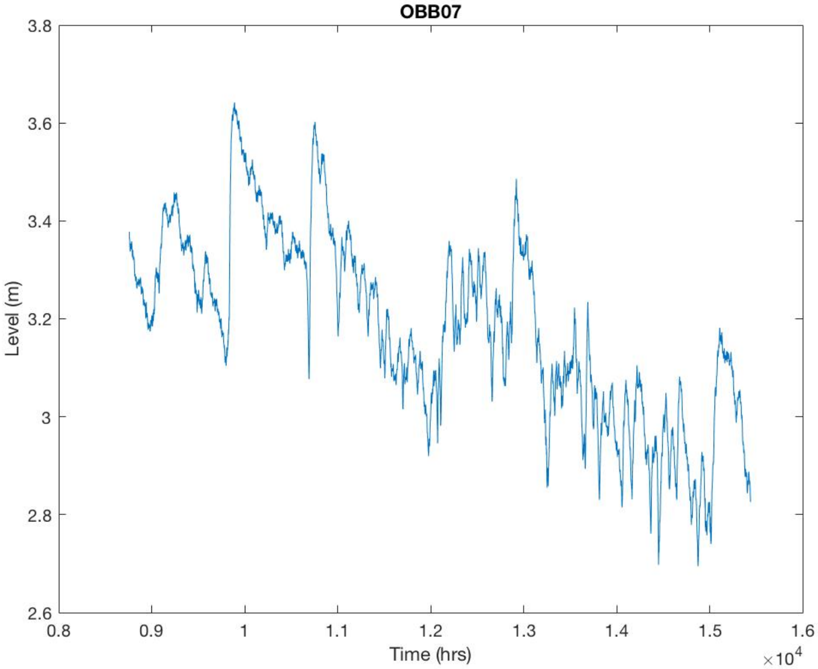
OBB07
Level (m)
3.8
3.6
3.4
3.2
3
2.8
2.6
0.8
0.9
1
1.1
1.2
1.3
1.4
1.5
1.6
Time (hrs)
×10^4

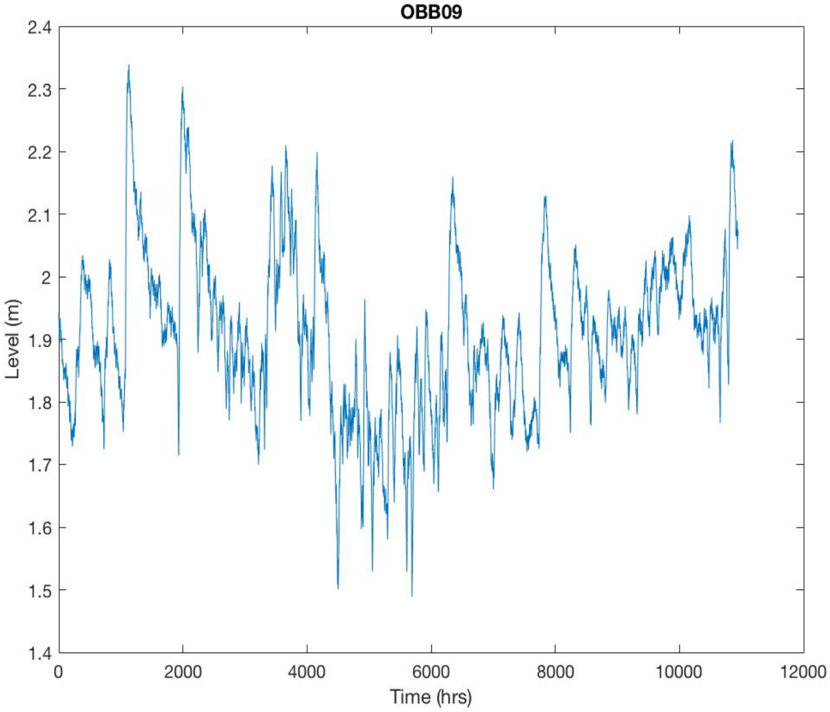
OBB09
Level (m)
2.4
2.3
2.2
2.1
2
1.9
1.8
1.7
1.6
1.5
1.4
0
2000
4000
6000
8000
10000
12000
Time (hrs)

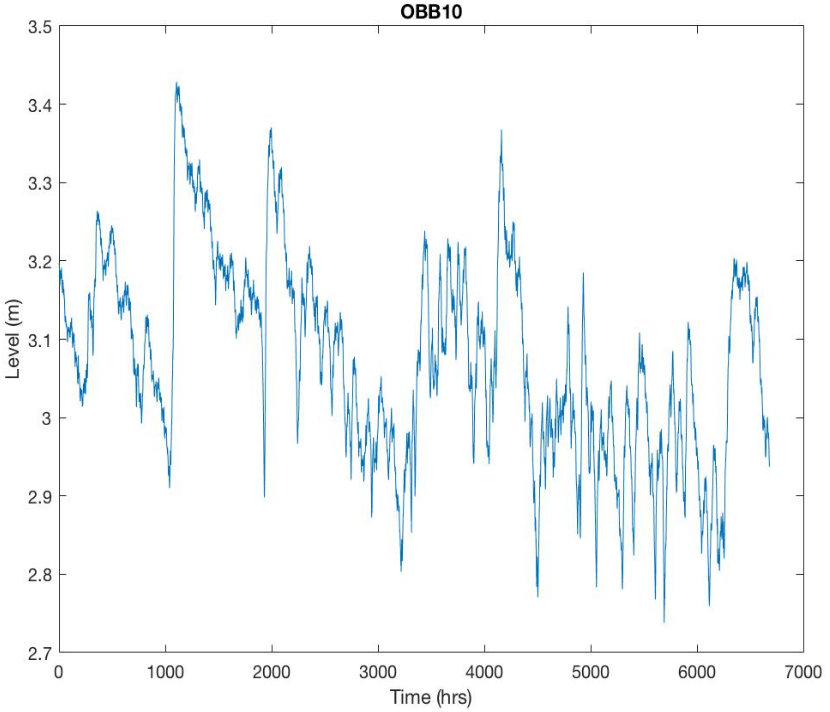
OBB10
Level (m)
3.5
3.4
3.3
3.2
3.1
3
2.9
2.8
2.7
0
1000
2000
3000
4000
5000
6000
7000
Time (hrs)

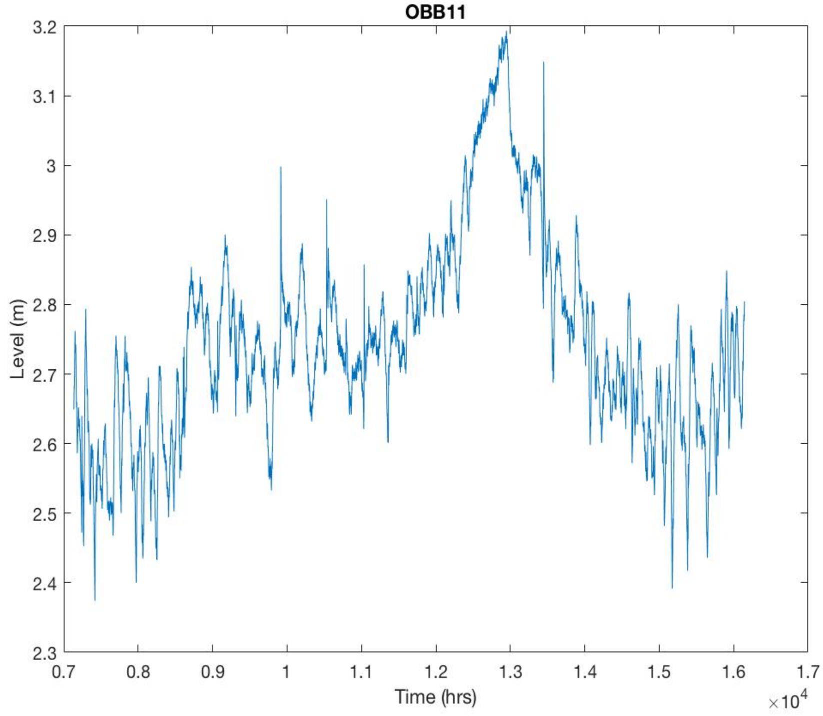
OBB11
Level (m)
3.2
3.1
3
2.9
2.8
2.7
2.6
2.5
2.4
2.3
0.7
0.8
0.9
1
1.1
1.2
1.3
1.4
1.5
1.6
1.7
Time (hrs)
×10^4

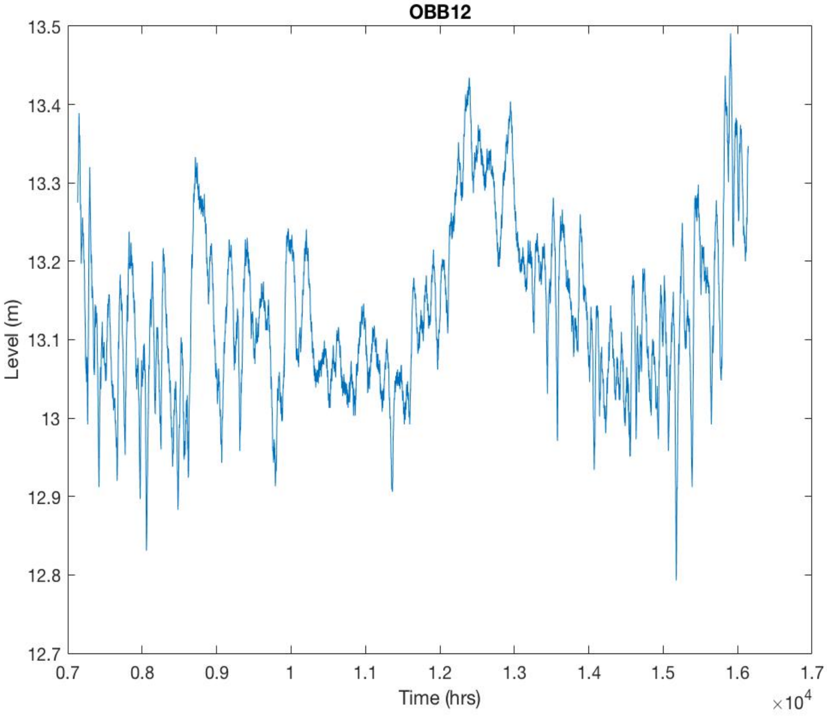
OBB12
Level (m)
13.5
13.4
13.3
13.2
13.1
13
12.9
12.8
12.7
0.7
0.8
0.9
1
1.1
1.2
1.3
1.4
1.5
1.6
1.7
Time (hrs)
×10^4

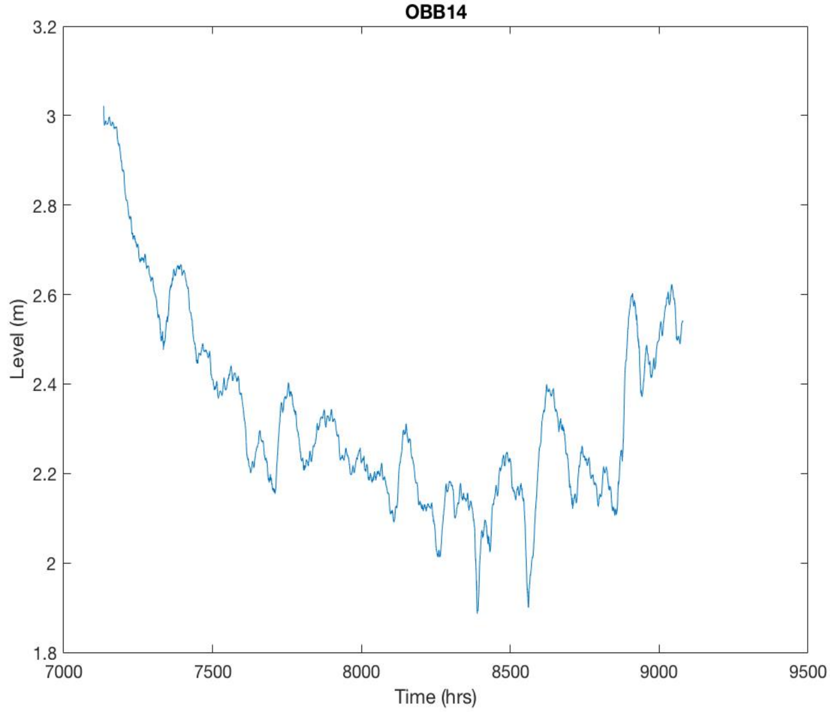
OBB14
Level (m)
3.2
3
2.8
2.6
2.4
2.2
2
1.8
7000
7500
8000
8500
9000
9500
Time (hrs)

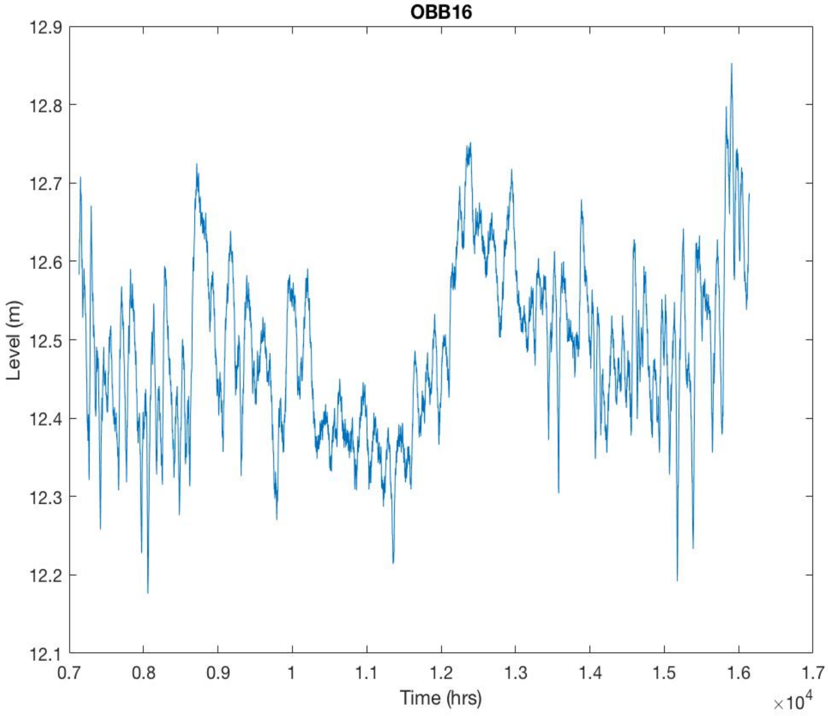
OBB16
Level (m)
12.9
12.8
12.7
12.6
12.5
12.4
12.3
12.2
12.1
0.7
0.8
0.9
1
1.1
1.2
1.3
1.4
1.5
1.6
1.7
Time (hrs)
×10^4

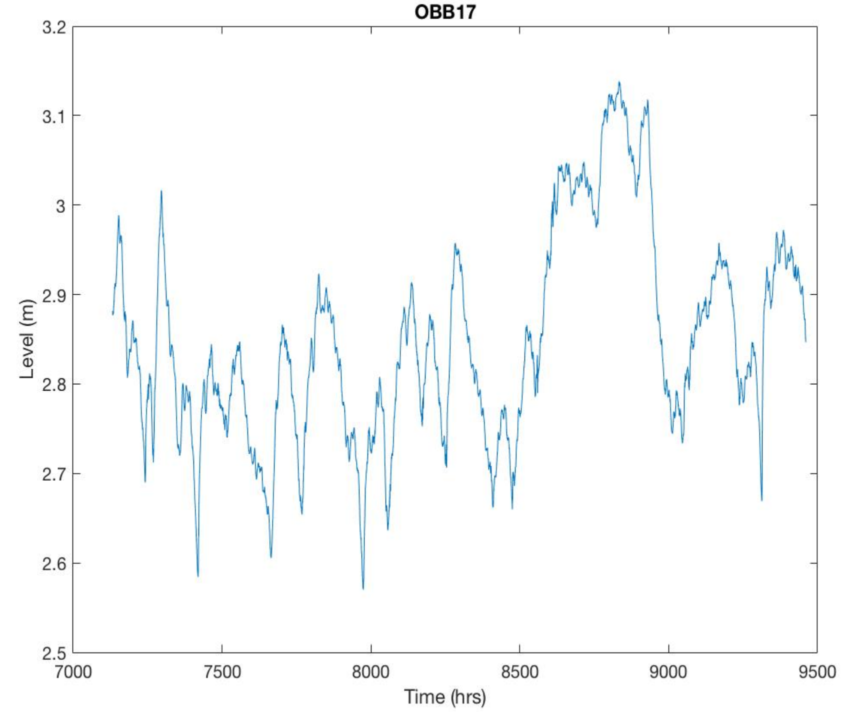
OBB17
Level (m)
3.2
3.1
3
2.9
2.8
2.7
2.6
2.5
7000
7500
8000
8500
9000
9500
Time (hrs)

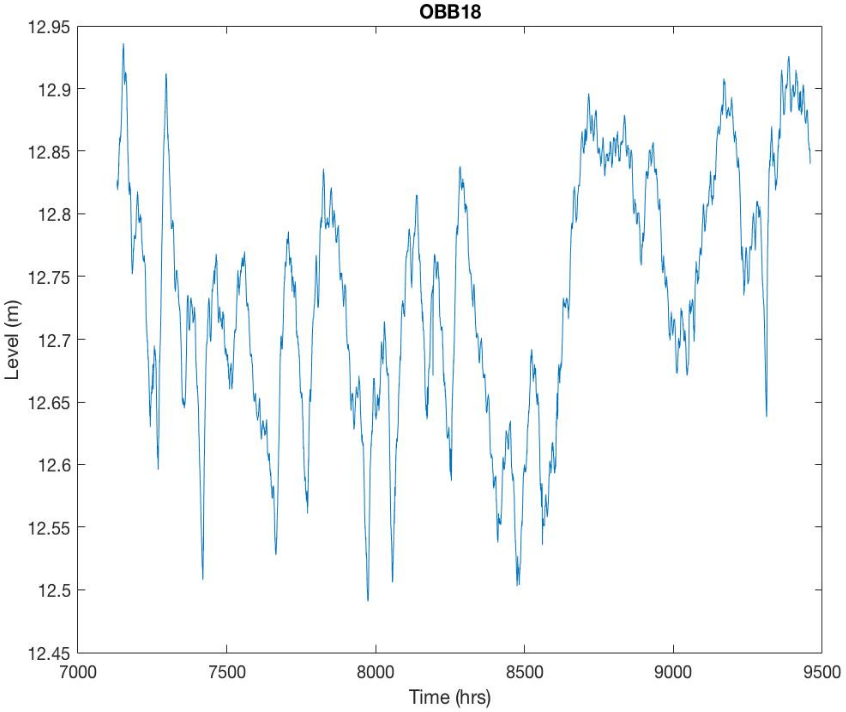
OBB18
Level (m)
12.95
12.9
12.85
12.8
12.75
12.7
12.65
12.6
12.55
12.5
12.45
7000
7500
8000
8500
9000
9500
Time (hrs)

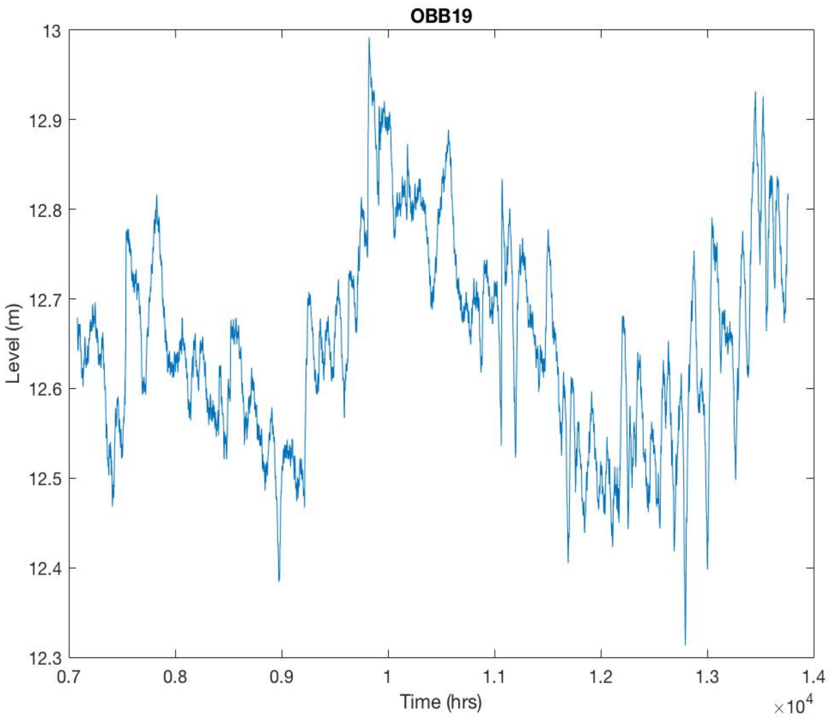
OBB19
Level (m)
12.3
12.4
12.5
12.6
12.7
12.8
12.9
13
Time (hrs)
0.7
0.8
0.9
1
1.1
1.2
1.3
1.4
×10^4

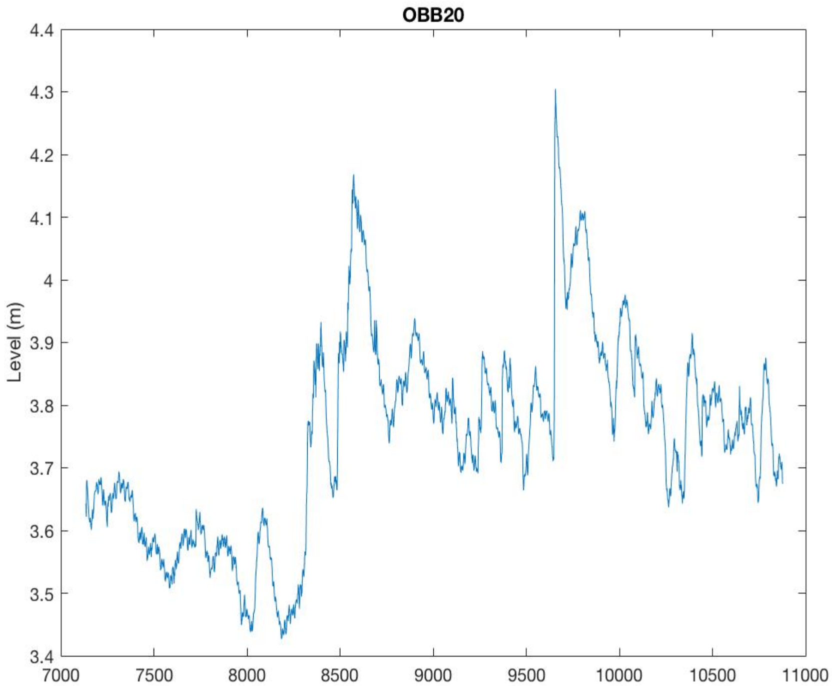
OBB20
Level (m)
3.4
3.5
3.6
3.7
3.8
3.9
4
4.1
4.2
4.3
4.4
Time (hrs)
7000
7500
8000
8500
9000
9500
10000
10500
11000

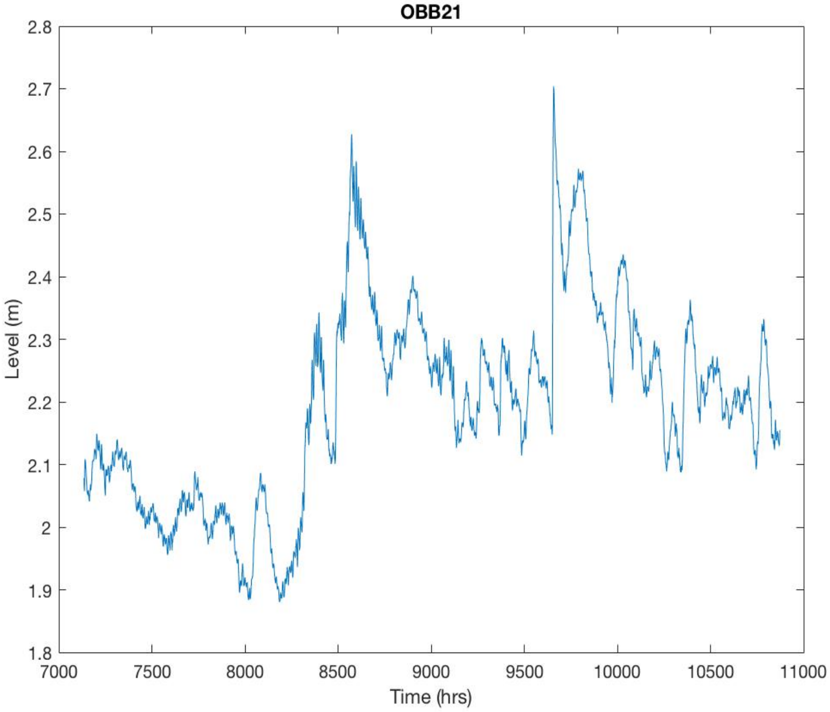
OBB21
Level (m)
2.8
2.7
2.6
2.5
2.4
2.3
2.2
2.1
2
1.9
1.8
7000
7500
8000
8500
9000
9500
10000
10500
11000
Time (hrs)

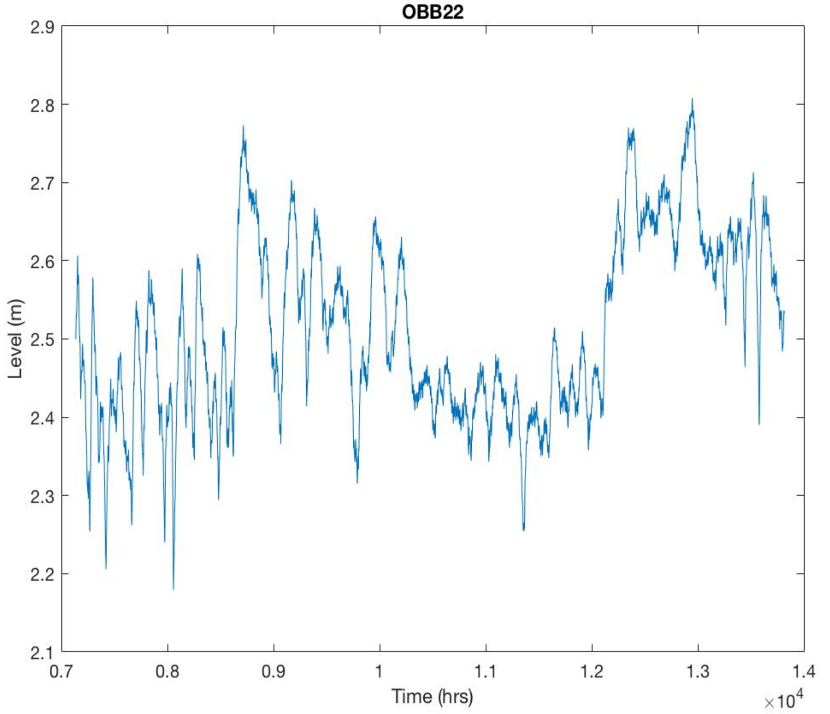
OBB22
Level (m)
2.9
2.8
2.7
2.6
2.5
2.4
2.3
2.2
2.1
0.7
0.8
0.9
1
1.1
1.2
1.3
1.4
Time (hrs)
×10^4

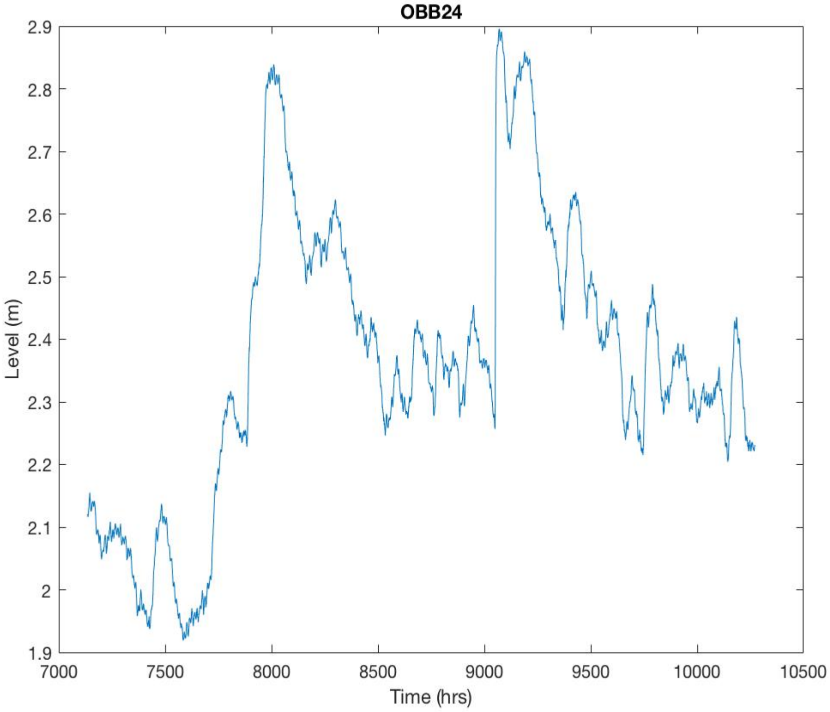
OBB24
Level (m)
Time (hrs)
2.9
2.8
2.7
2.6
2.5
2.4
2.3
2.2
2.1
2
1.9
7000
7500
8000
8500
9000
9500
10000
10500

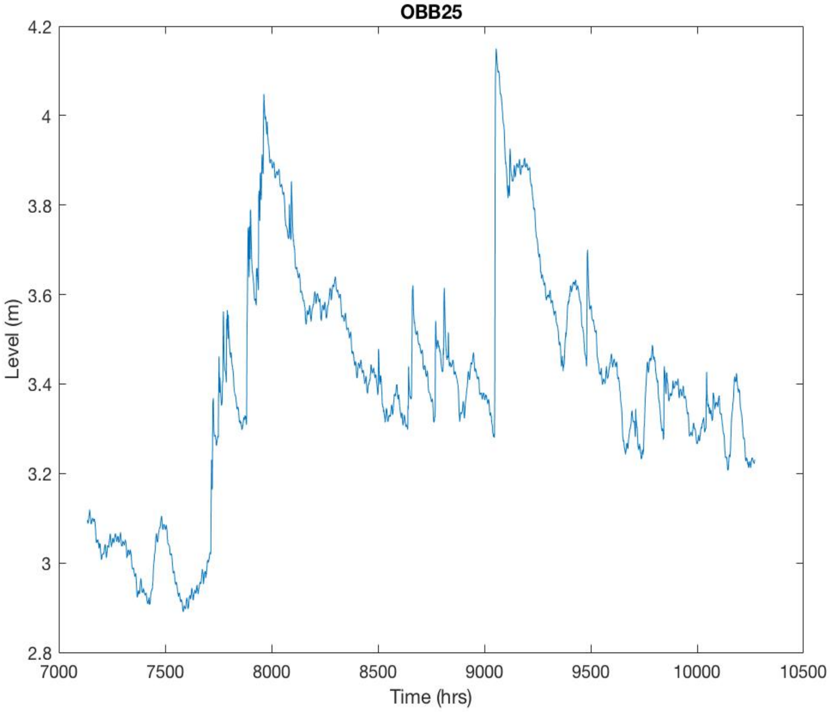
OBB25
Level (m)
Time (hrs)
4.2
4
3.8
3.6
3.4
3.2
3
2.8
7000
7500
8000
8500
9000
9500
10000
10500

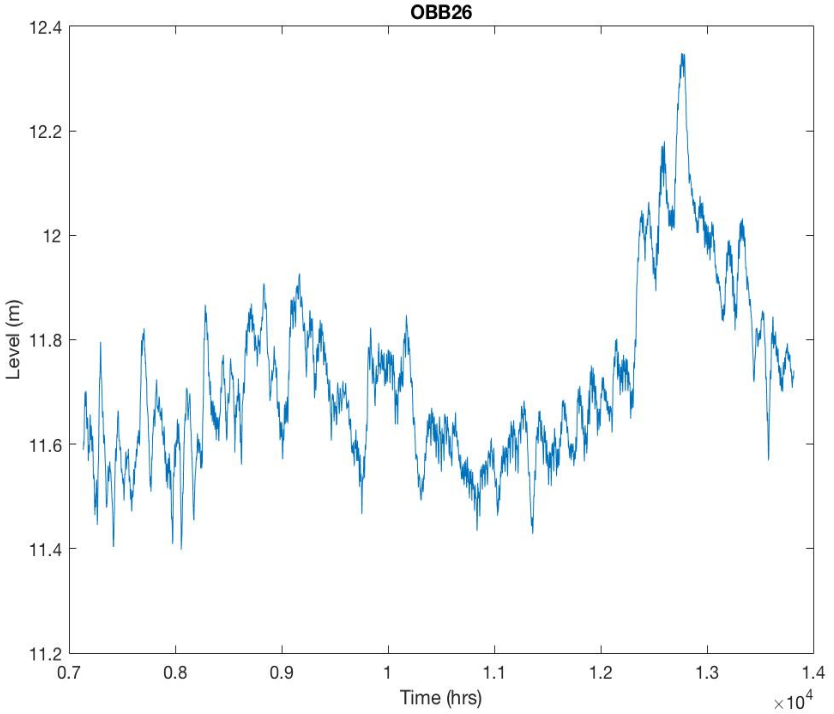
OBB26
Level (m)
12.4
12.2
12
11.8
11.6
11.4
11.2
0.7
0.8
0.9
1
1.1
1.2
1.3
1.4
Time (hrs)
×10^4

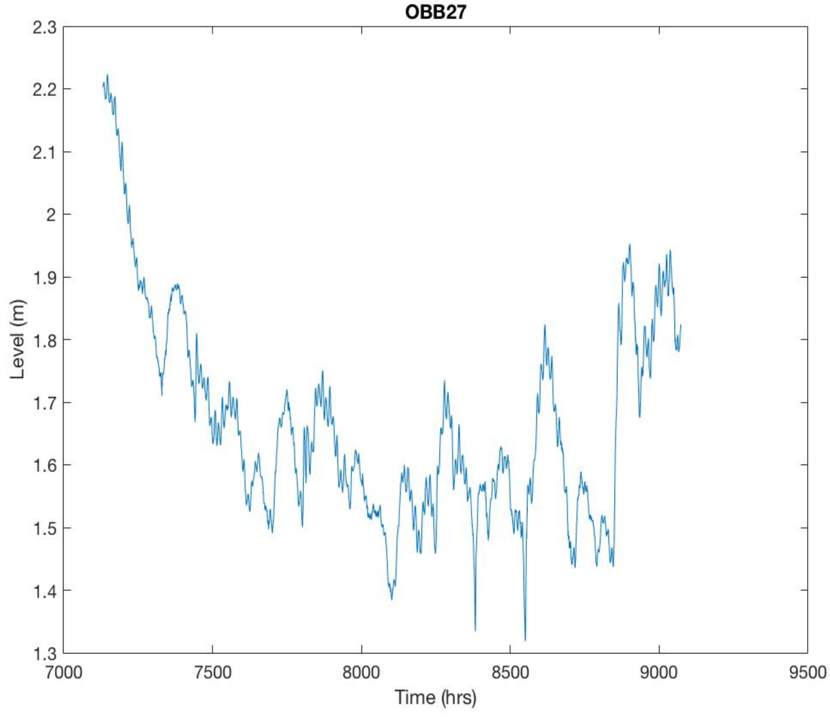
OBB27
Level (m)
2.3
2.2
2.1
2
1.9
1.8
1.7
1.6
1.5
1.4
1.3
7000
7500
8000
8500
9000
9500
Time (hrs)

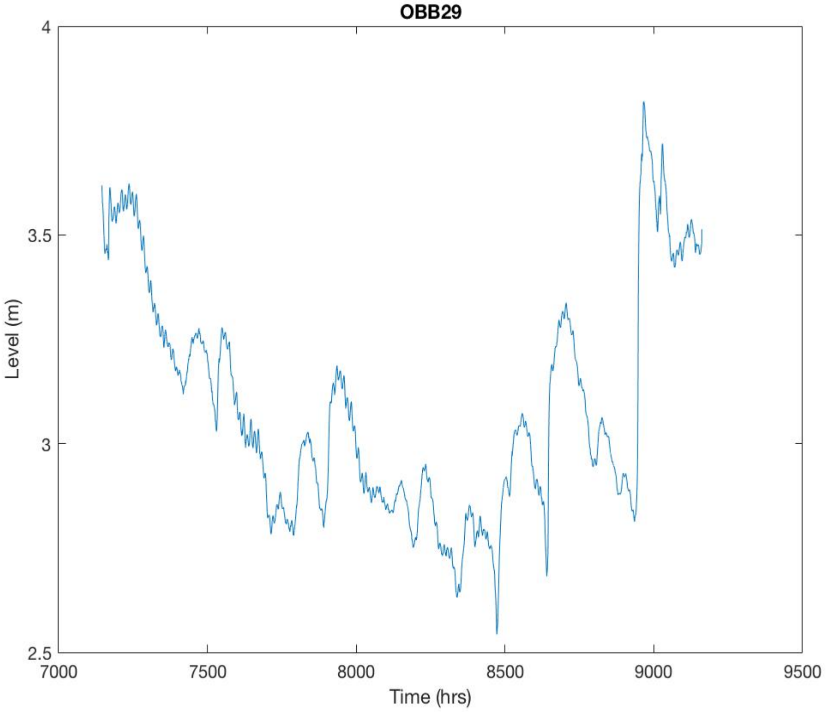
OBB29
Level (m)
4
3.5
3
2.5
7000
7500
8000
8500
9000
9500
Time (hrs)

E – Aquifer thickness and tidal amplitude maps.

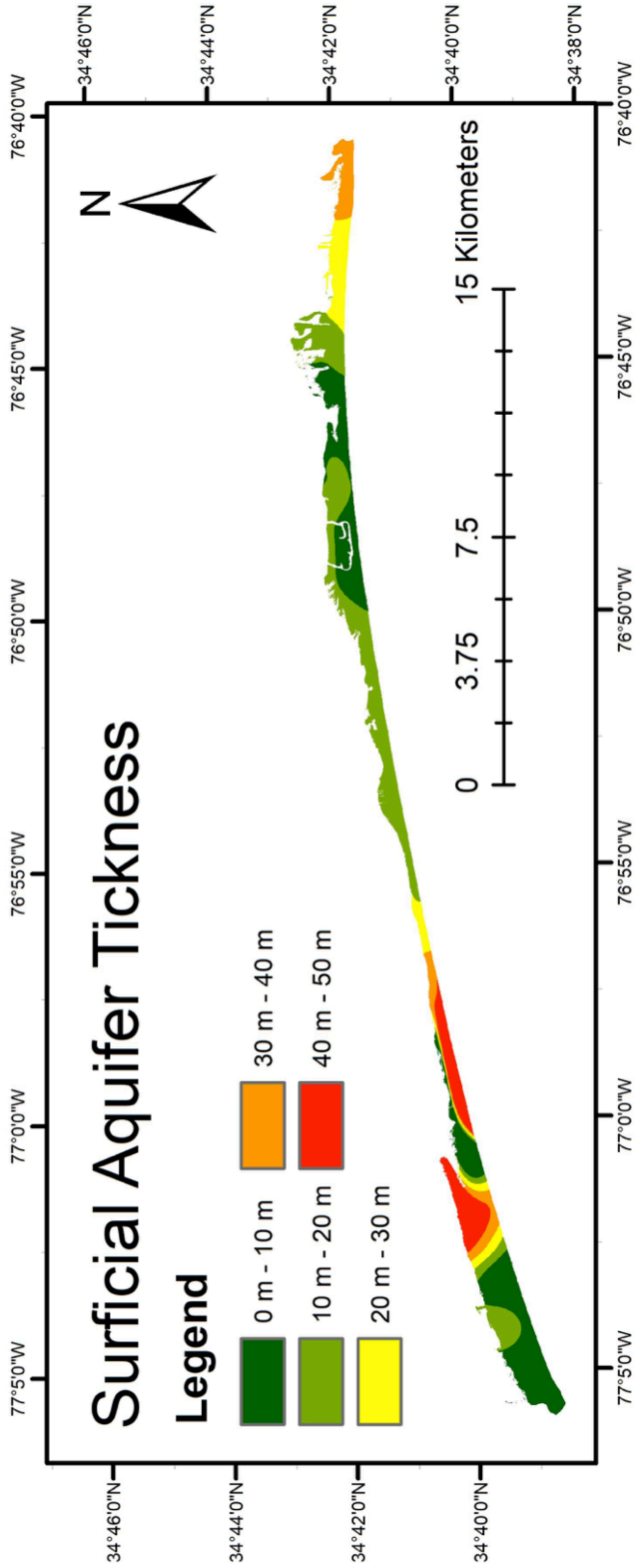

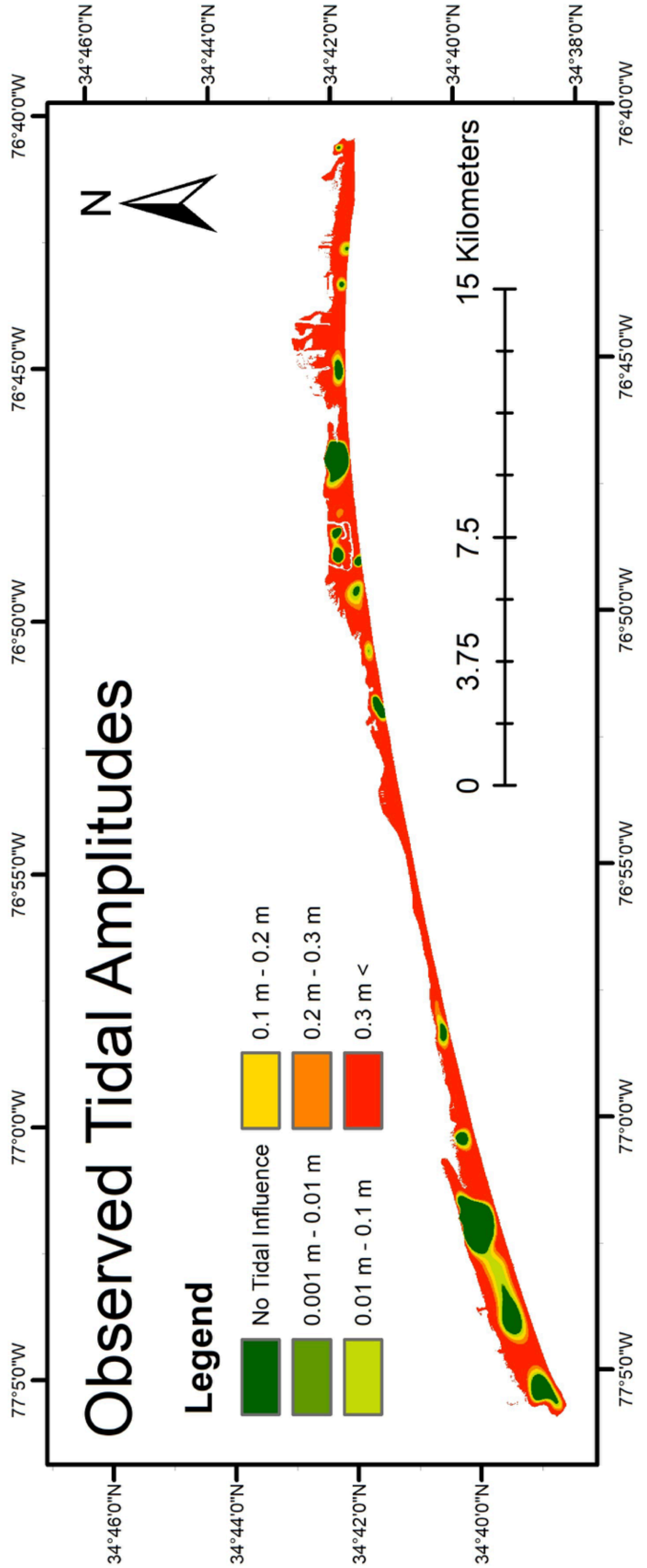

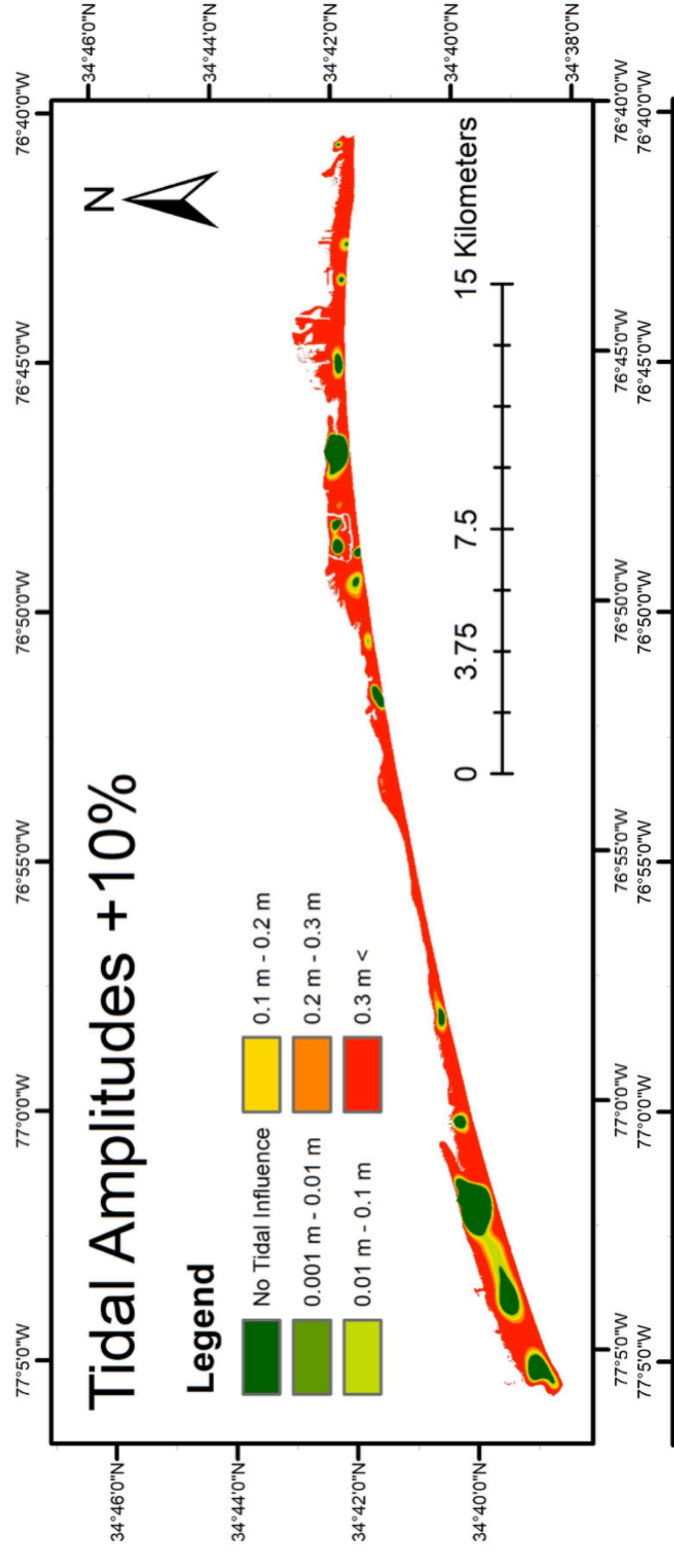
Tidal Amplitudes +10%
Legend
No Tidal Influence
0.001 m - 0.01 m
0.01 m - 0.1 m
0.1 m - 0.2 m
0.2 m - 0.3 m
0.3 m <
N
0
3.75
7.5
15 Kilometers
77°5'0"W
77°0'0"W
76°55'0"W
76°50'0"W
76°45'0"W
76°40'0"W
34°46'0"N
34°44'0"N
34°42'0"N
34°40'0"N
34°38'0"N

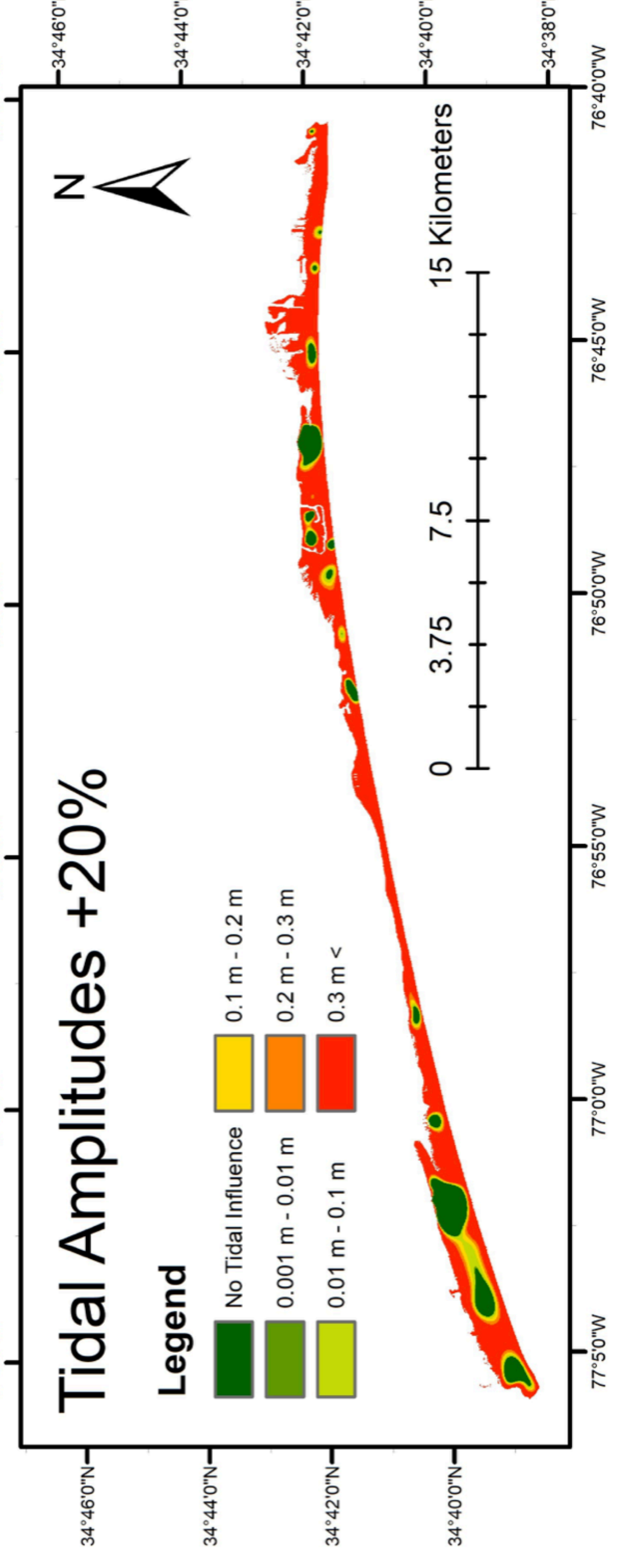
Tidal Amplitudes +20%
Legend
No Tidal Influence
0.001 m - 0.01 m
0.01 m - 0.1 m
0.1 m - 0.2 m
0.2 m - 0.3 m
0.3 m <
N
0
3.75
7.5
15 Kilometers
77°5'0"W
77°0'0"W
76°55'0"W
76°50'0"W
76°45'0"W
76°40'0"W
34°46'0"N
34°44'0"N
34°42'0"N
34°40'0"N
34°38'0"N

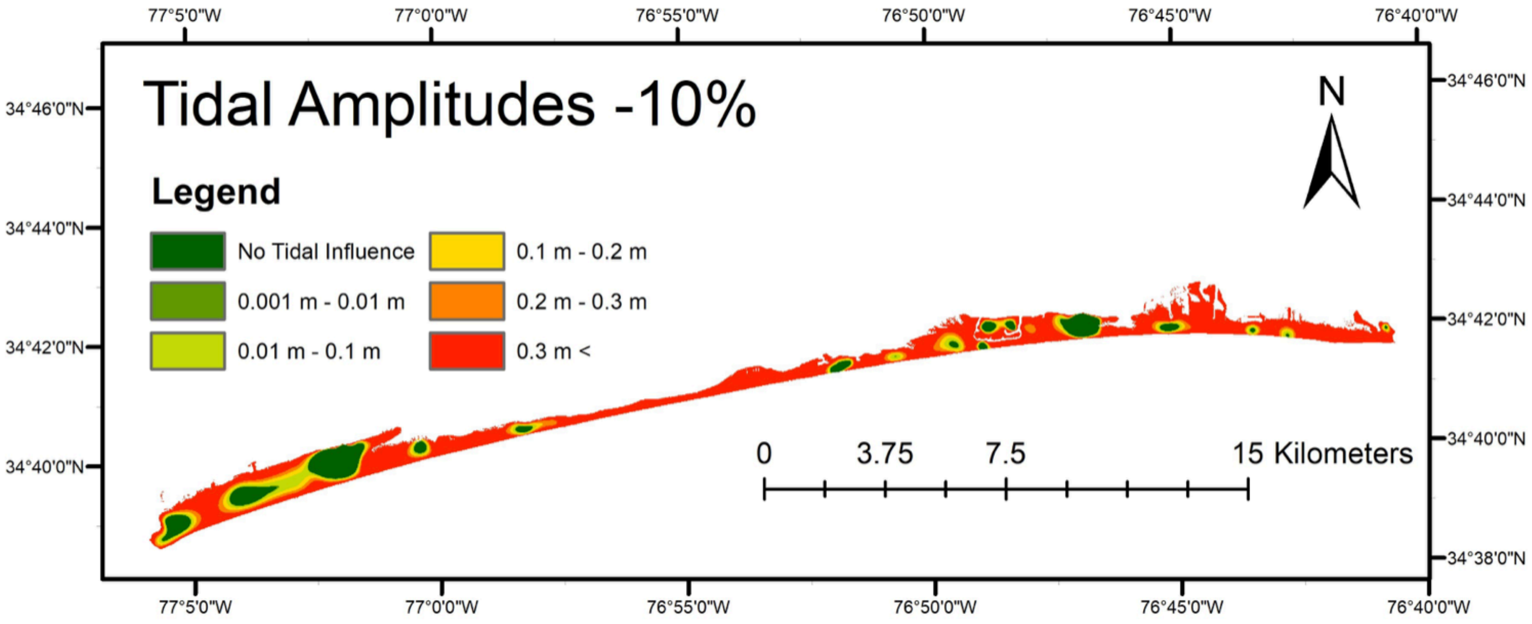
Tidal Amplitudes -10%
Legend
🟩 No Tidal Influence
🟩 0.001 m - 0.01 m
🟩 0.01 m - 0.1 m
🟨 0.1 m - 0.2 m
🟧 0.2 m - 0.3 m
🟥 0.3 m <
N
0
3.75
7.5
15 Kilometers
77°5'0"W
77°0'0"W
76°55'0"W
76°50'0"W
76°45'0"W
76°40'0"W
34°46'0"N
34°44'0"N
34°42'0"N
34°40'0"N
34°38'0"N

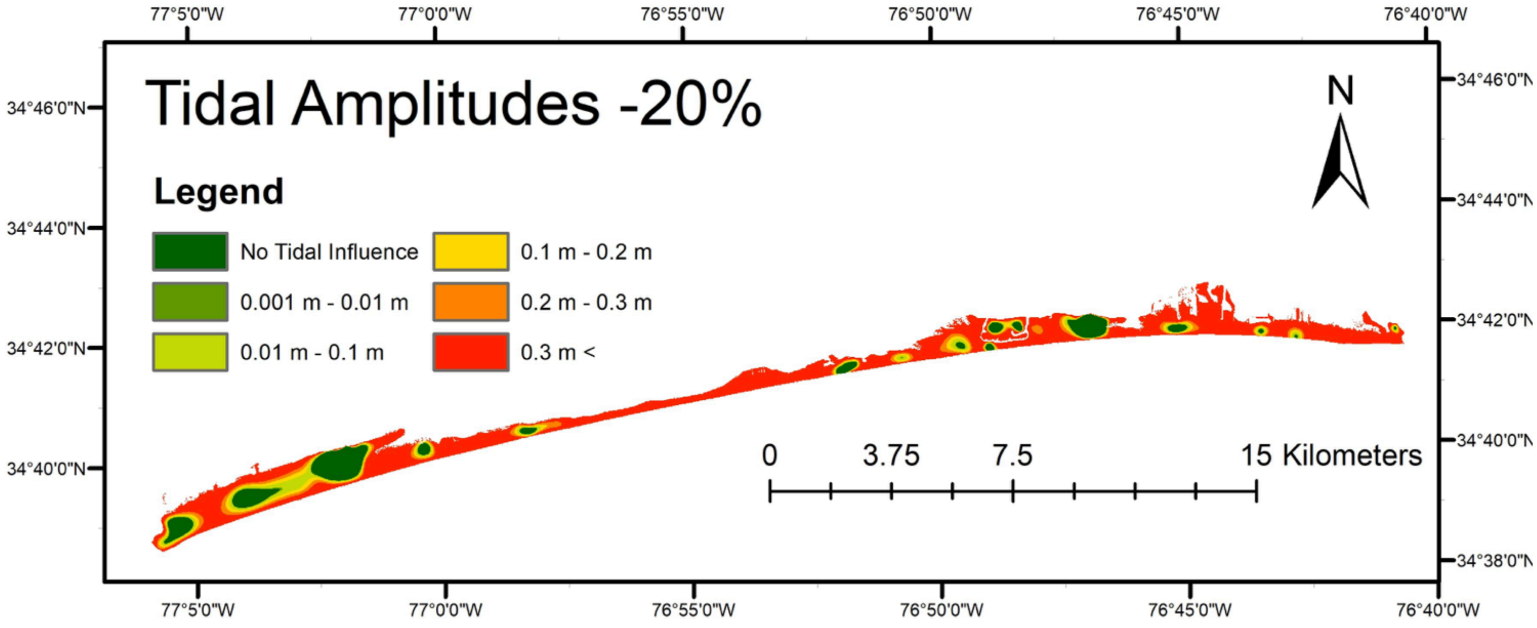
Tidal Amplitudes -20%
Legend
🟩 No Tidal Influence
🟩 0.001 m - 0.01 m
🟩 0.01 m - 0.1 m
🟨 0.1 m - 0.2 m
🟧 0.2 m - 0.3 m
🟥 0.3 m <
N
0
3.75
7.5
15 Kilometers
77°5'0"W
77°0'0"W
76°55'0"W
76°50'0"W
76°45'0"W
76°40'0"W
34°46'0"N
34°44'0"N
34°42'0"N
34°40'0"N
34°38'0"N

F- Expanded table displaying sea-level rise from 0-2 m and where the distance to the base of the saltwater wedge (toe). Equivalent pumping rates were calculated based off the location of the toe. The areas occupied by seawater were then compared to determine that sea-level rise would cause greater saltwater intrusion than groundwater pumping.

SLR (m)	Distance from shoreline to toe (m)	Area occupied by seawater due to SLR (m^2)	Percent of area occupied by seawater (SLR)	Pumping rates (GPD)	Area occupied by seawater due to pumping	Percent of area occupied by seawater (Pumping)	Percent difference (SLR-Pumping)
0	18.7	102.71	0.00	0.00	102.71	0.00	0.00
0.1	19.4	107.70	4.86	2282.43	106.92	4.10	0.76
0.2	19.9	110.81	7.88	45648.86	109.64	6.74	1.14
0.3	20.5	113.84	10.83	68473.29	112.49	9.52	1.31
0.4	21.0	120.73	17.54	91297.72	115.50	12.45	5.09
0.5	21.6	124.15	20.87	114122.16	118.67	15.54	5.33
0.6	22.2	128.47	25.07	136946.59	122.03	18.80	6.27
0.7	22.8	135.31	31.74	159771.02	125.57	22.26	9.48
0.8	23.5	141.06	37.33	187160.34	129.33	25.92	11.41
0.9	24.2	147.79	43.88	207702.33	133.32	29.80	14.08
1	25.0	155.53	51.42	228244.32	137.57	33.94	17.48
1.1	25.8	160.93	56.68	251068.75	142.10	38.34	18.33
1.2	26.7	167.23	62.81	273893.18	146.93	43.05	19.76
1.3	27.7	174.45	69.84	296717.61	152.10	48.09	21.75
1.4	28.7	180.08	75.33	319542.04	157.65	53.49	21.84
1.5	29.8	194.22	89.09	342366.48	163.63	59.30	29.78
1.6	30.9	201.68	96.35	374320.68	170.07	65.58	30.77
1.7	32.2	208.42	102.92	397145.11	177.04	72.36	30.56
1.8	33.6	222.82	116.94	419969.54	184.60	79.73	37.21
1.9	35.1	236.62	130.37	442793.98	192.84	87.75	42.62
2	36.7	248.07	141.52	456488.64	201.86	96.52	44.99

G – Inundation maps.

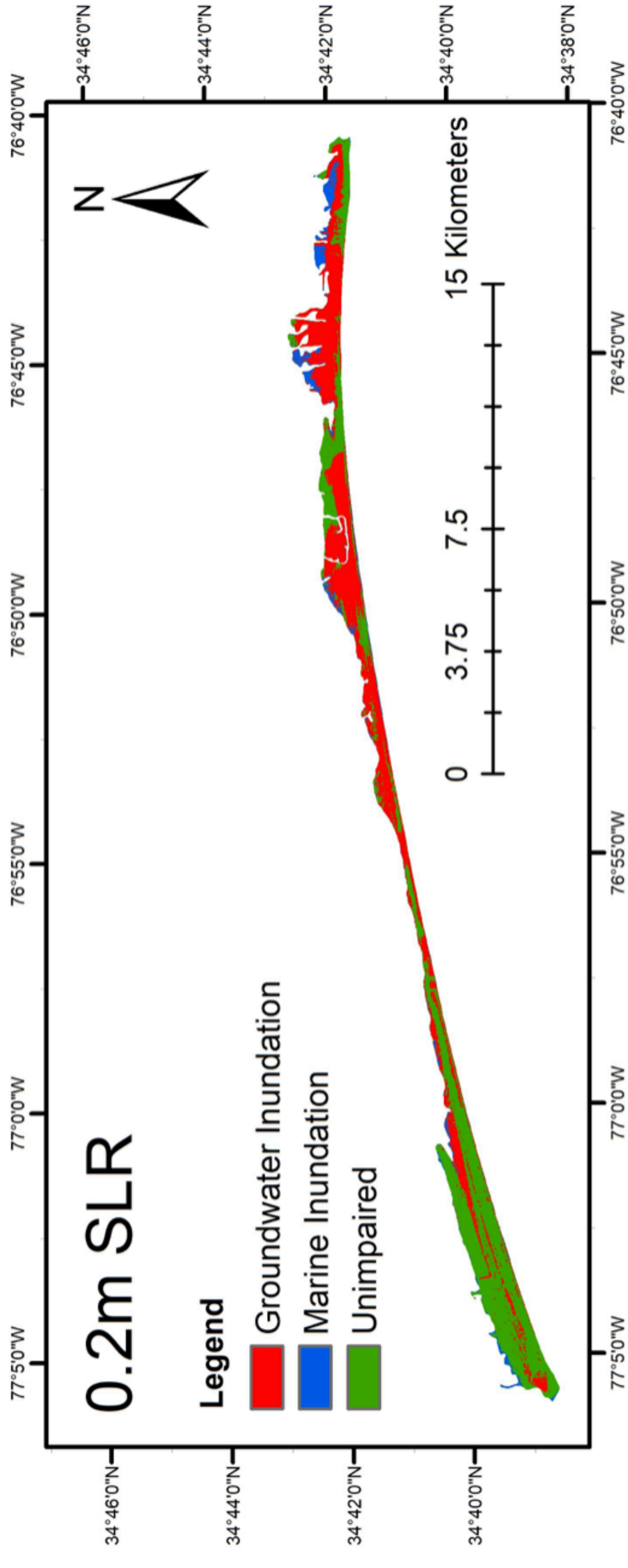

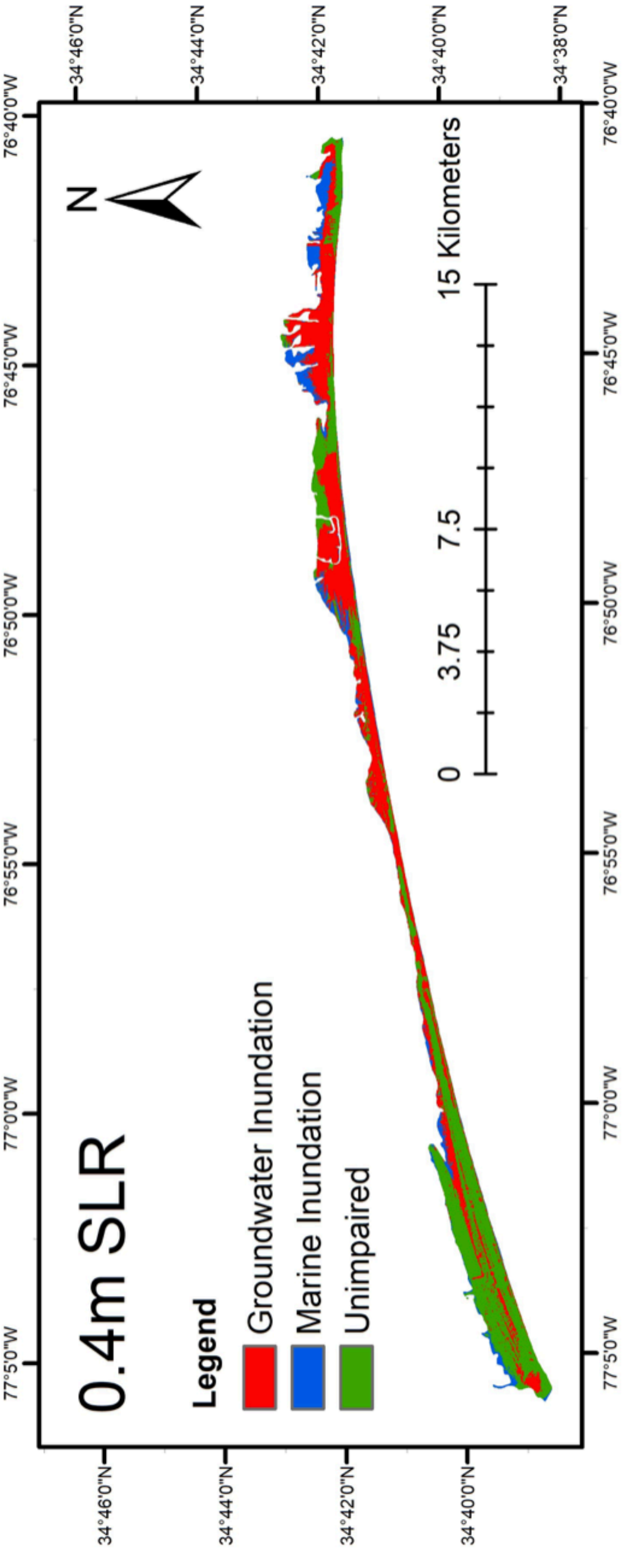

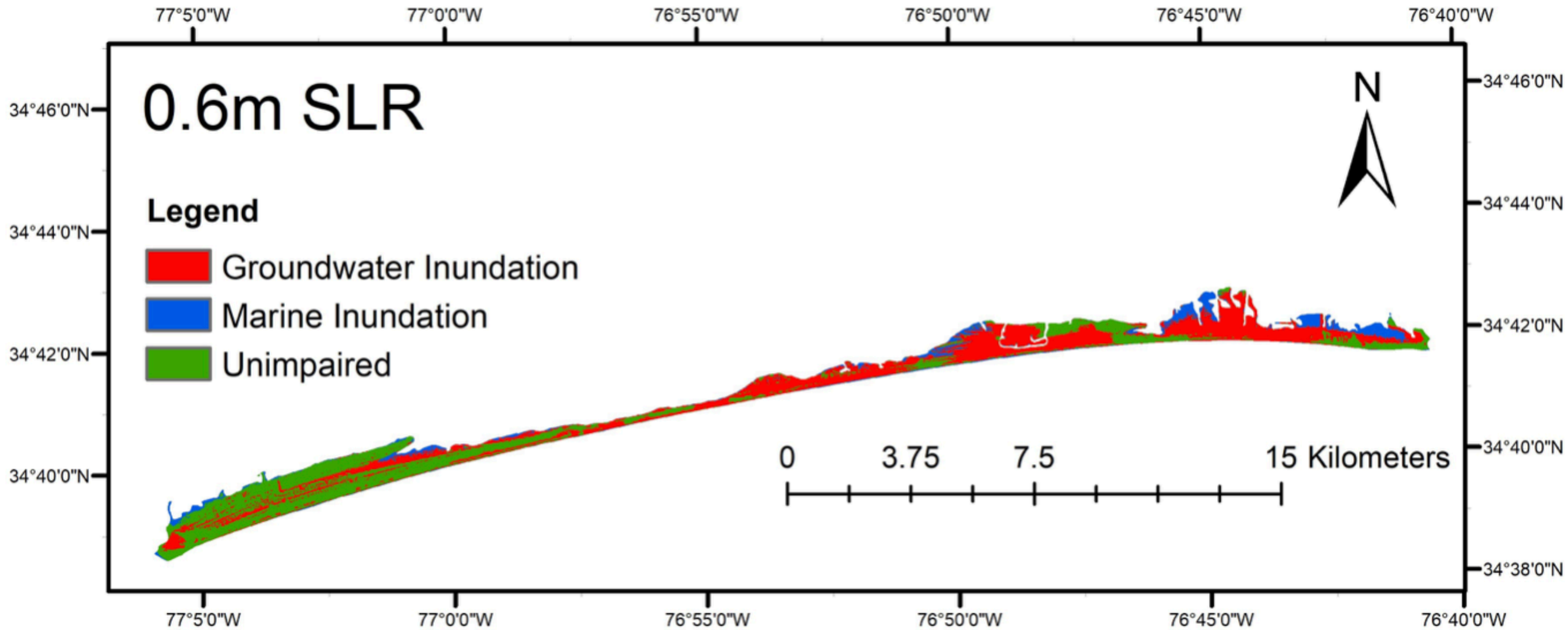
77°5'0"W
77°0'0"W
76°55'0"W
76°50'0"W
76°45'0"W
76°40'0"W
34°46'0"N
34°44'0"N
34°42'0"N
34°40'0"N
34°38'0"N
0.6m SLR
N
Legend
Groundwater Inundation
Marine Inundation
Unimpaired
0
3.75
7.5
15 Kilometers

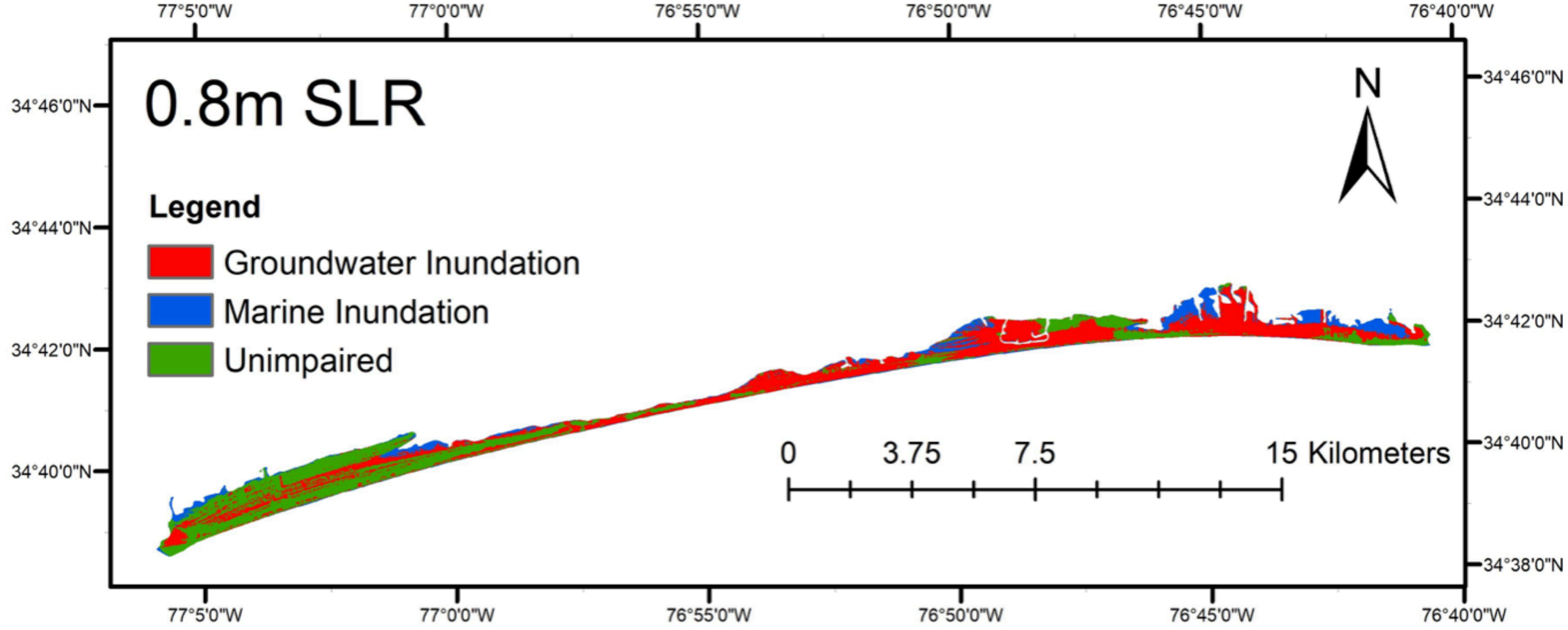
77°5'0"W
77°0'0"W
76°55'0"W
76°50'0"W
76°45'0"W
76°40'0"W
34°46'0"N
34°44'0"N
34°42'0"N
34°40'0"N
34°38'0"N
0.8m SLR
N
Legend
Groundwater Inundation
Marine Inundation
Unimpaired
0
3.75
7.5
15 Kilometers

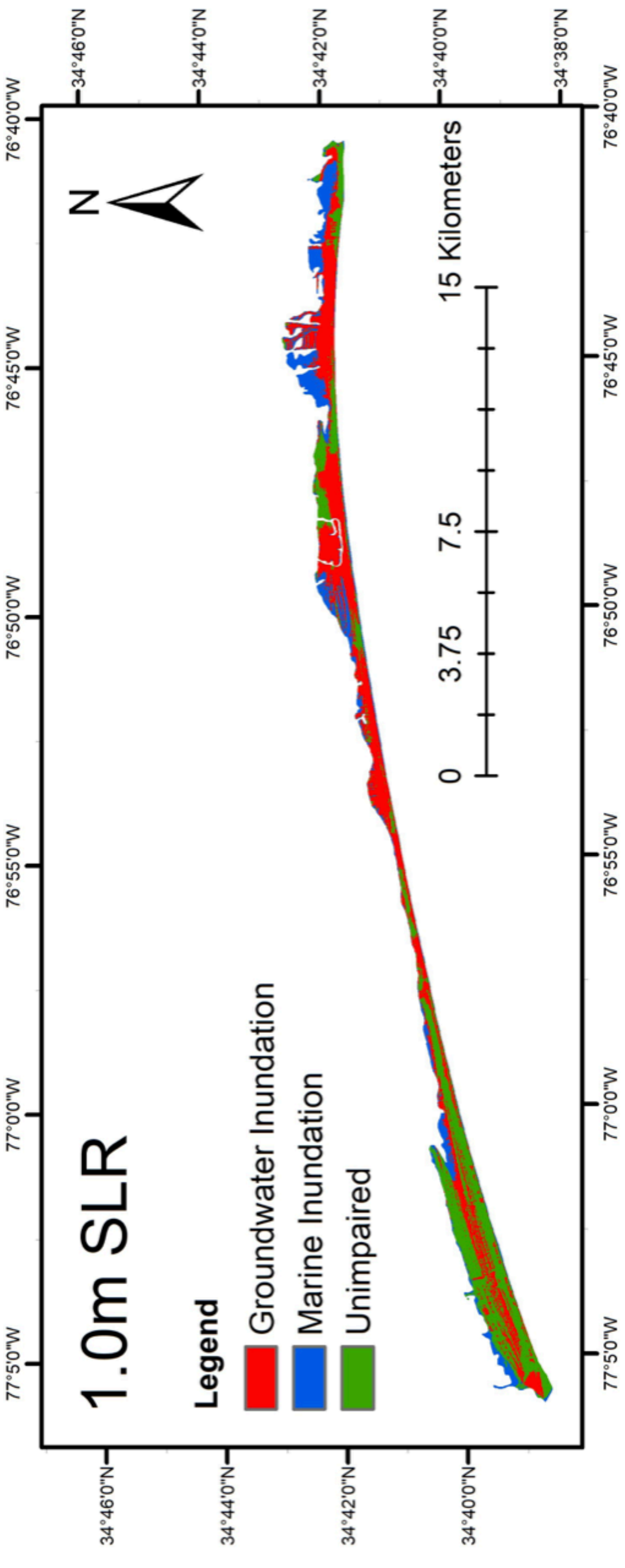
1.0m SLR
Legend
🟥 Groundwater Inundation
🟦 Marine Inundation
🟩 Unimpaired
N
0
3.75
7.5
15 Kilometers
77°5'0"W
77°0'0"W
76°55'0"W
76°50'0"W
76°45'0"W
76°40'0"W
34°46'0"N
34°44'0"N
34°42'0"N
34°40'0"N
34°38'0"N

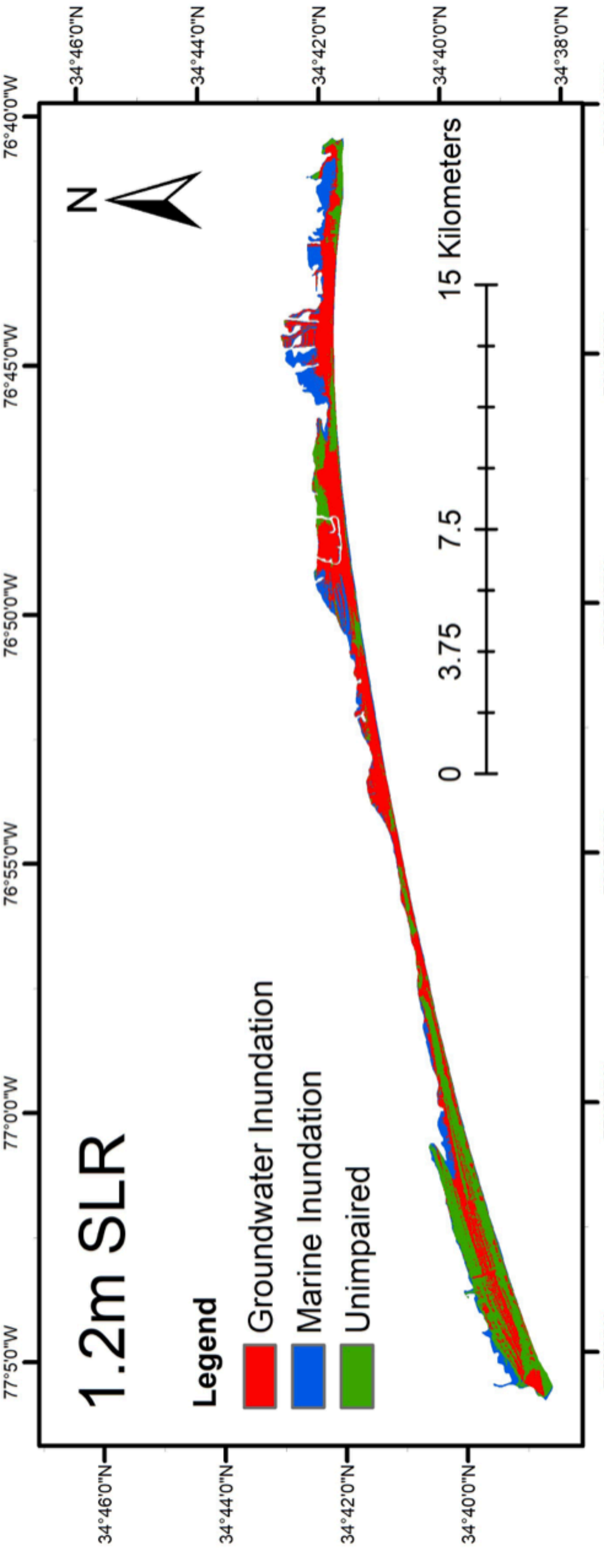
1.2m SLR
Legend
🟥 Groundwater Inundation
🟦 Marine Inundation
🟩 Unimpaired
N
0
3.75
7.5
15 Kilometers
77°5'0"W
77°0'0"W
76°55'0"W
76°50'0"W
76°45'0"W
76°40'0"W
34°46'0"N
34°44'0"N
34°42'0"N
34°40'0"N
34°38'0"N

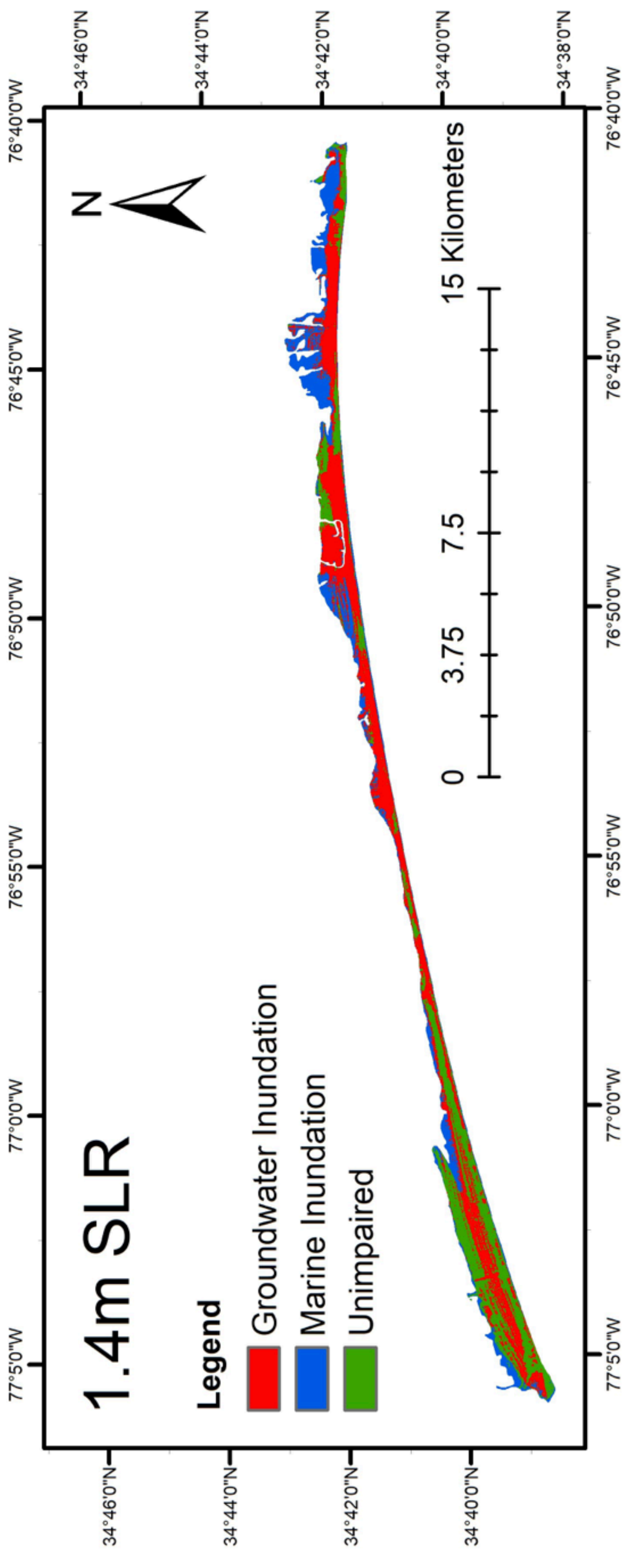
1.4m SLR
Legend
🟥 Groundwater Inundation
🟦 Marine Inundation
🟩 Unimpaired
N
0
3.75
7.5
15 Kilometers
77°5'0"W
77°0'0"W
76°55'0"W
76°50'0"W
76°45'0"W
76°40'0"W
34°46'0"N
34°44'0"N
34°42'0"N
34°40'0"N
34°38'0"N

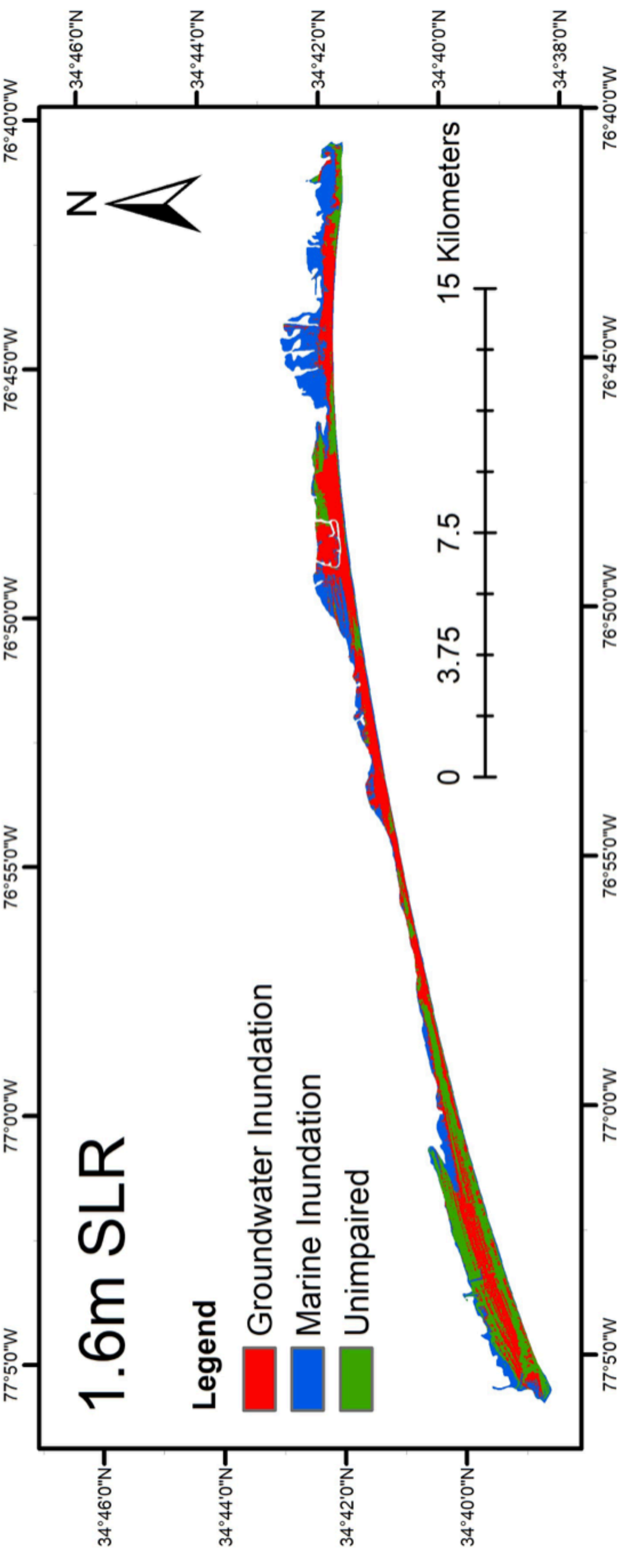
1.6m SLR
Legend
🟥 Groundwater Inundation
🟦 Marine Inundation
🟩 Unimpaired
N
0
3.75
7.5
15 Kilometers
77°5'0"W
77°0'0"W
76°55'0"W
76°50'0"W
76°45'0"W
76°40'0"W
34°46'0"N
34°44'0"N
34°42'0"N
34°40'0"N
34°38'0"N

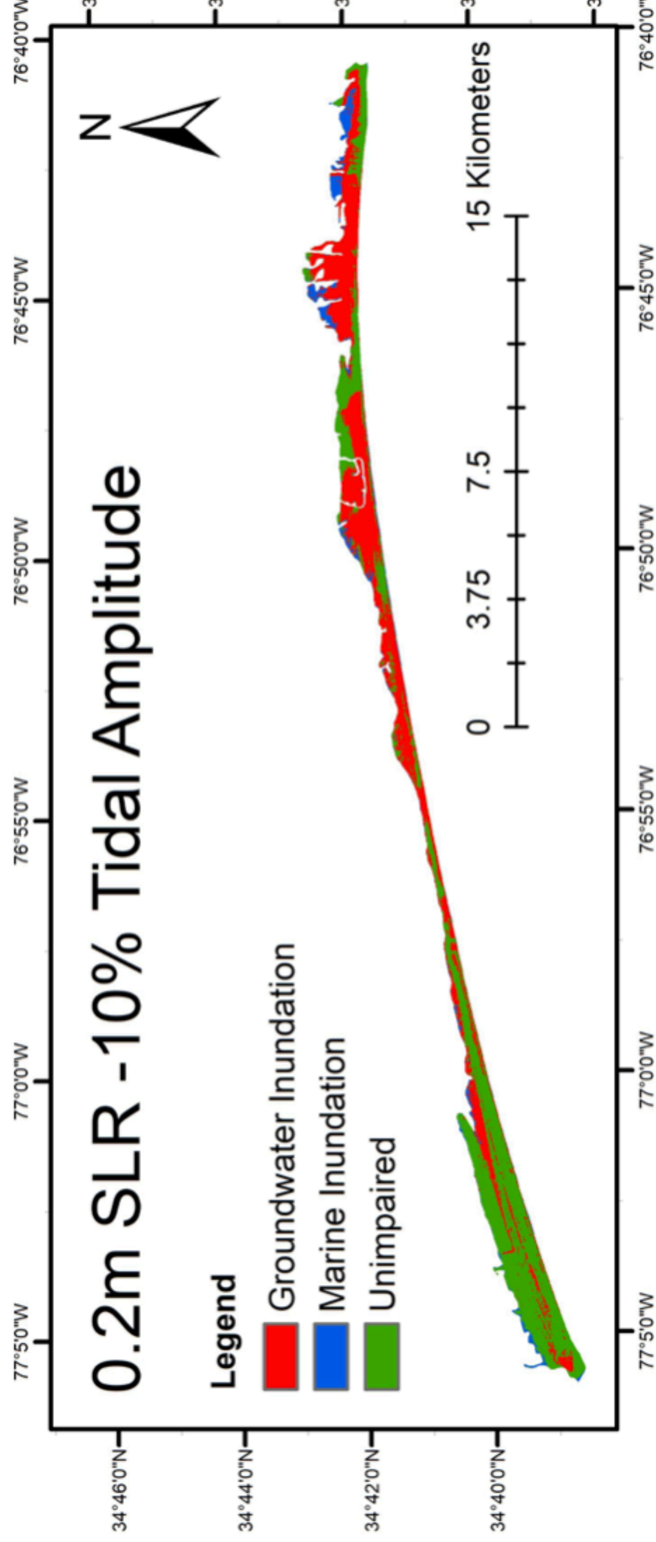
0.2m SLR -10% Tidal Amplitude
Legend
🟥 Groundwater Inundation
🟦 Marine Inundation
🟩 Unimpaired
N
0
3.75
7.5
15 Kilometers
77°5'0"W
77°0'0"W
76°55'0"W
76°50'0"W
76°45'0"W
76°40'0"W
34°46'0"N
34°44'0"N
34°42'0"N
34°40'0"N
34°38'0"N

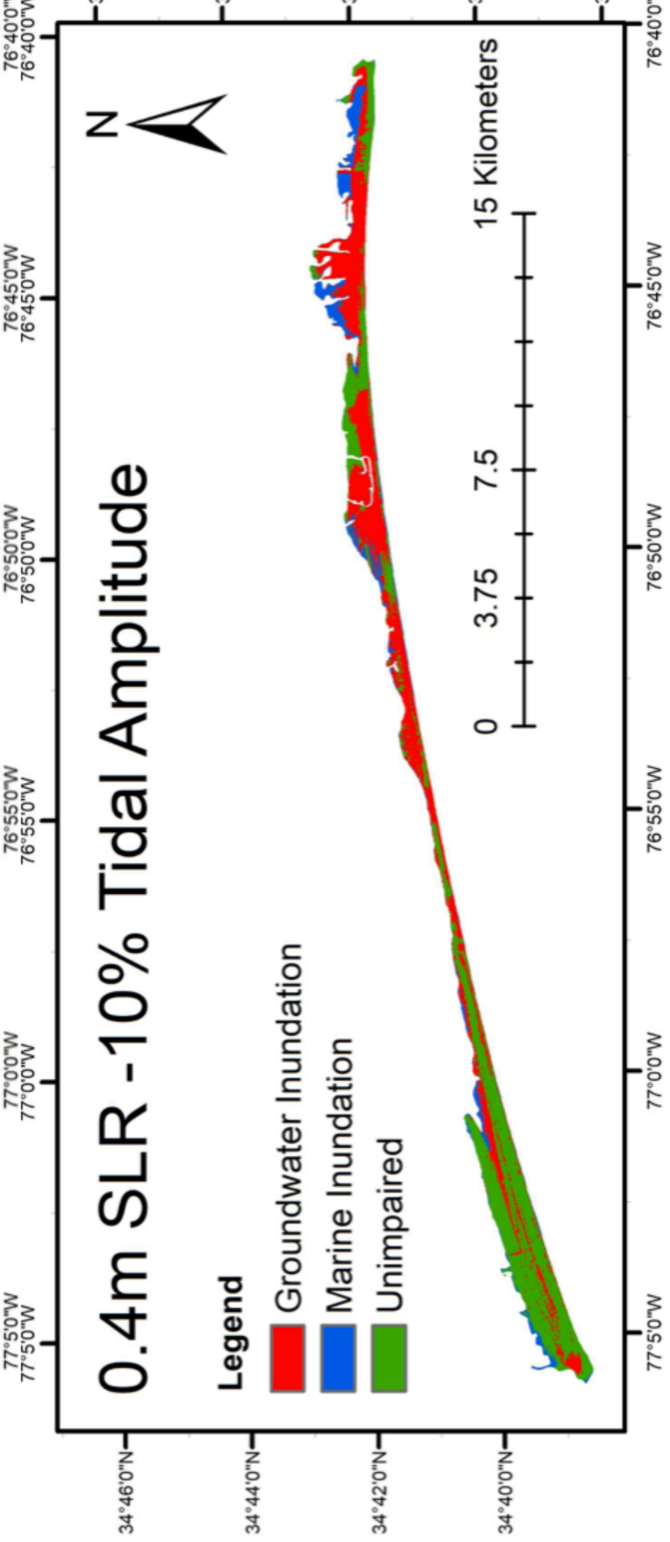
0.4m SLR -10% Tidal Amplitude
Legend
🟥 Groundwater Inundation
🟦 Marine Inundation
🟩 Unimpaired
N
0
3.75
7.5
15 Kilometers
77°5'0"W
77°0'0"W
76°55'0"W
76°50'0"W
76°45'0"W
76°40'0"W
34°46'0"N
34°44'0"N
34°42'0"N
34°40'0"N
34°38'0"N

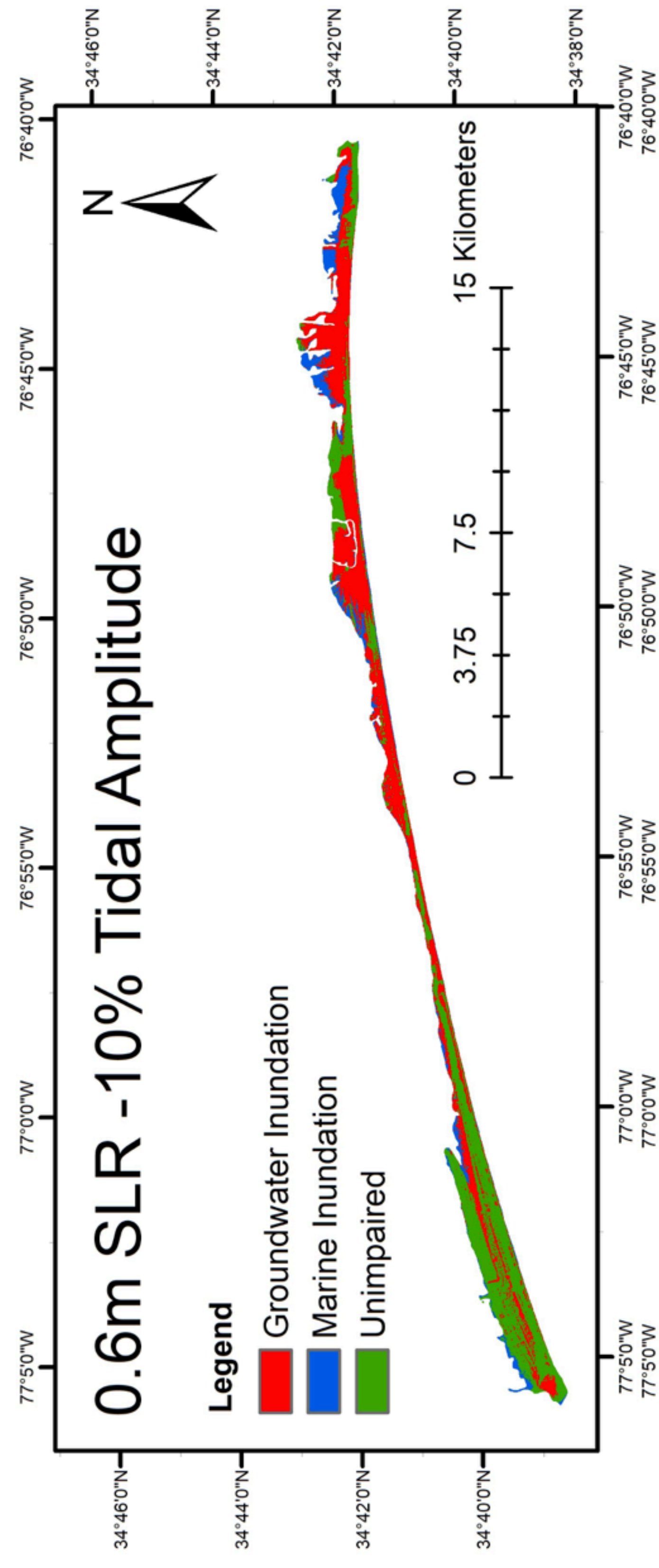
0.6m SLR -10% Tidal Amplitude
Legend
Groundwater Inundation
Marine Inundation
Unimpaired
N
0
3.75
7.5
15 Kilometers
77°5'0"W
77°0'0"W
76°55'0"W
76°50'0"W
76°45'0"W
76°40'0"W
34°46'0"N
34°44'0"N
34°42'0"N
34°40'0"N
34°38'0"N

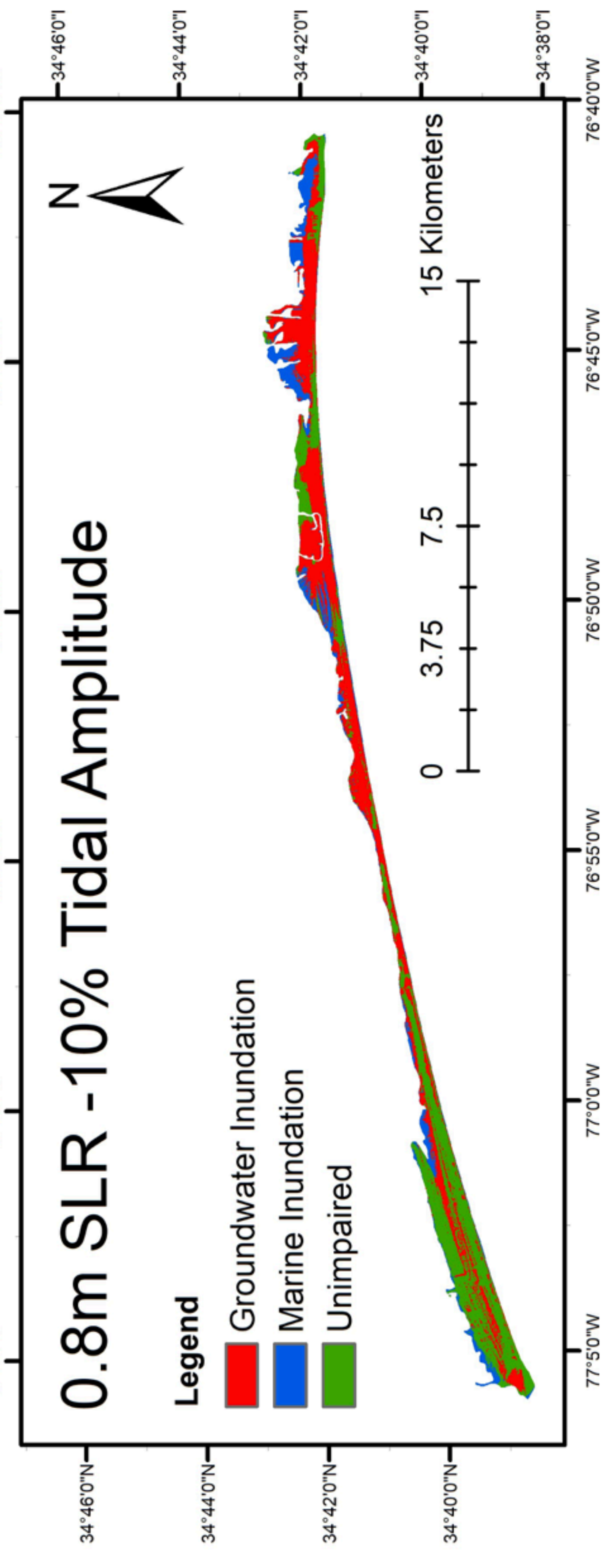
0.8m SLR -10% Tidal Amplitude
Legend
Groundwater Inundation
Marine Inundation
Unimpaired
N
0
3.75
7.5
15 Kilometers
77°5'0"W
77°0'0"W
76°55'0"W
76°50'0"W
76°45'0"W
76°40'0"W
34°46'0"N
34°44'0"N
34°42'0"N
34°40'0"N
34°38'0"N

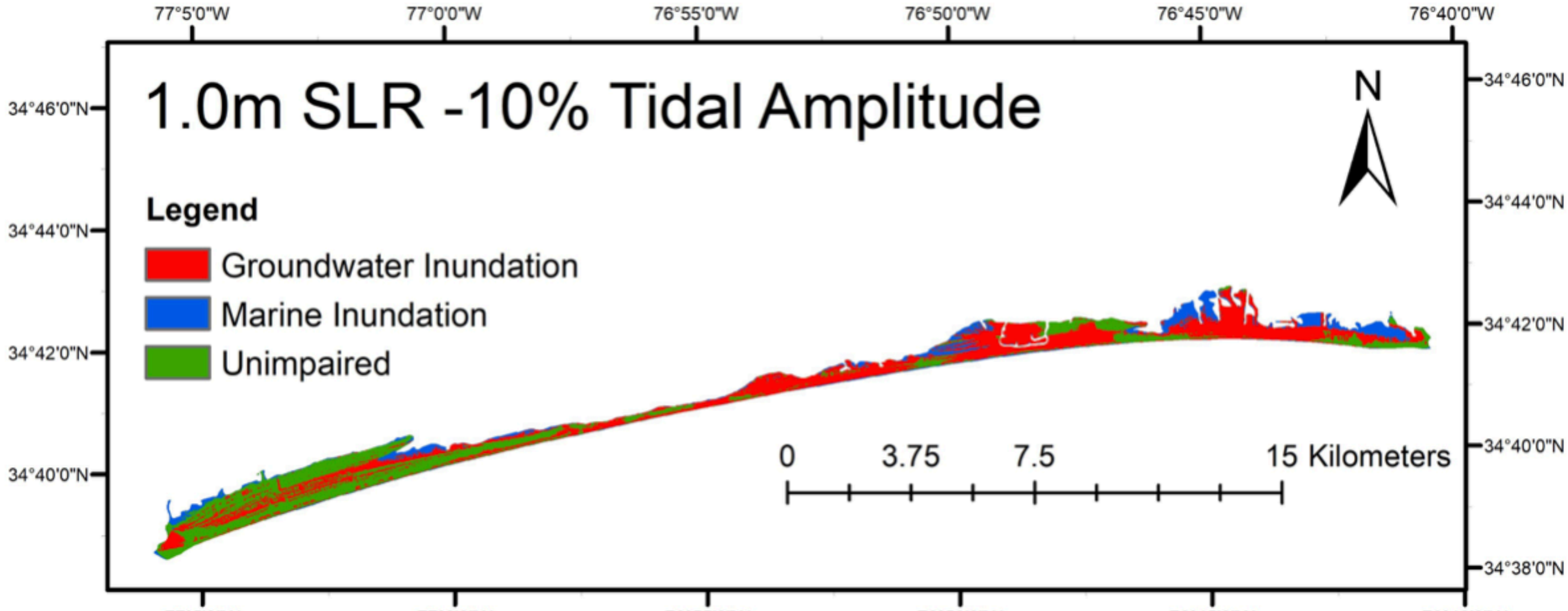
1.0m SLR -10% Tidal Amplitude
N
Legend
Groundwater Inundation
Marine Inundation
Unimpaired
0
3.75
7.5
15 Kilometers
77°5'0"W
77°0'0"W
76°55'0"W
76°50'0"W
76°45'0"W
76°40'0"W
34°46'0"N
34°44'0"N
34°42'0"N
34°40'0"N
34°38'0"N

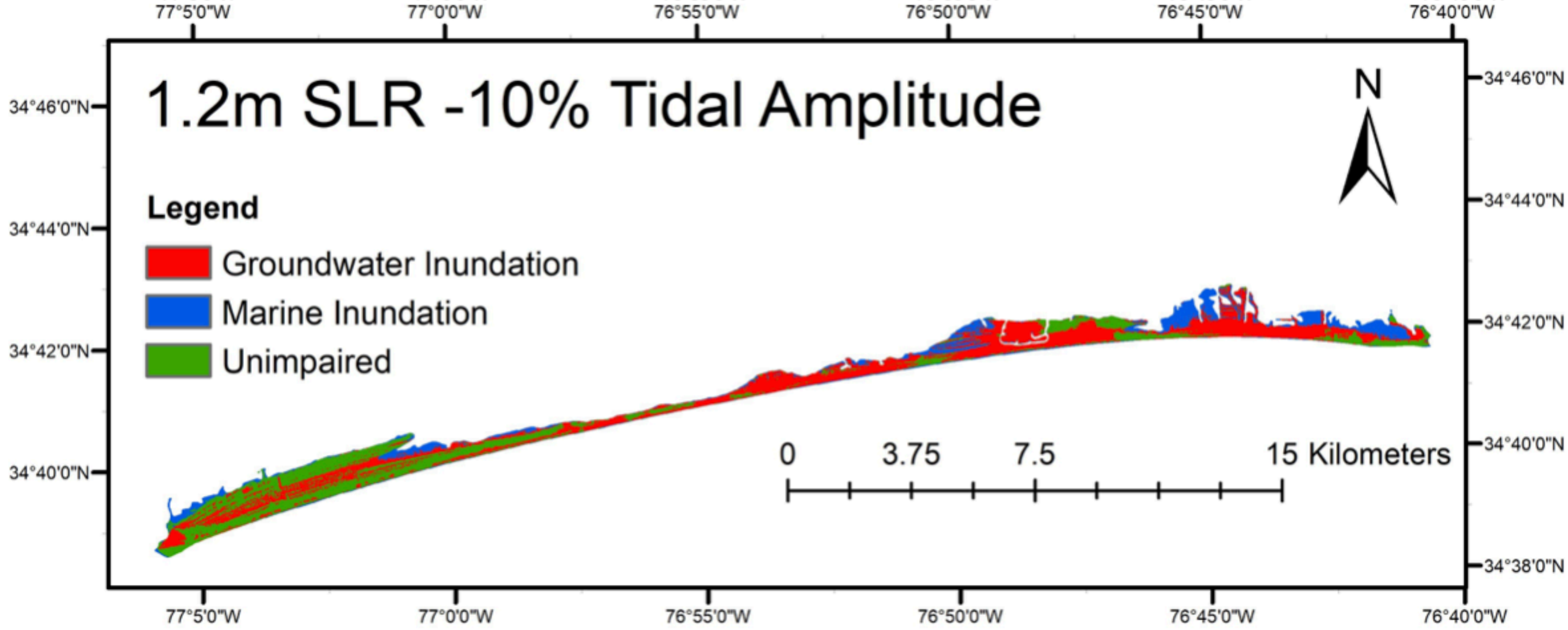
1.2m SLR -10% Tidal Amplitude
N
Legend
Groundwater Inundation
Marine Inundation
Unimpaired
0
3.75
7.5
15 Kilometers
77°5'0"W
77°0'0"W
76°55'0"W
76°50'0"W
76°45'0"W
76°40'0"W
34°46'0"N
34°44'0"N
34°42'0"N
34°40'0"N
34°38'0"N

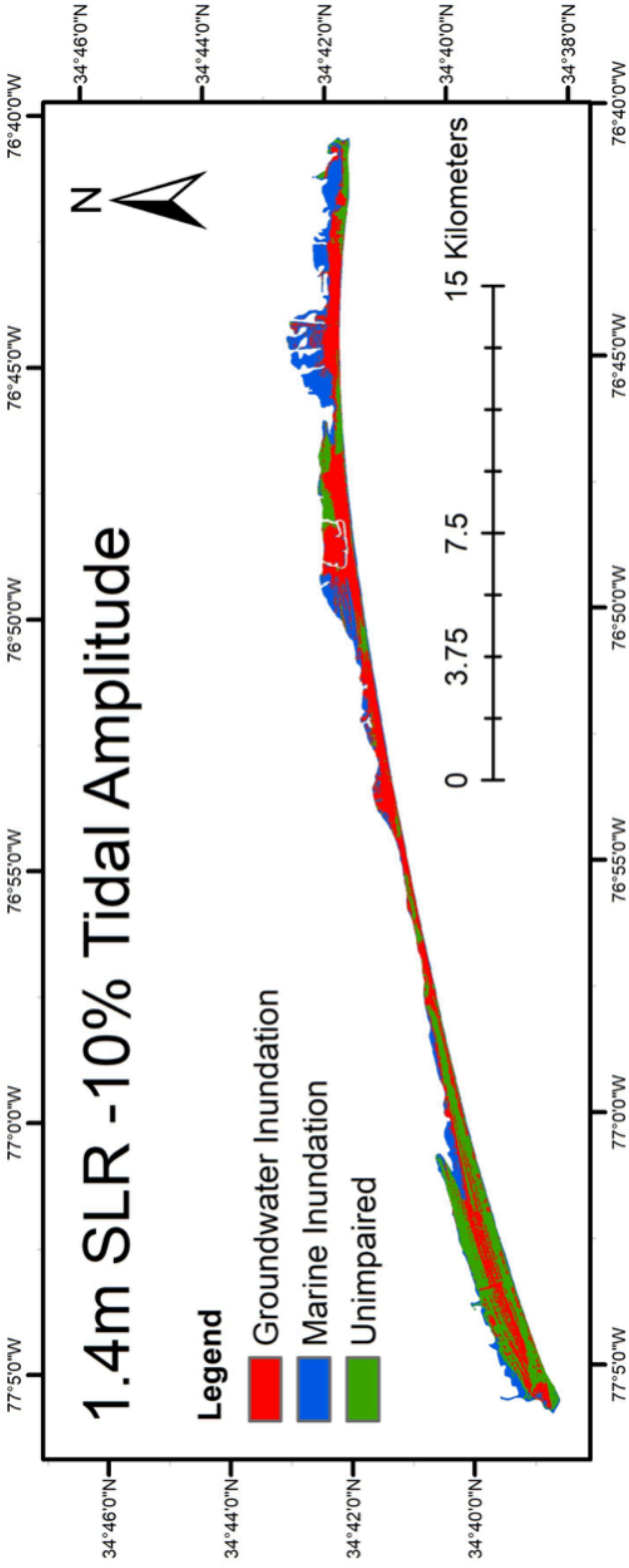
1.4m SLR -10% Tidal Amplitude
Legend
Groundwater Inundation
Marine Inundation
Unimpaired
N
0
3.75
7.5
15 Kilometers
77°5'0"W
77°0'0"W
76°55'0"W
76°50'0"W
76°45'0"W
76°40'0"W
34°46'0"N
34°44'0"N
34°42'0"N
34°40'0"N
34°38'0"N

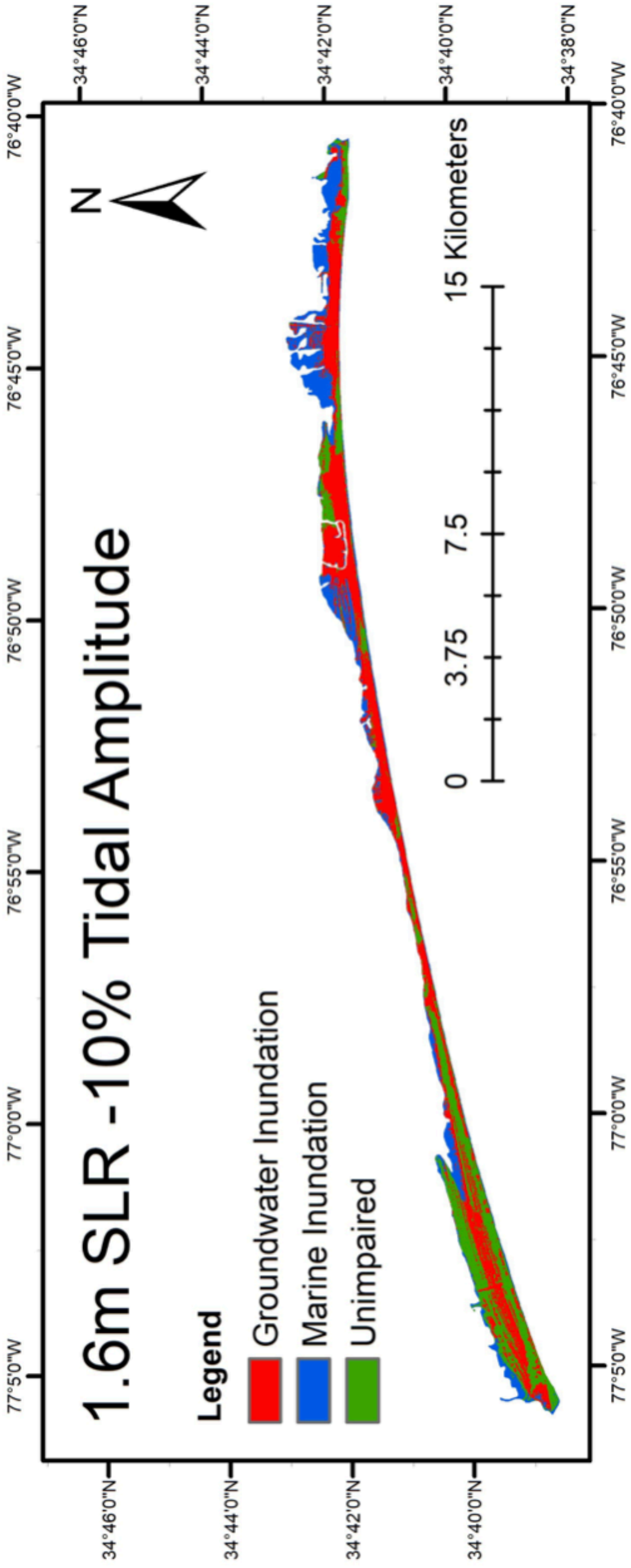
1.6m SLR -10% Tidal Amplitude
Legend
Groundwater Inundation
Marine Inundation
Unimpaired
N
0
3.75
7.5
15 Kilometers
77°5'0"W
77°0'0"W
76°55'0"W
76°50'0"W
76°45'0"W
76°40'0"W
34°46'0"N
34°44'0"N
34°42'0"N
34°40'0"N
34°38'0"N

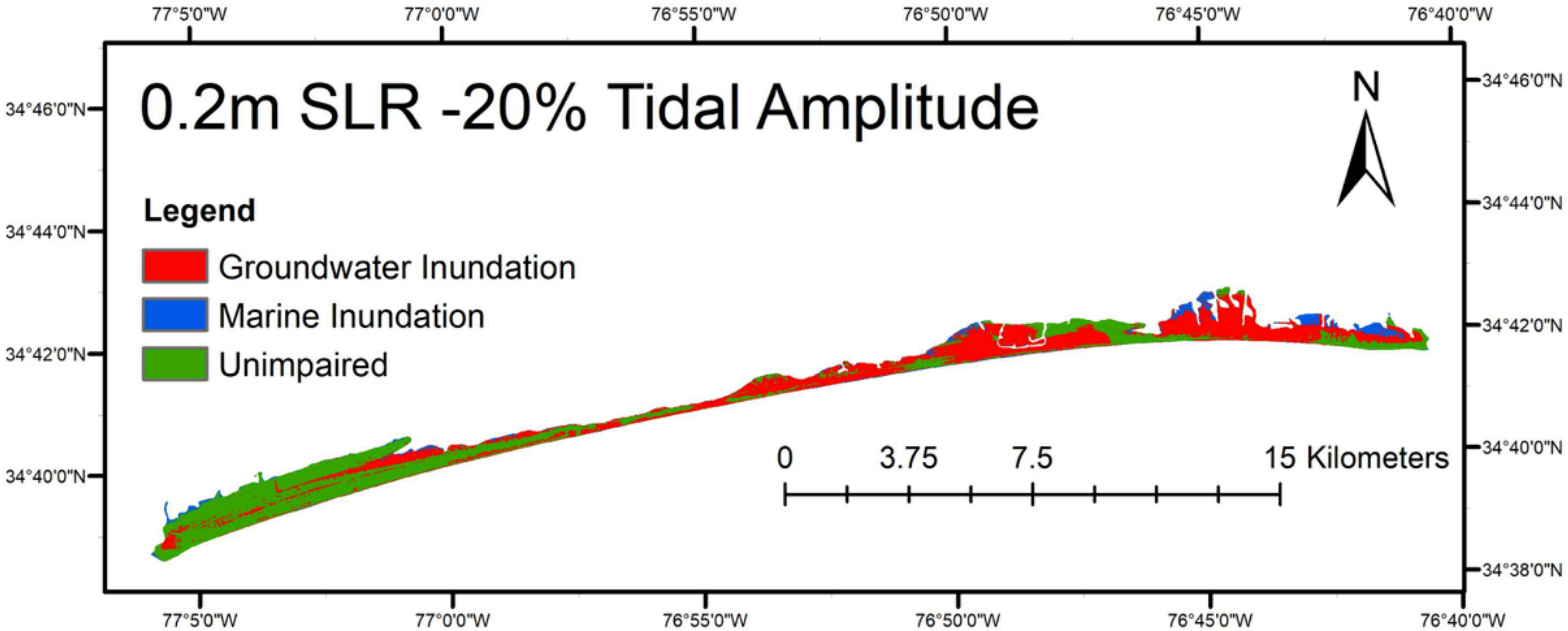
0.2m SLR -20% Tidal Amplitude
Legend
🟥 Groundwater Inundation
🟦 Marine Inundation
🟩 Unimpaired
N
0
3.75
7.5
15 Kilometers
77°5'0"W
77°0'0"W
76°55'0"W
76°50'0"W
76°45'0"W
76°40'0"W
34°46'0"N
34°44'0"N
34°42'0"N
34°40'0"N
34°38'0"N

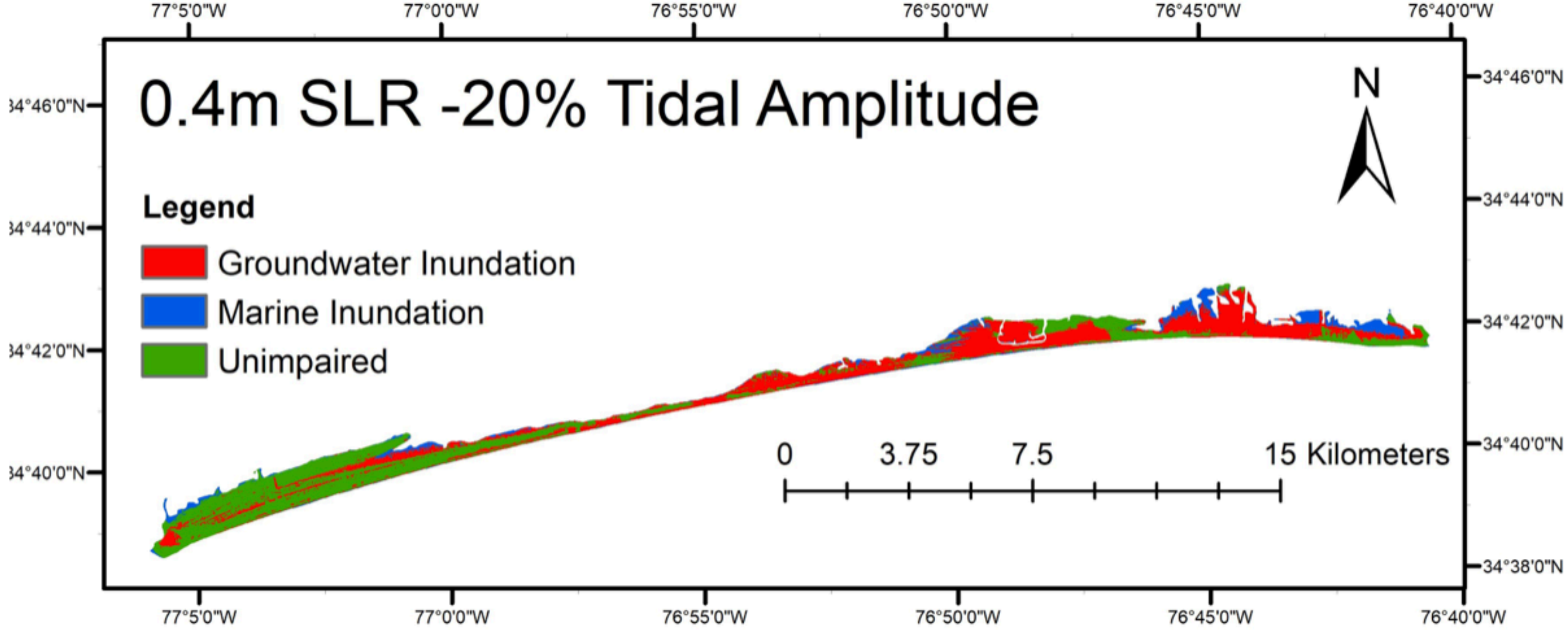
0.4m SLR -20% Tidal Amplitude
Legend
🟥 Groundwater Inundation
🟦 Marine Inundation
🟩 Unimpaired
N
0
3.75
7.5
15 Kilometers
77°5'0"W
77°0'0"W
76°55'0"W
76°50'0"W
76°45'0"W
76°40'0"W
34°46'0"N
34°44'0"N
34°42'0"N
34°40'0"N
34°38'0"N

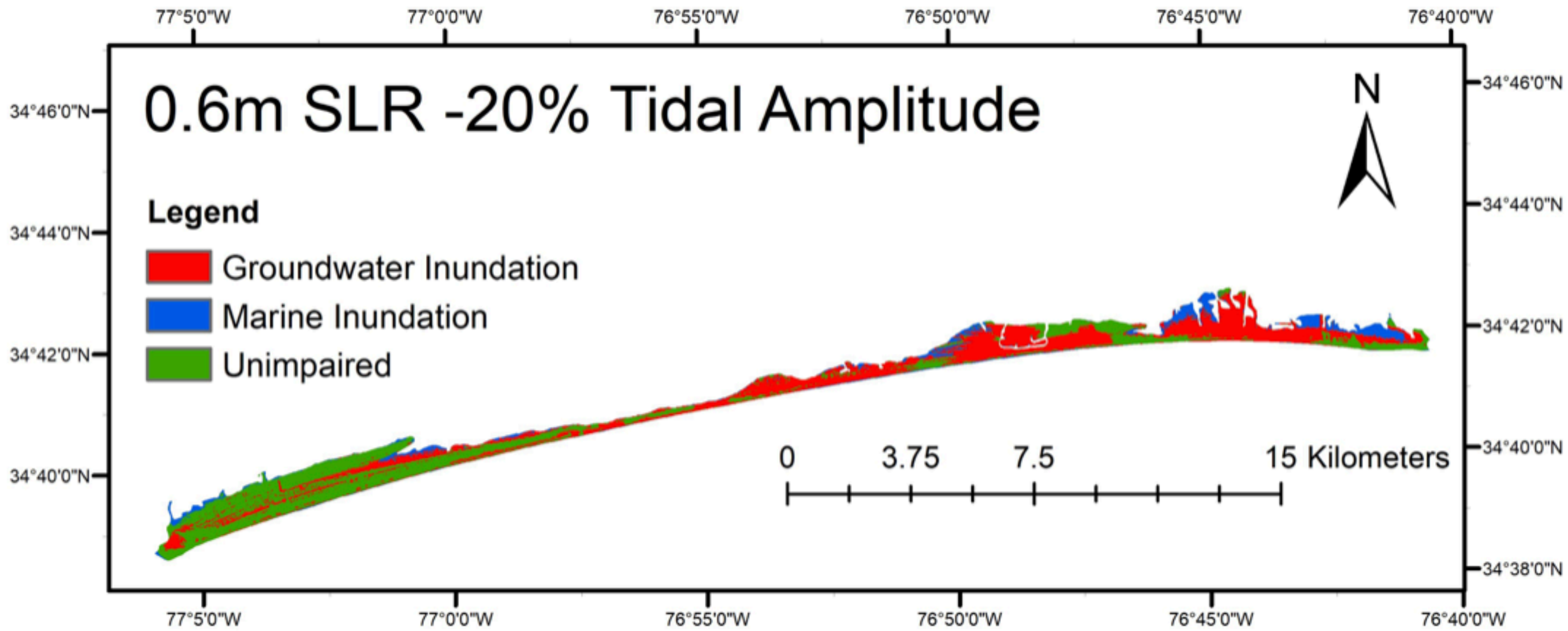
0.6m SLR -20% Tidal Amplitude
Legend
Groundwater Inundation
Marine Inundation
Unimpaired
N
0
3.75
7.5
15 Kilometers
77°5'0"W
77°0'0"W
76°55'0"W
76°50'0"W
76°45'0"W
76°40'0"W
34°46'0"N
34°44'0"N
34°42'0"N
34°40'0"N
34°38'0"N

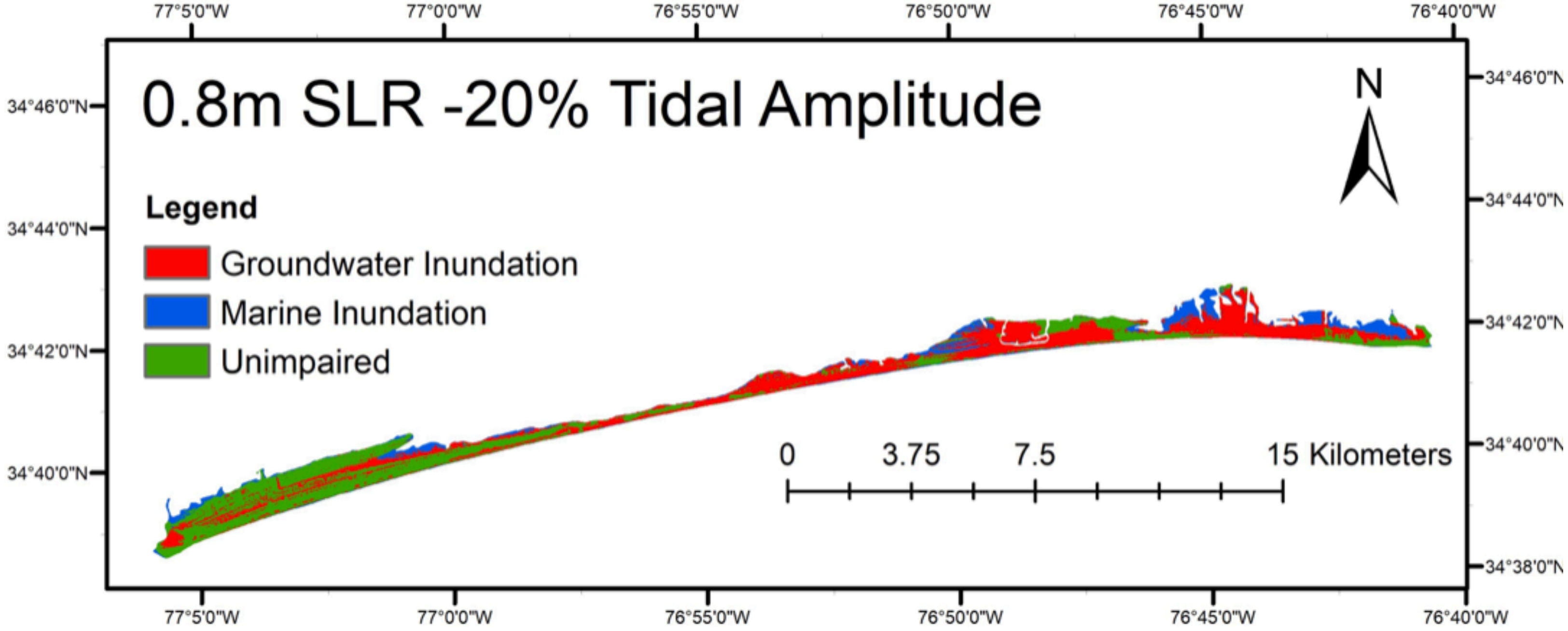
0.8m SLR -20% Tidal Amplitude
Legend
Groundwater Inundation
Marine Inundation
Unimpaired
N
0
3.75
7.5
15 Kilometers
77°5'0"W
77°0'0"W
76°55'0"W
76°50'0"W
76°45'0"W
76°40'0"W
34°46'0"N
34°44'0"N
34°42'0"N
34°40'0"N
34°38'0"N

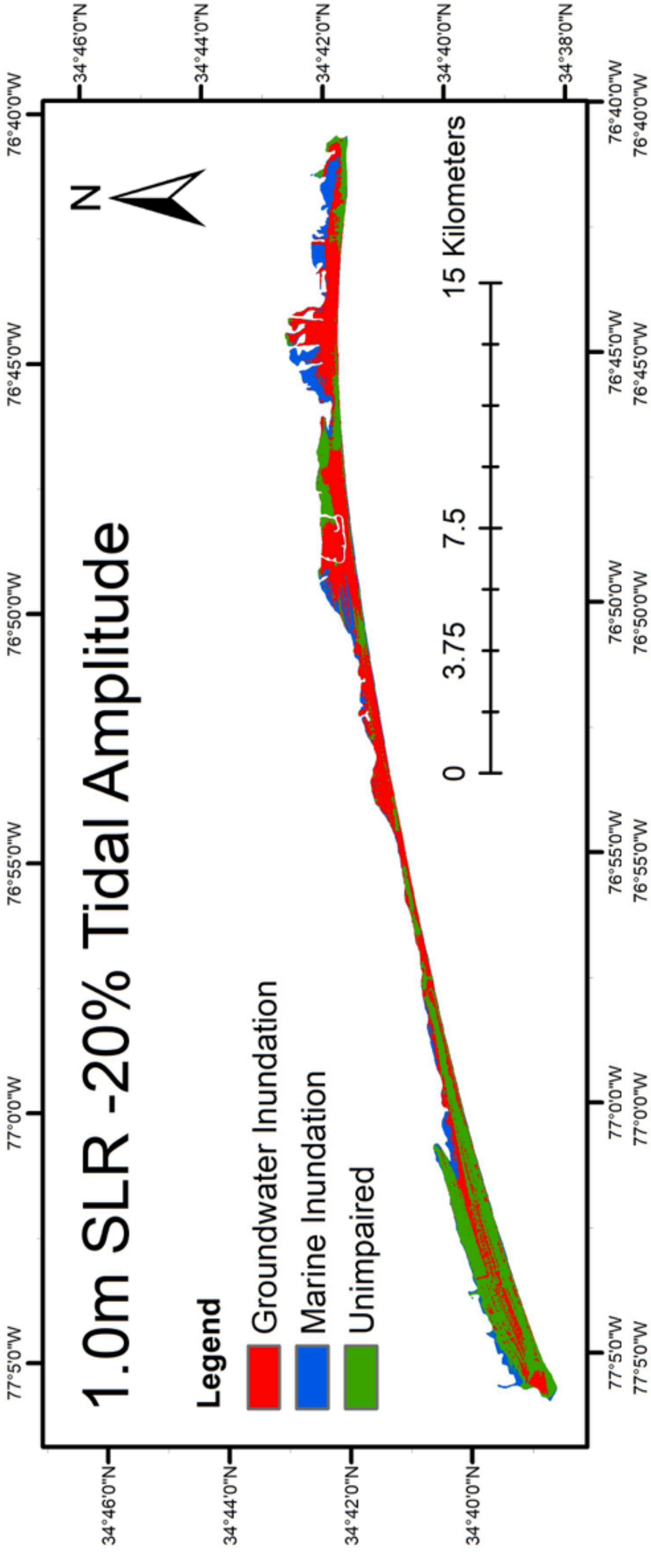
1.0m SLR -20% Tidal Amplitude
Legend
🟥 Groundwater Inundation
🟦 Marine Inundation
🟩 Unimpaired
N
0
3.75
7.5
15 Kilometers
77°5'0"W
77°0'0"W
76°55'0"W
76°50'0"W
76°45'0"W
76°40'0"W
34°46'0"N
34°44'0"N
34°42'0"N
34°40'0"N
34°38'0"N

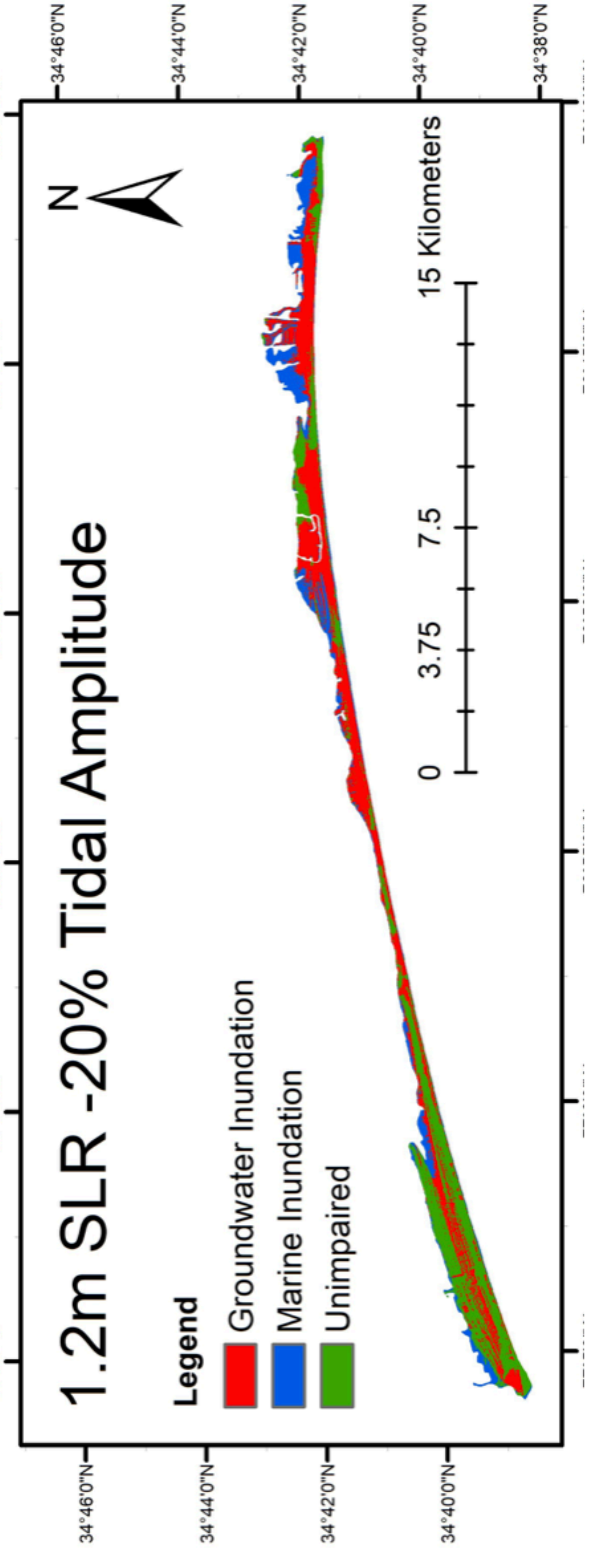
1.2m SLR -20% Tidal Amplitude
Legend
🟥 Groundwater Inundation
🟦 Marine Inundation
🟩 Unimpaired
N
0
3.75
7.5
15 Kilometers
77°5'0"W
77°0'0"W
76°55'0"W
76°50'0"W
76°45'0"W
76°40'0"W
34°46'0"N
34°44'0"N
34°42'0"N
34°40'0"N
34°38'0"N

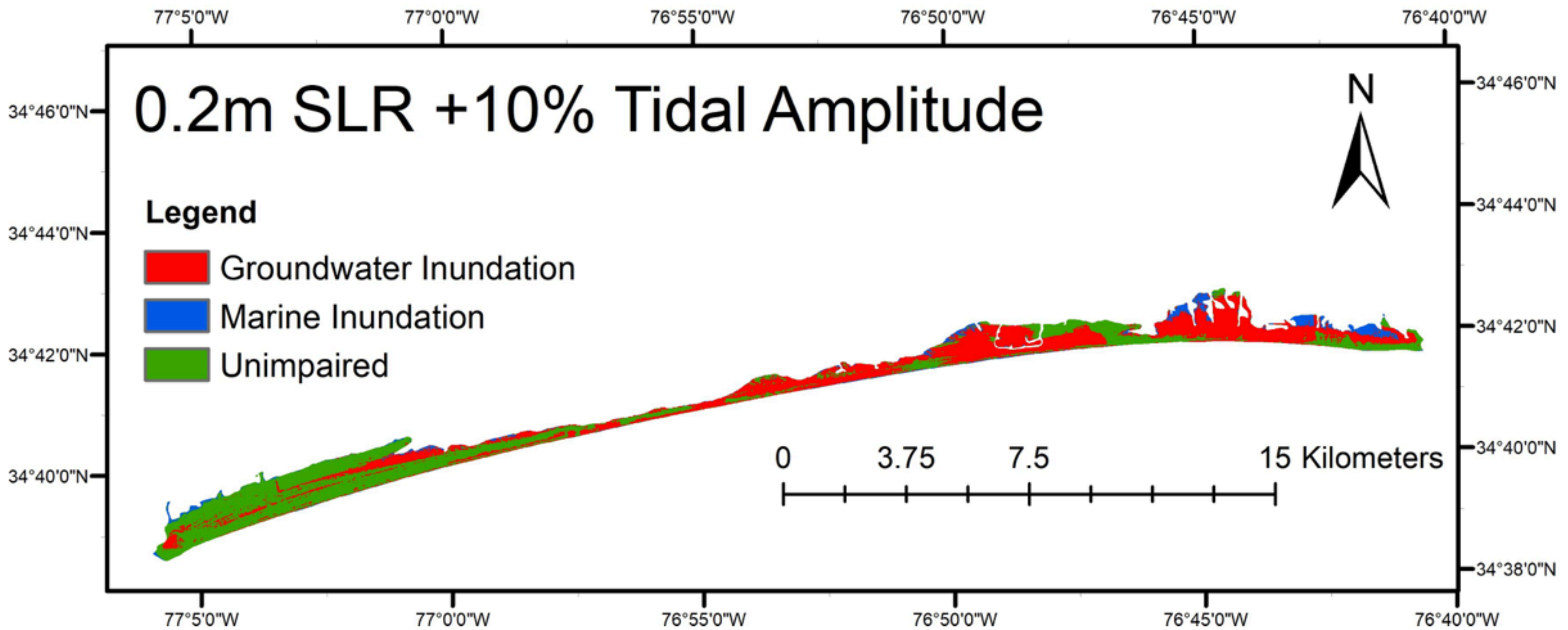
0.2m SLR +10% Tidal Amplitude
Legend
🟥 Groundwater Inundation
🟦 Marine Inundation
🟩 Unimpaired
N
0
3.75
7.5
15 Kilometers
77°5'0"W
77°0'0"W
76°55'0"W
76°50'0"W
76°45'0"W
76°40'0"W
34°46'0"N
34°44'0"N
34°42'0"N
34°40'0"N
34°38'0"N

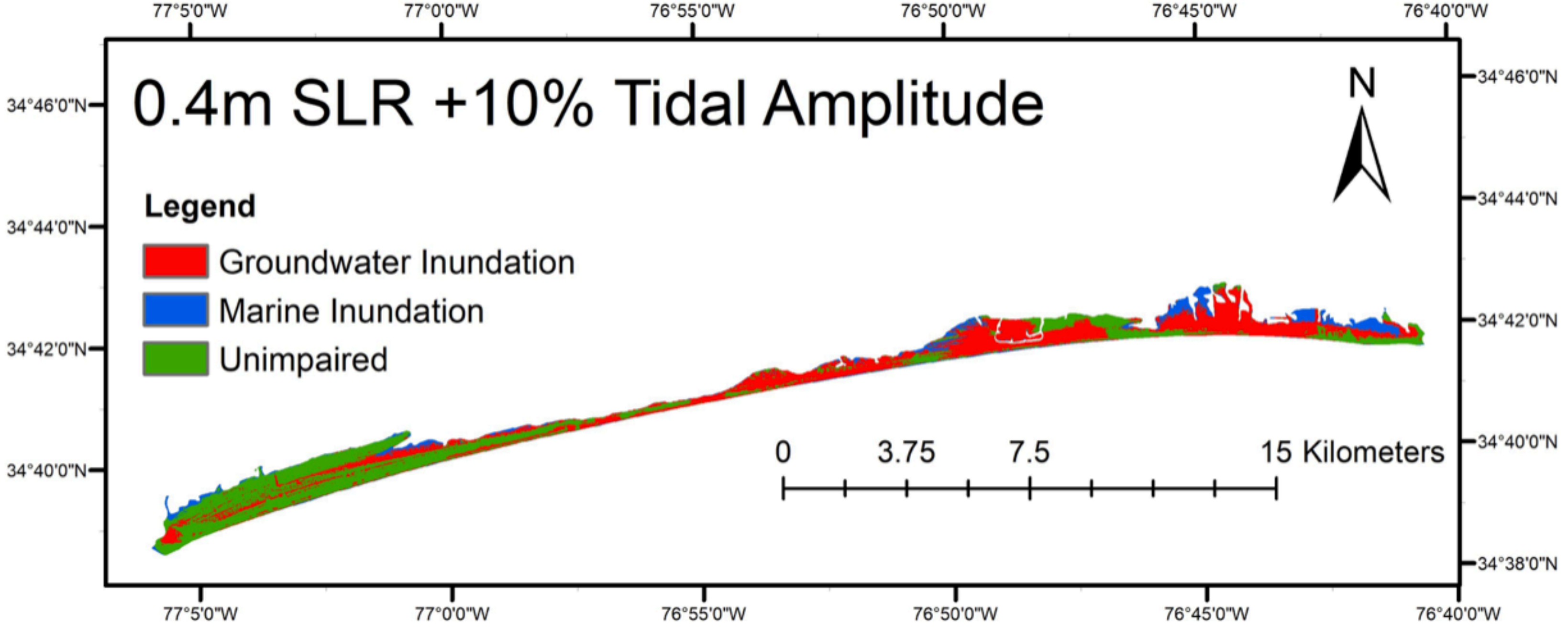
0.4m SLR +10% Tidal Amplitude
Legend
🟥 Groundwater Inundation
🟦 Marine Inundation
🟩 Unimpaired
N
0
3.75
7.5
15 Kilometers
77°5'0"W
77°0'0"W
76°55'0"W
76°50'0"W
76°45'0"W
76°40'0"W
34°46'0"N
34°44'0"N
34°42'0"N
34°40'0"N
34°38'0"N

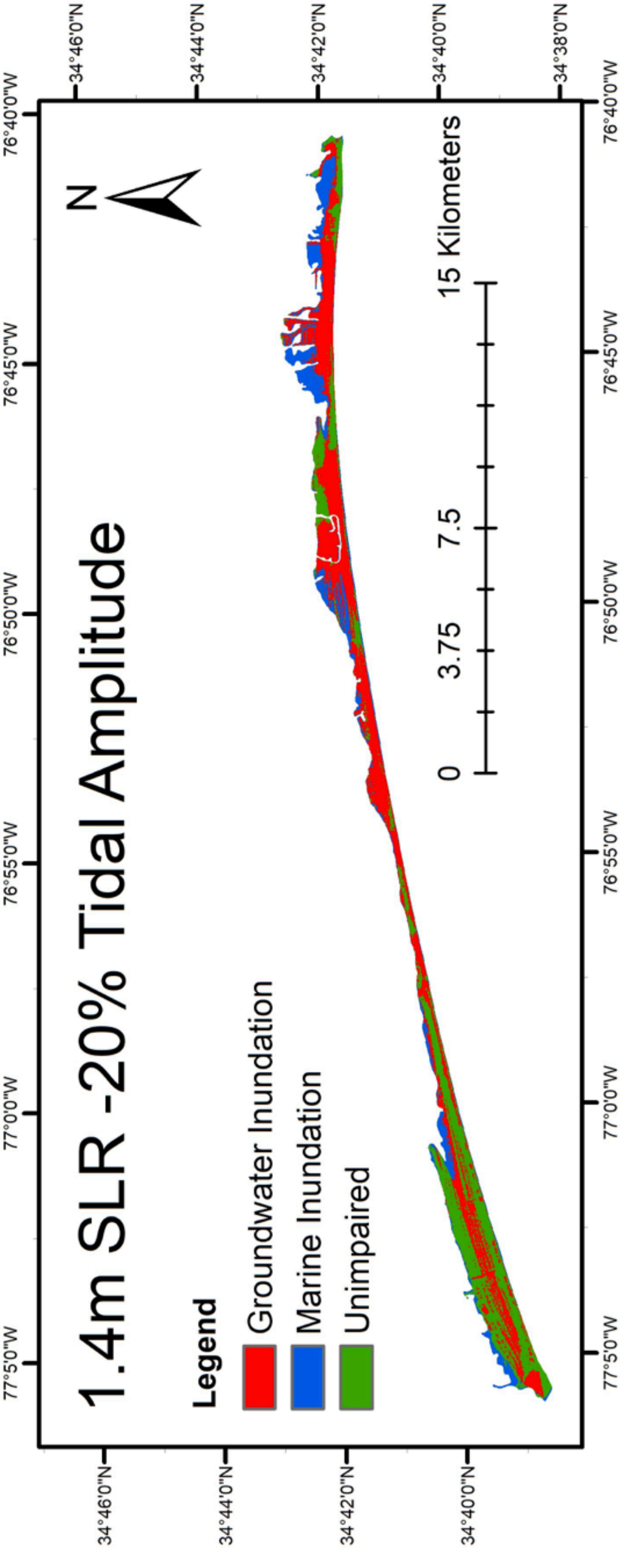
1.4m SLR -20% Tidal Amplitude
Legend
🟥 Groundwater Inundation
🟦 Marine Inundation
🟩 Unimpaired
N
0
3.75
7.5
15 Kilometers
77°5'0"W
77°0'0"W
76°55'0"W
76°50'0"W
76°45'0"W
76°40'0"W
34°46'0"N
34°44'0"N
34°42'0"N
34°40'0"N
34°38'0"N

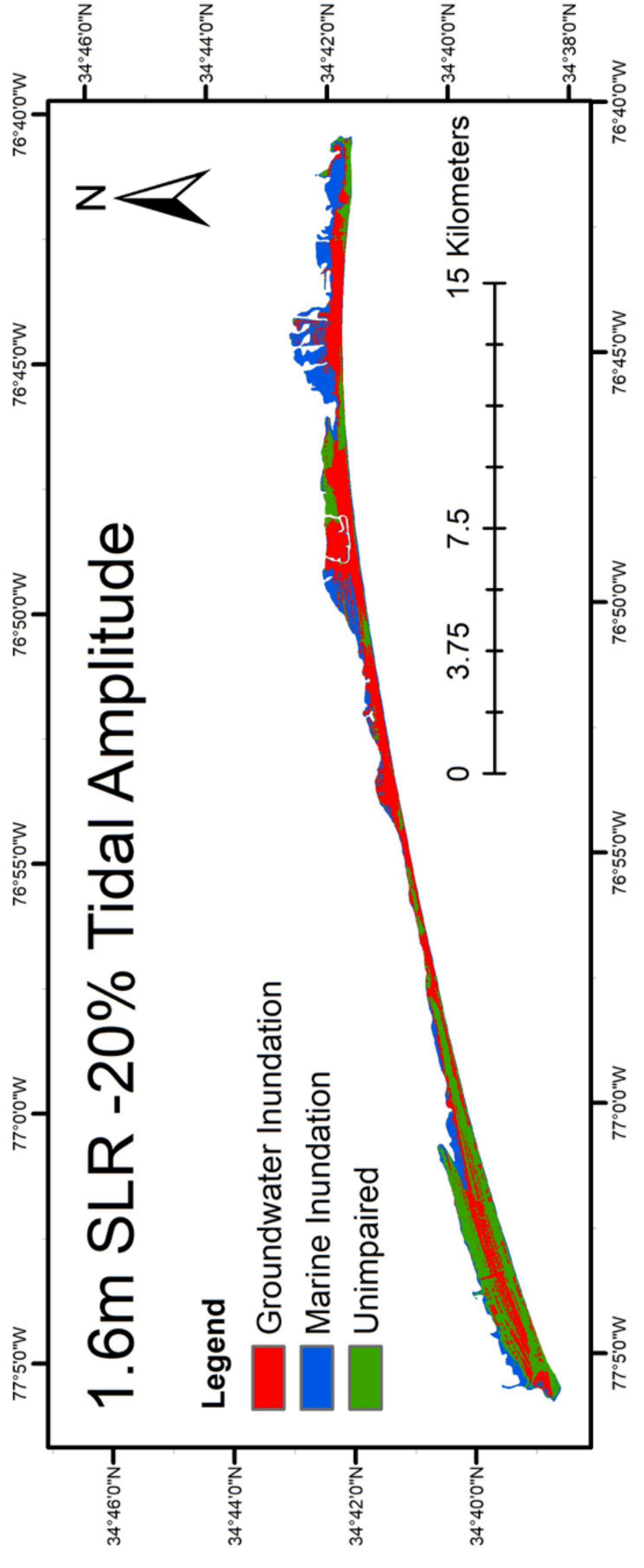
1.6m SLR -20% Tidal Amplitude
Legend
🟥 Groundwater Inundation
🟦 Marine Inundation
🟩 Unimpaired
N
0
3.75
7.5
15 Kilometers
77°5'0"W
77°0'0"W
76°55'0"W
76°50'0"W
76°45'0"W
76°40'0"W
34°46'0"N
34°44'0"N
34°42'0"N
34°40'0"N
34°38'0"N

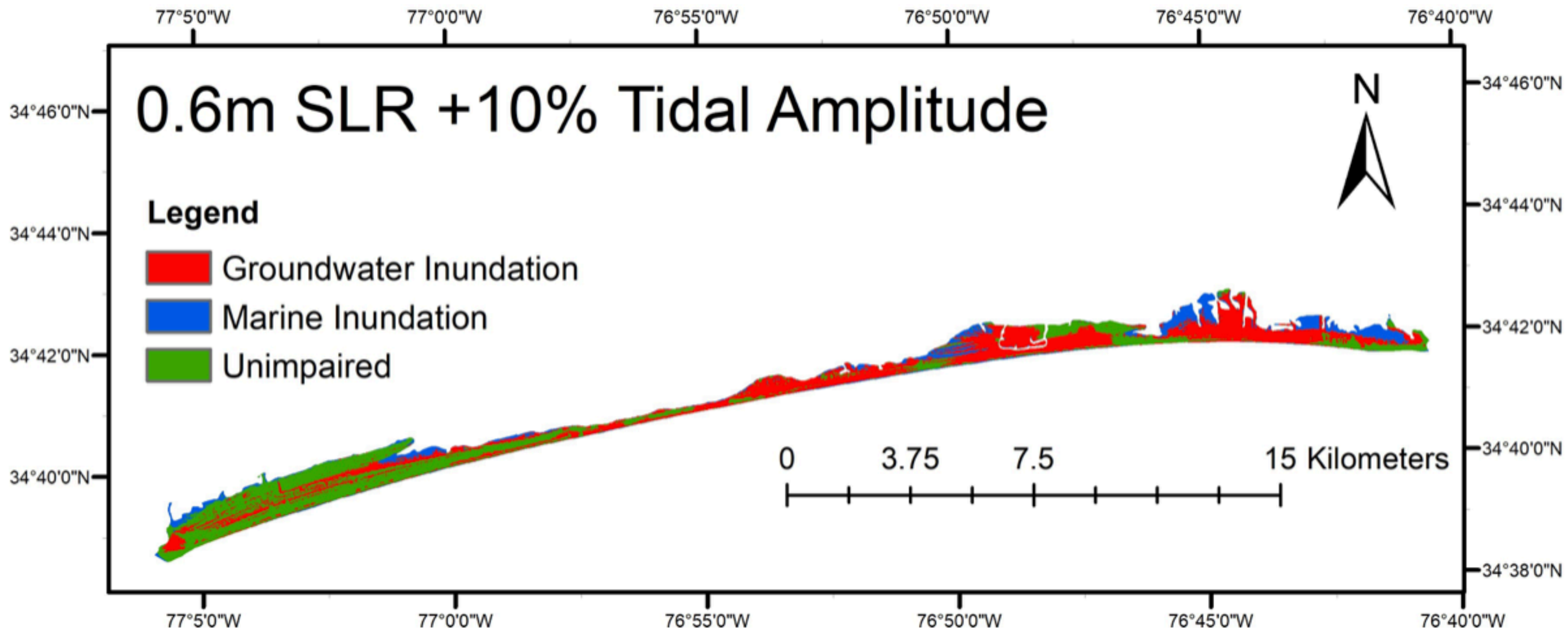
0.6m SLR +10% Tidal Amplitude
Legend
🟥 Groundwater Inundation
🟦 Marine Inundation
🟩 Unimpaired
N
0
3.75
7.5
15 Kilometers
77°5'0"W
77°0'0"W
76°55'0"W
76°50'0"W
76°45'0"W
76°40'0"W
34°46'0"N
34°44'0"N
34°42'0"N
34°40'0"N
34°38'0"N

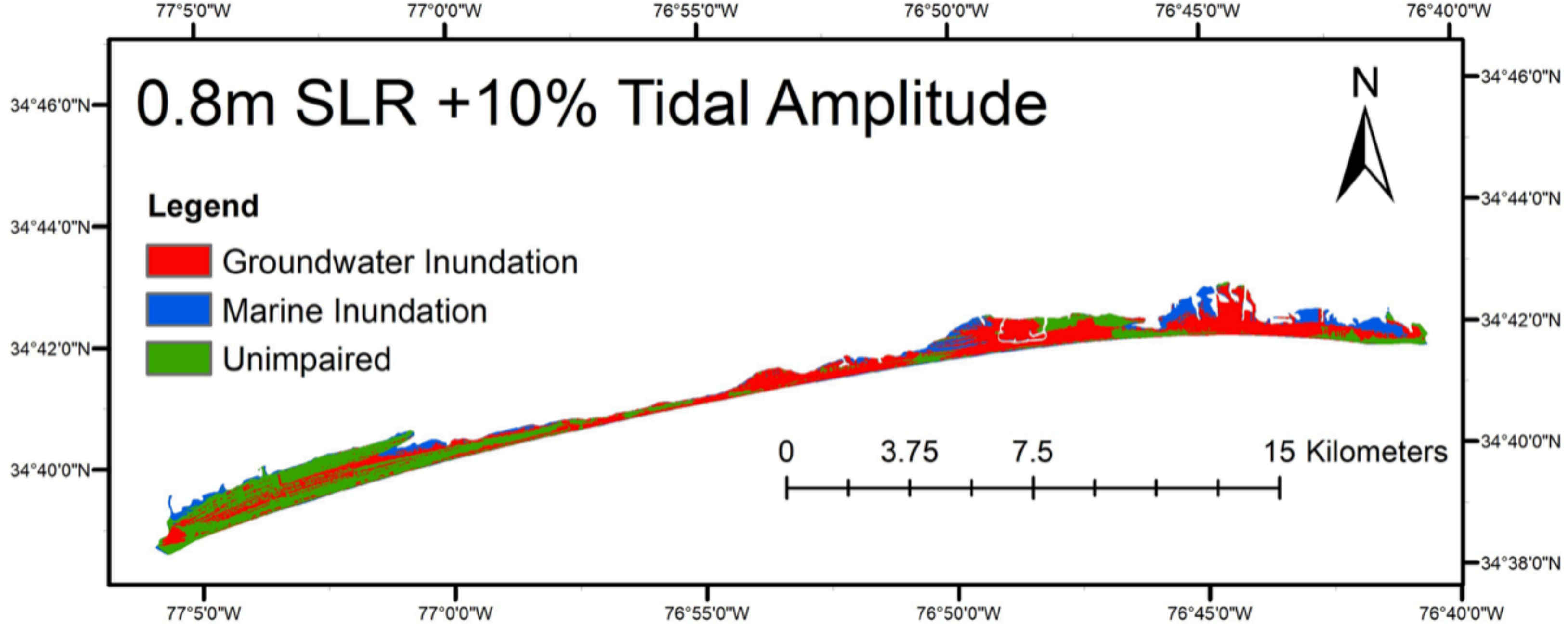
0.8m SLR +10% Tidal Amplitude
Legend
🟥 Groundwater Inundation
🟦 Marine Inundation
🟩 Unimpaired
N
0
3.75
7.5
15 Kilometers
77°5'0"W
77°0'0"W
76°55'0"W
76°50'0"W
76°45'0"W
76°40'0"W
34°46'0"N
34°44'0"N
34°42'0"N
34°40'0"N
34°38'0"N

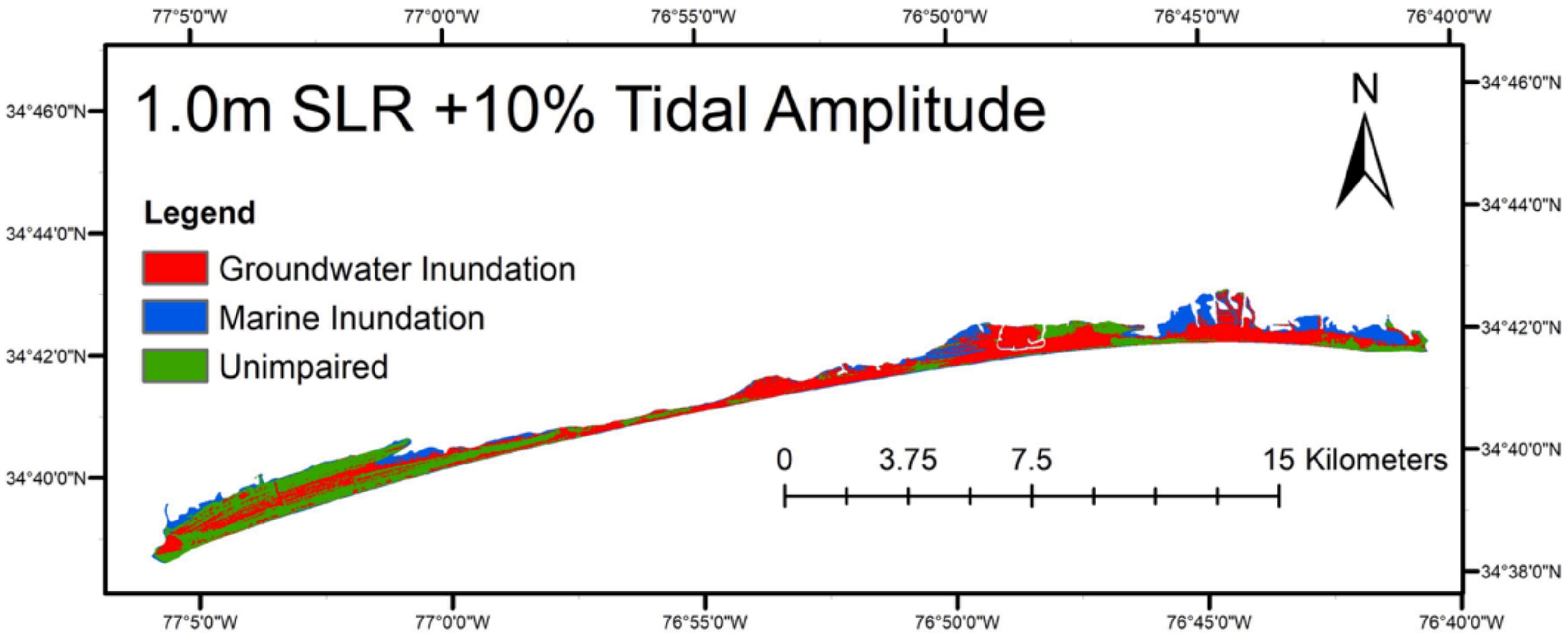
1.0m SLR +10% Tidal Amplitude
Legend
🟥 Groundwater Inundation
🟦 Marine Inundation
🟩 Unimpaired
N
0
3.75
7.5
15 Kilometers
77°5'0"W
77°0'0"W
76°55'0"W
76°50'0"W
76°45'0"W
76°40'0"W
34°46'0"N
34°44'0"N
34°42'0"N
34°40'0"N
34°38'0"N

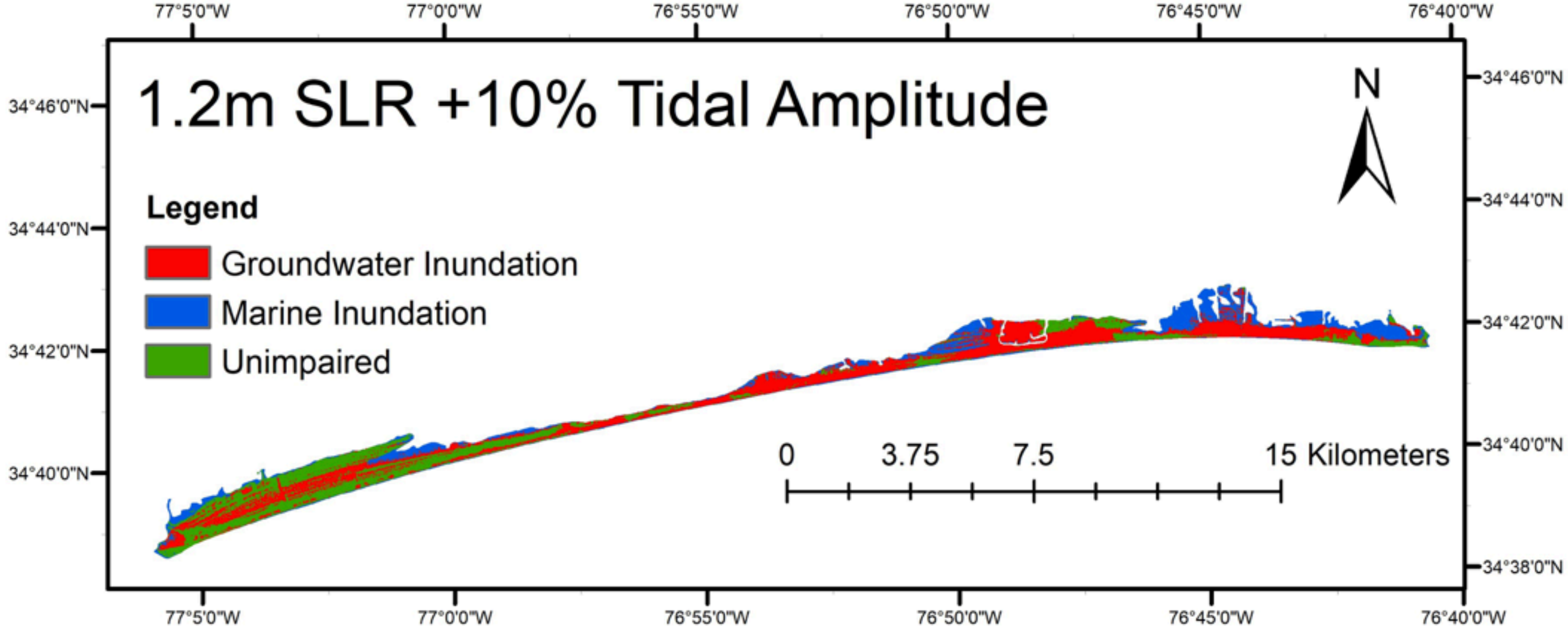
1.2m SLR +10% Tidal Amplitude
Legend
🟥 Groundwater Inundation
🟦 Marine Inundation
🟩 Unimpaired
N
0
3.75
7.5
15 Kilometers
77°5'0"W
77°0'0"W
76°55'0"W
76°50'0"W
76°45'0"W
76°40'0"W
34°46'0"N
34°44'0"N
34°42'0"N
34°40'0"N
34°38'0"N

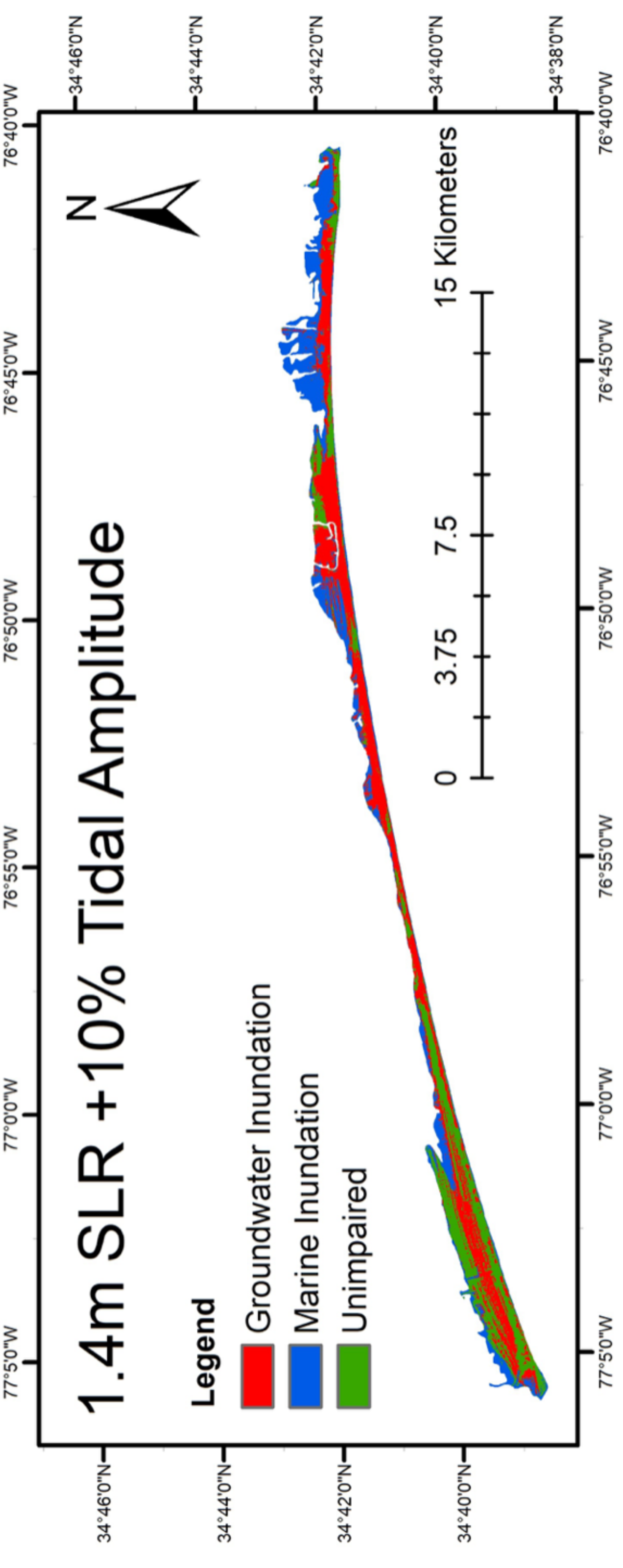
1.4m SLR +10% Tidal Amplitude
Legend
🟥 Groundwater Inundation
🟦 Marine Inundation
🟩 Unimpaired
N
0
3.75
7.5
15 Kilometers
77°5'0"W
77°0'0"W
76°55'0"W
76°50'0"W
76°45'0"W
76°40'0"W
34°46'0"N
34°44'0"N
34°42'0"N
34°40'0"N
34°38'0"N

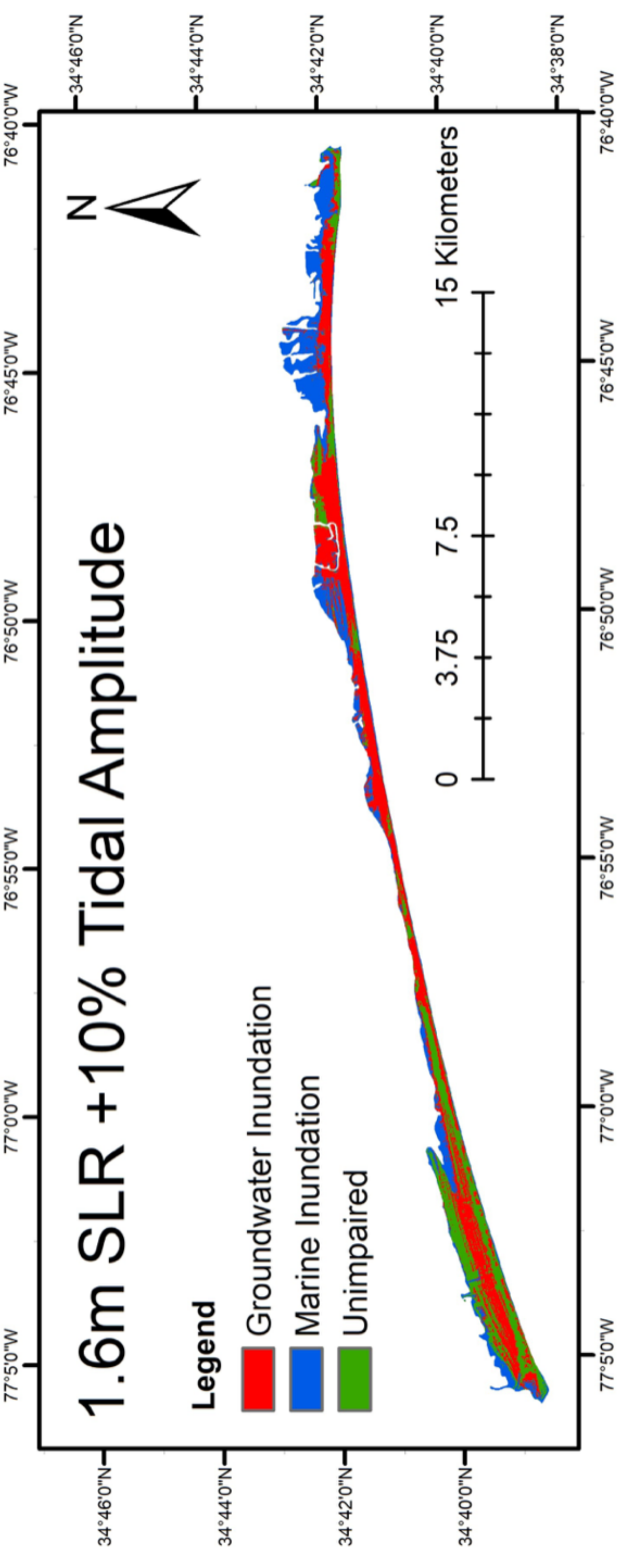
1.6m SLR +10% Tidal Amplitude
Legend
🟥 Groundwater Inundation
🟦 Marine Inundation
🟩 Unimpaired
N
0
3.75
7.5
15 Kilometers
77°5'0"W
77°0'0"W
76°55'0"W
76°50'0"W
76°45'0"W
76°40'0"W
34°46'0"N
34°44'0"N
34°42'0"N
34°40'0"N
34°38'0"N

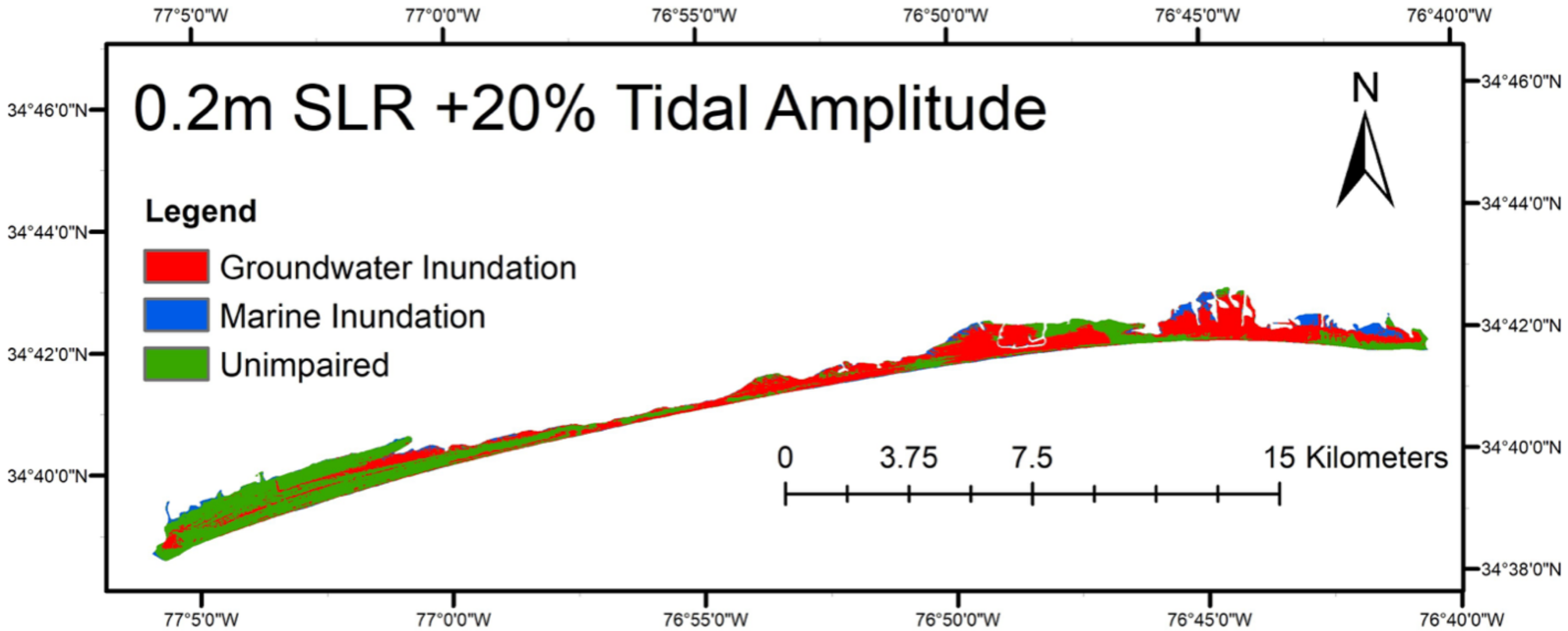
0.2m SLR +20% Tidal Amplitude
N
Legend
🟥 Groundwater Inundation
🟦 Marine Inundation
🟩 Unimpaired
0
3.75
7.5
15 Kilometers
77°5'0"W
77°0'0"W
76°55'0"W
76°50'0"W
76°45'0"W
76°40'0"W
34°46'0"N
34°44'0"N
34°42'0"N
34°40'0"N
34°38'0"N

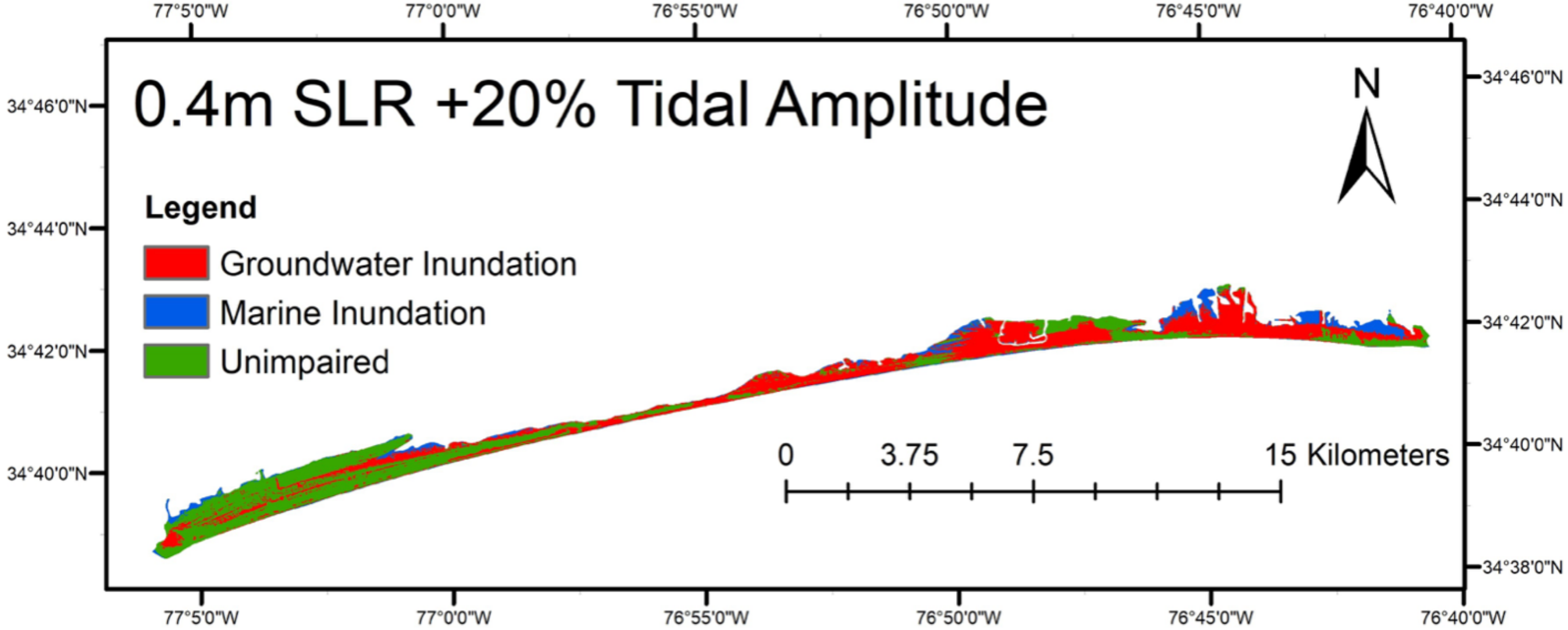
0.4m SLR +20% Tidal Amplitude
N
Legend
🟥 Groundwater Inundation
🟦 Marine Inundation
🟩 Unimpaired
0
3.75
7.5
15 Kilometers
77°5'0"W
77°0'0"W
76°55'0"W
76°50'0"W
76°45'0"W
76°40'0"W
34°46'0"N
34°44'0"N
34°42'0"N
34°40'0"N
34°38'0"N

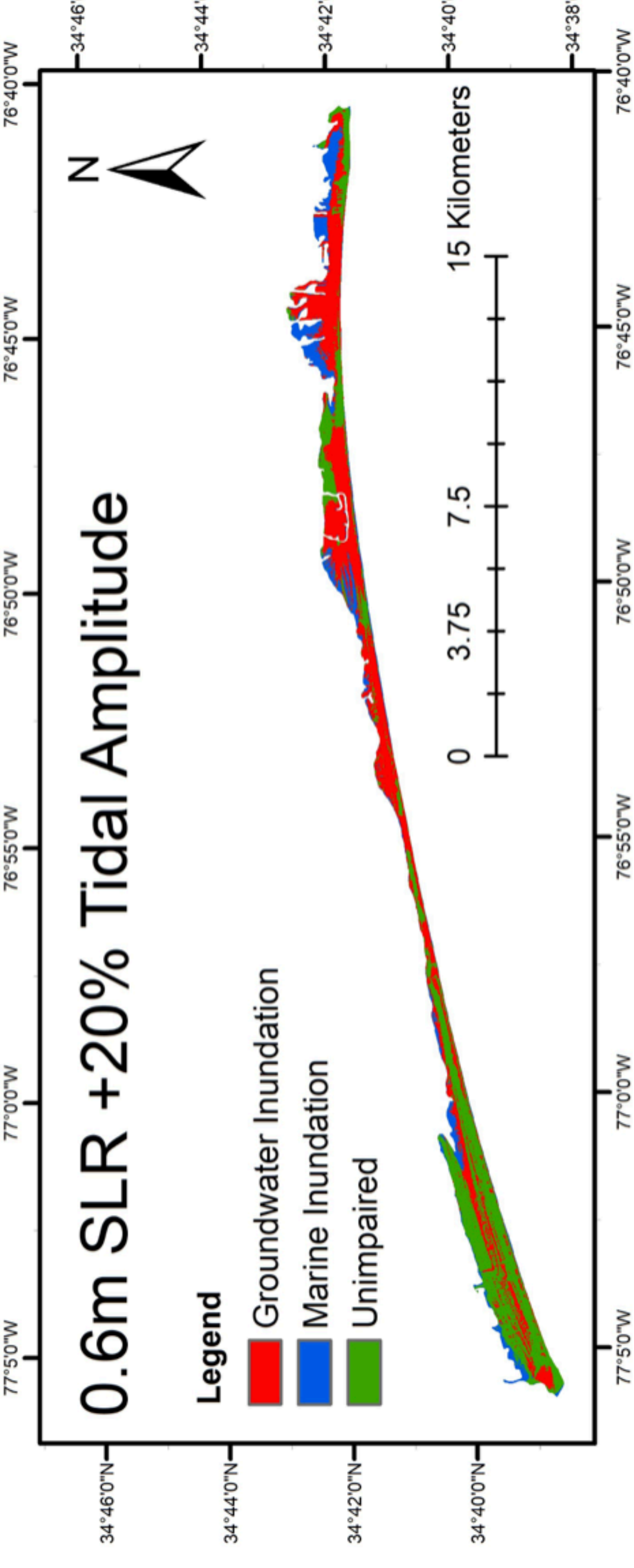
0.6m SLR +20% Tidal Amplitude
Legend
🟥 Groundwater Inundation
🟦 Marine Inundation
🟩 Unimpaired
N
0
3.75
7.5
15 Kilometers
77°5'0"W
77°0'0"W
76°55'0"W
76°50'0"W
76°45'0"W
76°40'0"W
34°46'0"N
34°44'0"N
34°42'0"N
34°40'0"N
34°38'0"N

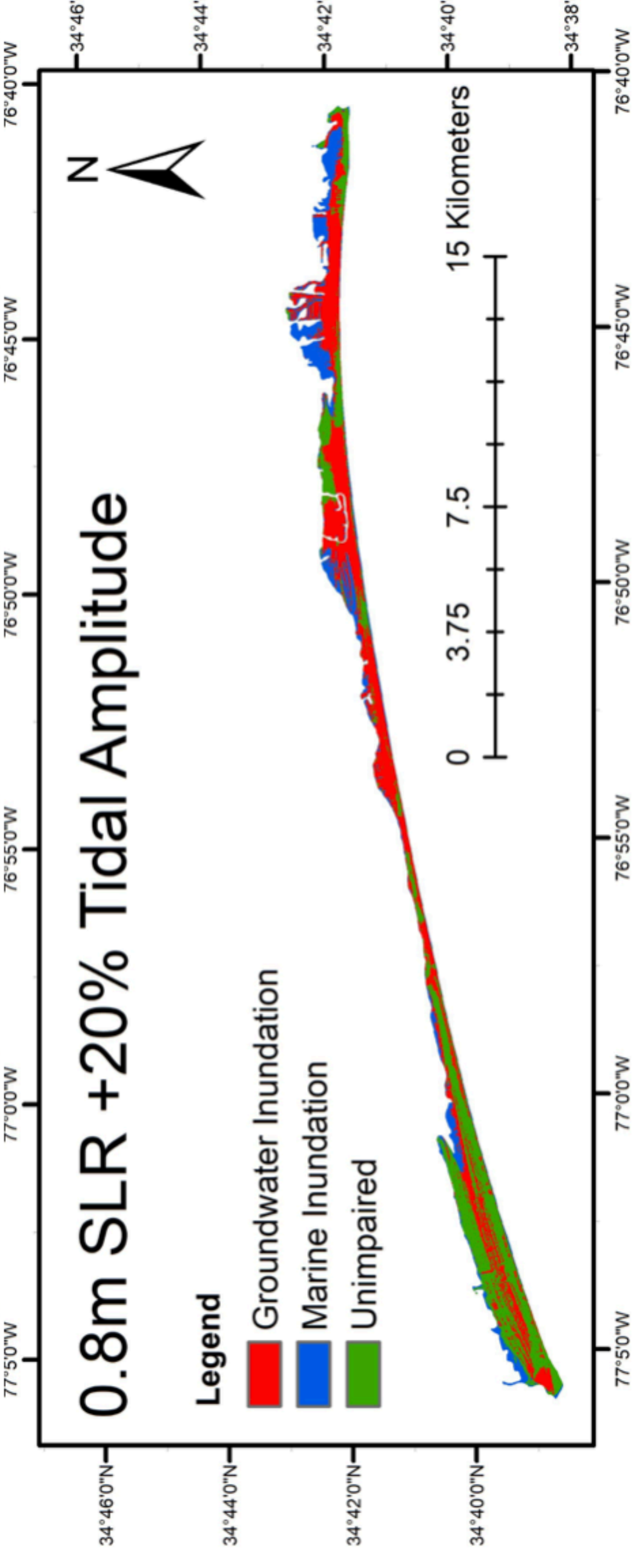
0.8m SLR +20% Tidal Amplitude
Legend
🟥 Groundwater Inundation
🟦 Marine Inundation
🟩 Unimpaired
N
0
3.75
7.5
15 Kilometers
77°5'0"W
77°0'0"W
76°55'0"W
76°50'0"W
76°45'0"W
76°40'0"W
34°46'0"N
34°44'0"N
34°42'0"N
34°40'0"N
34°38'0"N

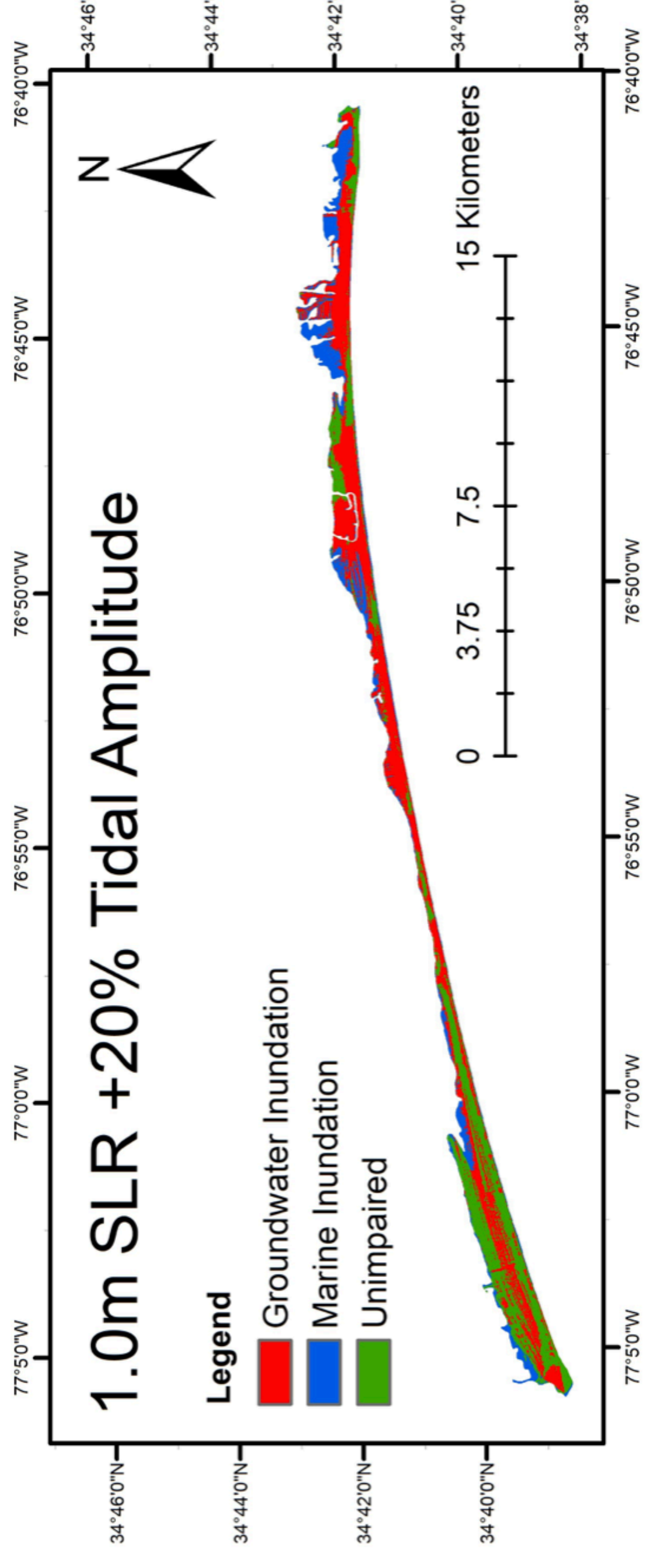
1.0m SLR +20% Tidal Amplitude
Legend
🟥 Groundwater Inundation
🟦 Marine Inundation
🟩 Unimpaired
N
0
3.75
7.5
15 Kilometers
77°5'0"W
77°0'0"W
76°55'0"W
76°50'0"W
76°45'0"W
76°40'0"W
34°46'0"N
34°44'0"N
34°42'0"N
34°40'0"N
34°38'0"N

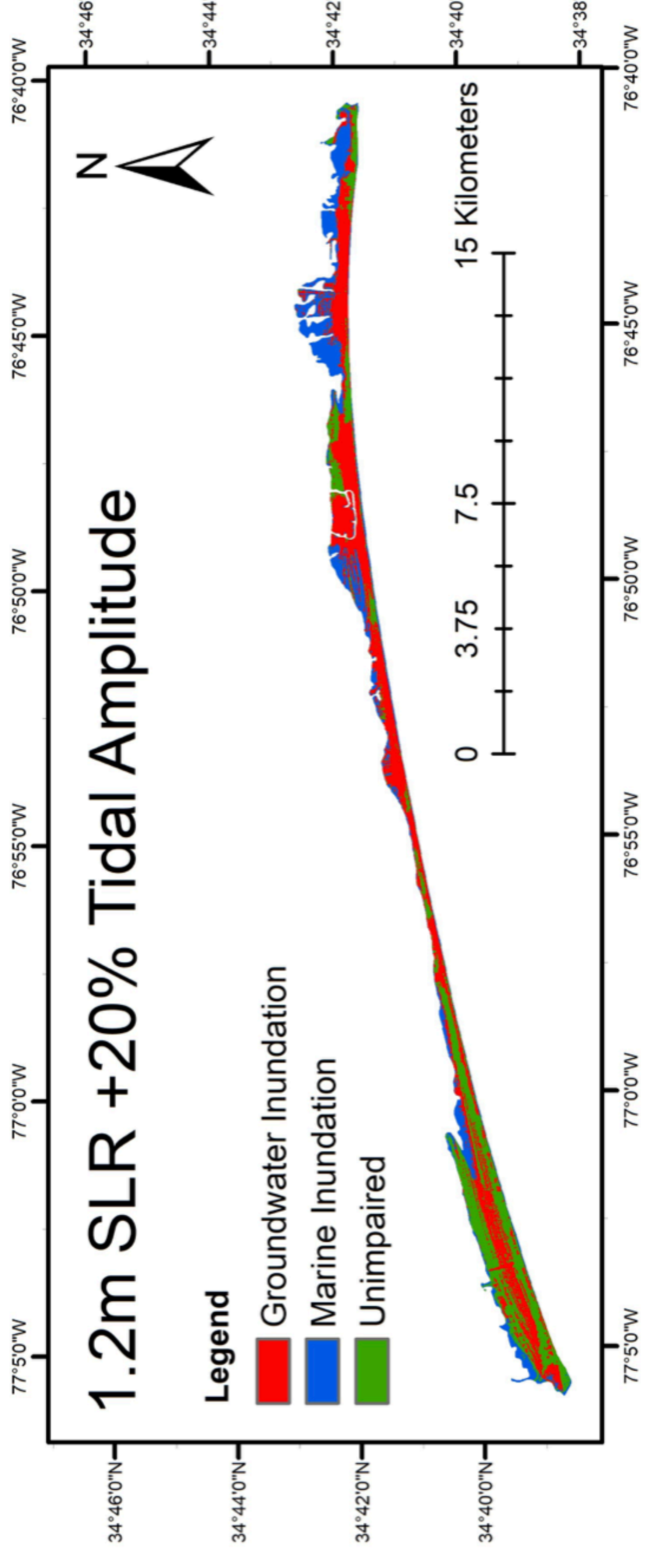
1.2m SLR +20% Tidal Amplitude
Legend
🟥 Groundwater Inundation
🟦 Marine Inundation
🟩 Unimpaired
N
0
3.75
7.5
15 Kilometers
77°5'0"W
77°0'0"W
76°55'0"W
76°50'0"W
76°45'0"W
76°40'0"W
34°46'0"N
34°44'0"N
34°42'0"N
34°40'0"N
34°38'0"N

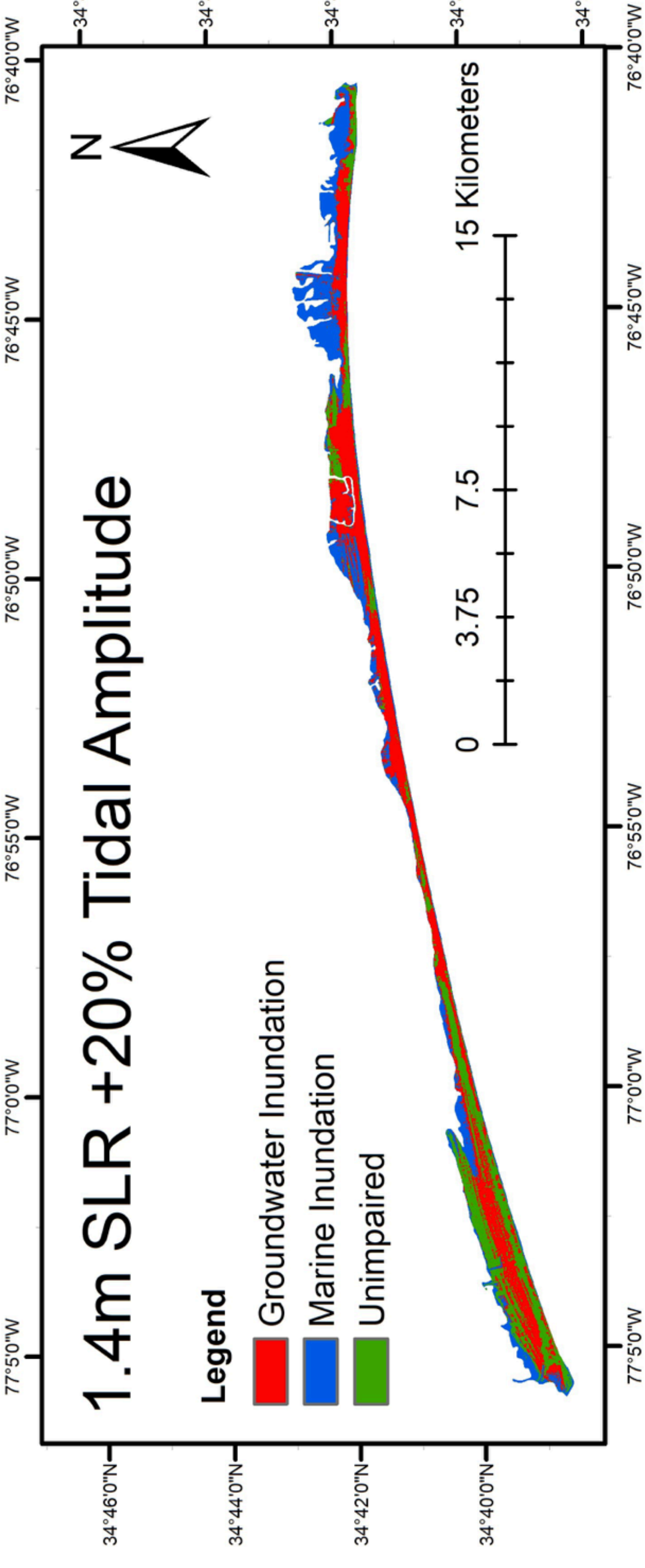
1.4m SLR +20% Tidal Amplitude
Legend
🟥 Groundwater Inundation
🟦 Marine Inundation
🟩 Unimpaired
N
0
3.75
7.5
15 Kilometers
34°46'0"N
34°44'0"N
34°42'0"N
34°40'0"N
34°38'0"N
76°40'0"W
76°45'0"W
76°50'0"W
76°55'0"W
77°0'0"W
77°5'0"W

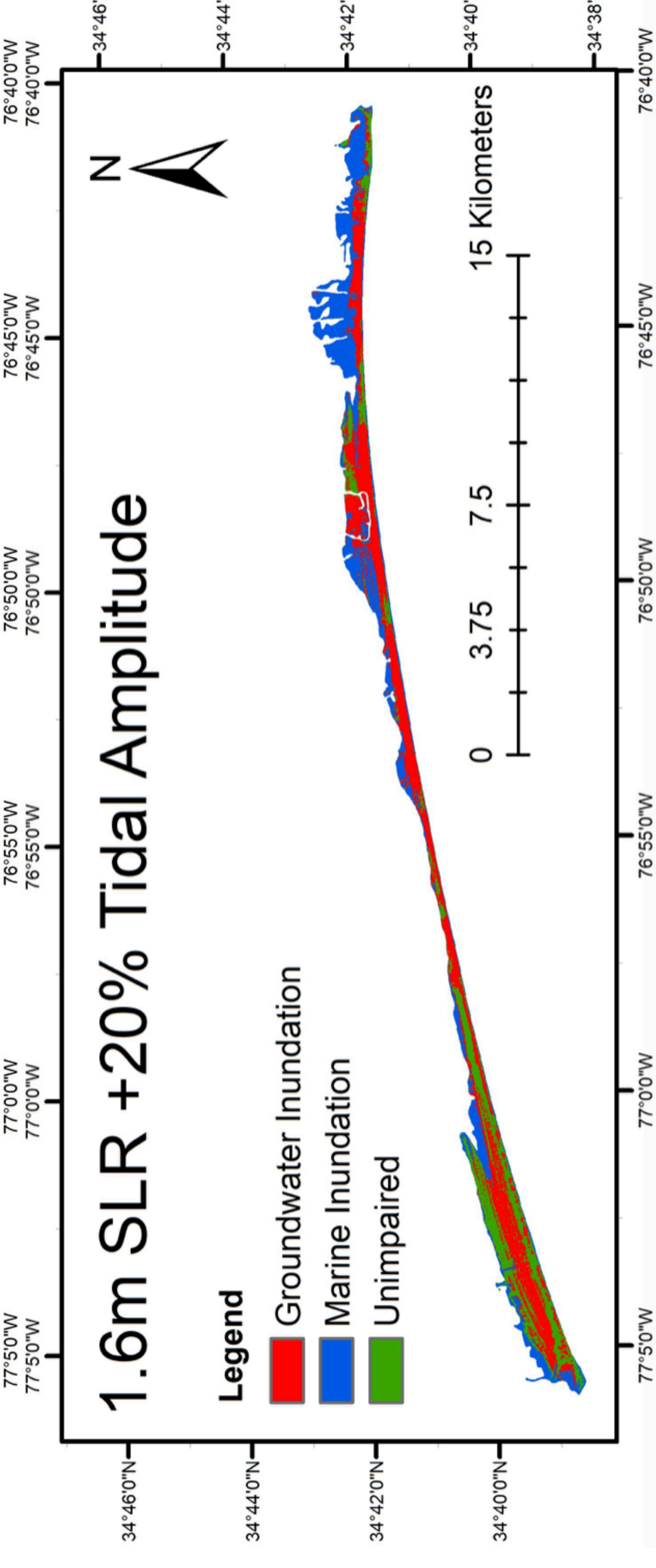
1.6m SLR +20% Tidal Amplitude
Legend
🟥 Groundwater Inundation
🟦 Marine Inundation
🟩 Unimpaired
N
0
3.75
7.5
15 Kilometers
34°46'0"N
34°44'0"N
34°42'0"N
34°40'0"N
34°38'0"N
76°40'0"W
76°45'0"W
76°50'0"W
76°55'0"W
77°0'0"W
77°5'0"W